ISSN 1175-1584

MINISTRY OF FISHERIES
Te Tautiaki i nga tini a Tangaroa

The 2003 stock assessment of paua (*Haliotis iris*) in PAU 7

P. A. Breen
S. W. Kim

New Zealand Fisheries Assessment Report 2003/35
September 2003

The 2003 stock assessment of paua (*Haliotis iris*) in PAU 7

P. A. Breen
S. W. Kim

NIWA
Private Bag 14901
Wellington

New Zealand Fisheries Assessment Report 2003/35
September 2003

Published by Ministry of Fisheries
Wellington
2003

ISSN 1175-1584

Citation:
Breen, P.A.; Kim, S.W. (2003).
The 2003 stock assessment of paua (*Haliotis iris*) in PAU 7.
New Zealand Fisheries Assessment Report 2003/35. 112 p.

This series continues the informal
New Zealand Fisheries Assessment Research Document series
which ceased at the end of 1999.

EXECUTIVE SUMMARY

Breen, P.A.; Kim, S.W. (2003): The 2003 stock assessment of paua (*Haliotis iris*) in PAU 7.

***New Zealand Fishery Assessment Report 2003/35.* 112p.**

A revised length-based model was used to assess the PAU 7 stock of paua (abalone) (*Haliotis iris*). The assessment used Bayesian techniques to estimate model parameters, the state of the stock, future states of the stock, and their uncertainties. Point estimates from the mode of the joint posterior distribution were used to explore sensitivity of the results to model assumptions and the input data; the assessment itself was based on marginal posterior distributions generated from Markov chain-Monte Carlo simulation.

The model was revised from the 2002 assessment model by re-parameterising the growth model and incorporating an alternative growth model, estimating the catchability coefficients as parameters, integrating maturity-at-length by fitting the model to a dataset, using mid-season biomass and numbers to make predictions, and estimating the selectivity of the commercial fishery. Other minor changes were made for various reasons, and a full description of the revised model is provided.

The model was applied to six datasets from PAU 7: standardised CPUE, a standardised index of relative abundance from research diver surveys, proportions-at-length from commercial catch sampling and population surveys, tag-recapture data, and maturity-at-length data.

Iterative re-weighting of the datasets produced a base case result in which the standard deviations of the normalised residuals were close to unity for all datasets. Model results for PAU 7 suggest a stock currently exploited at a rate of about 80%, and with recruited and spawning biomass below those in an arbitrary reference period, 1985–87, during which the stock was moderately stable. Results were not unduly sensitive to the exclusion of single datasets, and were robust to other modelling choices. Retrospective analyses were reasonably favourable.

At the current catch levels and minimum legal size, recruited biomass has a high likelihood (92%) of decreasing over the next 5 years. Spawning biomass has a 41% chance of decreasing. There is no chance that either could reach the reference levels in the next five years.

The assessment may be too optimistic – possible mechanisms causing such a result are discussed.

Table of Contents

1. INTRODUCTION

1.1 Overview

This document presents a Bayesian stock assessment of paua (abalone) (*Haliotis iris*) in PAU 7 (Marlborough) using data to the end of 2001–02 and some data from the 2002–03 fishing season. The assessment is made with a further revision of the length-based model first used in 1999 for PAU 5B (Breen et al. 2000a), and revised for subsequent assessments in PAU 5B (Stewart Island) and PAU 7 (Andrew et al. 2000a, Breen et al. 2000b, Breen et al. (unpublished results), Breen et al. 2001). This model is driven by reported commercial catches from 1974 to 2003 and is fitted to six sets of data described below: standardised CPUE, a standardised research diver survey index (RDSI) (Andrew et al. 2000b, 2002), proportion-at-length data from commercial catch sampling and from research diver surveys (Andrew et al. 2000a), a set of growth increment data, and a set of maturity-at-length data. This document contains a full description of the current model.

This document describes the model, the datasets used in the assessment, assumptions made in fitting, the basic fit of the model to the data, and how the point estimates of model parameters respond to a variety of changes to datasets and other modelling choices in sensitivity trials. The assessment is based on posterior distributions of model and derived parameters, which are obtained from Markov chain-Monte Carlo (McMC) simulations. Diagnostics from these are discussed and results are summarised. The document presents some further sensitivity trials based on McMC chains. Finally, at the request of the Ministry we explore the predicted effects of various catch reductions on an agreed set of indicators.

1.2 Description of the fishery

The paua fishery was summarised by Schiel (1992), by Annala et al. (2002), and in numerous previous assessment documents (e.g., Schiel 1989, McShane et al. 1994, 1996, Breen et al. 2000a, 2000b, 2001).

The fishing year for paua is from 1 October to 30 September. In what follows we refer to fishing year by the second portion; thus we call the 1997–98 fishing year "1998".

2. MODEL

This section describes the model used for stock assessment of PAU 7 in 2003. The model was developed for use in PAU 5B in 1999 and has been revised each year for subsequent assessments. The model revisions in many cases echo changes made to the rock lobster assessment model (Breen et al. 2002), which is a similar but more complex length-based Bayesian model.

2.1 Changes to the 2002 assessment model

2.1.1 Maturity-at-length

Maturity is now estimated in the model, in an integrated approach, by fitting to some maturity-at-length data. In previous model versions, maturity was estimated outside the model and the maturity ogive parameters were fed to the model in a sequential approach.

This change should have little or no effect on the MPD (modes of the joint posterior distribution) maturity schedule, because the model has only the maturity-at-length data from which to estimate maturity. However, the sequential approach discards the uncertainty associated with the maturity parameters and thus gives posterior distributions of spawning biomass that are too narrow, a typical consequence of the sequential approach.

The change added two new parameters to be estimated: L_{50} and L_{95-50}.

A fully integrated approach would see CPUE and the RDSI indices standardised within the model rather than outside it. Because of the huge number of CPUE records, this would slow down the model considerably, probably for only a small gain. The effect of standardising is small when compared with the raw data and standard errors are small. Still, this approach should some day be explored.

2.1.2 Growth model

Two changes were made. First, the growth model was re-parameterised. Instead of using the length-based von Bertalanffy model with parameters L_∞ and K, the assessment model now uses the Francis (1988) parameterisation. For arbitrary lengths α and β, the parameters are g_α and g_β, the expected annual growth increment at these two sizes. This change should have little effect, because it is just a re-parameterisation of the underlying model.

Second, we added an alternative growth model, based on the same parameters, in which the expected increment does not decline linearly with increasing length but instead declines at a decreasing rate. Test using only the tag-recapture data did not favour one model over the other, and both were tested with the full model in choosing a base case.

Trials were made, using only the tag-recapture data, on an alternative error structure for the growth increments – an assumed lognormal distribution instead of normal made little difference to the growth estimates. This change was not programmed into the model.

The growth model has five parameters: g_α and g_β, the c.v. of the expected increment, the minimum standard deviation, and the observation error standard deviation (the last was fixed). In preliminary explorations of possible base cases, it eventually became clear that the four-parameter model was over-parameterised, leading to problems with local minima and with the Hessian matrix. The minimum standard deviation is confounded with both the c.v. and g_β, and after experimentation we fixed the minimum standard deviation at 1.

2.1.3 Estimated *qs*

In previous assessments, catchability coefficients were treated as nuisance parameters and were calculated as the weighted geometric mean of the annual estimates obtained from the observed abundance estimate (CPUE or RDSI) and model biomass (for CPUE) or model numbers (for RDSI). This became complicated when variance components for each year's data were used in calculating the likelihoods for the data. In this assessment we estimated the catchability coefficients as simple parameters q^I for CPUE and q^J for RDSI.

2.1.4 Mid-season biomass and length frequencies

In previous versions of this model, predicted abundance indices and proportions-at-length were calculated from the numbers present at the beginning of the year. In this version they are based on mid-season numbers by subtracting half the catch (in numbers) from the numbers present at the beginning of the year. We do not simulate growth or natural mortality in the mid-year step.

The main model dynamics are unchanged – mid-year numbers are calculated only for making predictions. The effect of this change appears to be small except that estimated recruited biomass is lower by definition.

2.1.5 Selectivity of the commercial fishery

In previous assessments it was assumed that the fishery operates only on animals above the minimum legal size (MLS) of 125 mm. In commercial catch sampling data, some animals are observed below the MLS, either because the commercial measurement of length differs from the scientific, or because some fishers land some undersized paua. In PAU 7, 7–15% of the paua in the catch sampling data are below 124 mm shell length, so the assumption of knife-edged selection at 125 mm is violated.

The model can estimate commercial diver selectivity instead of using the MLS to model the commercial fishery (MLS continues to be used in calculating recruited biomass as an indicator). The model was changed so that either procedure can be used, and after initial testing the assessment was based on estimated commercial selectivity. In this version MLS is used only to calculate recruited biomass.

2.2 Model description

The model (LAMBASTA:Length-based Model for Bayesian Stock Assessment) does not use age, instead it uses 51 length bins, each of 2 mm shell length. The left-hand edge of the first bin is 70 mm; the largest bin is a plus-group representing abalone 170 mm and larger. Sexes are not distinguished. The time step is one year for the main dynamics. There is no spatial structure within the area modelled. The model is implemented in AD Model Builder™ (Otter Research Ltd., http://otter-rsch.com/admodel.htm) version 5.0.1, compiled with the Borland 5.01 compiler.

2.2.1 Estimated parameters

Parameters estimated by the model are as follows. The whole parameter vector is referred to as θ.

$\ln(R0)$	natural logarithm of base recruitment
M	instantaneous rate of natural mortality
g_α	expected annual growth increment at length α
g_β	expected annual growth increment at length β
ϕ	c.v. of the expected growth increment
q^I	scalar between recruited biomass and CPUE
q^J	scalar between numbers and the RDSI
L_{50}	length at which maturity is 50%
L_{95-50}	distance between L_{50} and L_{95}
T_{50}	length at which research diver selectivity is 50%
T_{95-50}	distance between T_{50} and T_{95}
D_{50}	length at which commercial diver selectivity is 50%
D_{95-50}	distance between D_{50} and D_{95}
$\tilde{\sigma}$	common component of error
h	shape of CPUE *vs* biomass relation
ε	vector of annual recruitment deviations

2.2.2 Constants

l_k	length of an abalone at the midpoint of the *k*th length class (l_k for class 1 is 71 mm, for class 2 is 73 mm, and so on)
σ_{MIN}	minimum standard deviation of the expected growth increment (assumed to be 1)
σ_{obs}	standard deviation of the observation error around the growth increment (assumed to be 0.25 mm)
MLS_t	Minimum legal size (125 mm)
$P_{k,t}$	a switch based whether abalone in the *k*th length class in year *t* are above the MLS ($P_{k,t} = 1$) or below ($P_{k,t} = 0$)
a, b	constants for the length-weight relation, taken from Schiel & Breen (1991); a = 2.592E-8; b = 3.322 where length is in mm and weight in kg.
w_k	the weight of an abalone at length l_k
ϖ^I	relative weight assigned to the CPUE dataset. This and the following relative weights are specified in the data file, but can be varied between runs; described further below under "Fitting".
ϖ^J	relative weight assigned to the research diver survey index dataset
ϖ^r	relative weight assigned to proportions-at-length from research diver surveys
ϖ^s	relative weight assigned to proportions-at-length from commercial catch sampling
ϖ^{mat}	relative weight assigned to maturity-at-length data
κ_t^s	square root of the number measured greater than the MLS in commercial catch sampling in year *t*, normalised by the lowest year
κ_t^r	square root of the number measured greater than 90 mm in research diver surveys in year *t*, normalised by the lowest year
$U^{\max}$	exploitation rate above which a limiting function was invoked, set at 0.80
μ_M	mean of the prior distribution for *M*, assumed to be 0.10 based on a literature review by Shepherd & Breen (1992)
σ_M	assumed standard deviation of the prior distribution for *M*, set at 0.35 based on inspection of the prior
σ_ε	assumed standard deviation of recruitment deviations in log space (part of the prior for recruitment deviations), set arbitrarily at 0.40
n_ε	number of recruitment deviations (30).
α	length associated with g_α
β	length associated with g_β

2.2.3 Observations

C_t	total observed catch in year *t*
I_t	standardised CPUE in year *t*
σ_t^I	standard deviation of the estimate of observed CPUE in year *t*, obtained from the standardisation model
J_t	standardised RDSI in year *t*

σ_t^J	the standard deviation of the estimate of research survey index in year t, obtained from the standardisation model
$p_{k,t}^r$	observed proportion in the *k*th length class in year *t* in research diver sampling
$p_{k,t}^s$	observed proportion in the *k*th length class in year *t* in commercial catch sampling
l_j	initial length for the *j*th tag-recapture record
d_j	observed length increment of the *j*th tag-recapture record
Δt_j	time at liberty for the *j*th tag-recapture record
p_k^{mat}	observed proportion mature in the *k*th length class in the maturity dataset

2.2.4 Derived variables

$R0$	base number of annual recruits
$N_{k,t}$	number of abalone in the *k*th length class at the start of year *t*
$N_{k,t+0.5}$	number of abalone in the *k*th length class in the mid-season of year *t*
$R_{k,t}$	recruits to the model in the *k*th length class in year *t*
Δl_k	expected annual growth increment for abalone in the *k*th length class
$\sigma^{\Delta l_k}$	standard deviation of the expected growth increment for abalone in the *k*th length class, used in calculating $\mathbf{G}$
$\mathbf{G}$	growth transition matrix
m_k	proportion of mature abalone at length l_k
$B_{t+0.5}$	biomass of abalone above the MLS in the mid-season of year *t*
$\breve{B}_t$	biomass of abalone available to the commercial fishery at the beginning of year *t*
$S_{t+0.5}$	biomass of mature abalone in the mid-season of year *t*
U_t	exploitation rate in year *t*
$SF_{k,t}$	finite rate of survival from fishing for abalone in the *k*th length class in year *t*
V_k^r	relative selectivity of research divers for abalone in the *k*th length class
V_k^s	relative selectivity of commercial divers for abalone in the *k*th length class
$\sigma_{k,t}^r$	error of the predicted proportion in the *k*th length class in year *t* in research diver surveys
$\sigma_{k,t}^s$	error of the predicted proportion in the *k*th length class in year *t* in commercial catch sampling
σ_j^d	standard deviation of the predicted length increment for the *j*th tag-recapture record
σ_j^{tag}	total error predicted for the *j*th tag-recapture record
σ_k^{mat}	error of the proportion mature-at-length for the *k*th length class
$-\ln(\mathbf{L})$	negative log-likelihood
f	total function value

2.2.5 Predictions

$\hat{I}_t$	predicted CPUE in year t
$\hat{J}_t$	predicted RDSI in year t
$\hat{p}^r_{k,t}$	predicted proportion in the kth length class in year t in research diver surveys
$\hat{p}^s_{k,t}$	predicted proportion in the kth length class in year t in commercial catch sampling
$\hat{d}_j$	predicted length increment of the jth tag-recapture record
$\hat{p}^{mat}_k$	predicted proportion mature in the kth length class

2.2.6 Initial conditions

The initial population is assumed to be in equilibrium with zero fishing mortality and the base recruitment. The model is run for 60 years with no fishing to obtain near equilibrium in numbers-at-length. Recruitment is evenly divided among the first five length bins:

(1) $R_{k,t} = 0.2R0 \qquad \text{for} 1 \le k \le 5$

(2) $R_{k,t} = 0 \qquad \text{for} k > 5$

A growth transition matrix is calculated inside the model from the estimated growth parameters. If the growth model is linear, the expected annual growth increment for the kth length class is

(3) $$\Delta l_k = \left(\frac{\beta g_\alpha - \alpha g_\beta}{g_\alpha - g_\beta} - l_k \right) \left[1 - \left(1 + \frac{g_\alpha - g_\beta}{\alpha - \beta} \right) \right]$$

The model uses the AD ModelBuilder™ function *posfun*, with a dummy penalty only, to ensure a positive expected increment at all lengths, using a smooth differentiable function. The *posfun* function is also used with a real penalty to prevent the quantity $\left(1 + \frac{g_\alpha - g_\beta}{\alpha - \beta} \right)$ from becoming negative. If the growth model is exponential, the expected annual growth increment for the kth length class is

(4) $$\Delta l_k = g_\alpha \left(g_\beta / g_\alpha \right)^{(l_k - \alpha)/(\beta - \alpha)}$$

again using *posfun* with a dummy penalty to ensure a positive expected increment at all lengths.

The standard deviation of Δl_k is assumed to be proportional to Δl_k with minimum σ_{MIN}:

(5) $$\sigma^{\Delta l_k} = \left(\Delta l_k \phi - \sigma_{MIN} \right) \left(\frac{1}{\pi} \tan^{-1} \left(10^6 \left(\Delta l_k \phi - \sigma_{MIN} \right) \right) + 0.5 \right) + \sigma_{MIN}$$

From the expected increment and standard deviation for each length class, the probability distribution of growth increments for an abalone of length l_k is calculated from the normal distribution, and translated into the vector of probabilities of transition from the kth length bin to other length bins to form the growth transition matrix **G**. Zero and negative growth increments are permitted, i.e. the probability of staying in the same bin or moving to a smaller bin can be non-zero.

In the initialisation, the vector $\mathbf{N}_t$ of numbers-at-length is determined from numbers in the previous year, survival from natural mortality, the growth transition matrix $\mathbf{G}$ and the vector of recruitment $\mathbf{R}_t$:

$$(6) \qquad \mathbf{N}_t = \left(\mathbf{N}_{t-1}\, e^{-M}\right) \bullet \mathbf{G} + \mathbf{R}_t$$

where the prime (′) denotes vector transposition and the dot (•) denotes matrix multiplication.

2.2.7 Dynamics

2.2.7.1 Sequence of operations

In the estimation phase (i.e., for the years with catch data, after the burn-in period and before any projections), the dynamics are sequenced as follows:

- numbers at the beginning of year t-1 are subjected to natural mortality, then fishing, then growth to produce the numbers at the beginning of year t.
- recruitment is added to the numbers at the beginning of year t.
- biomass available to the fishery is calculated, and used with catch to calculate the exploitation rate, which is constrained if necessary.
- half the exploitation rate is applied to obtain mid-year numbers, from which the predicted abundance indices and proportions-at-length are calculated. Mid-year numbers are not used further.

2.2.7.2 Main dynamics

For each year, t, the model calculates the start-of-the-year biomass available to the commercial fishery. Biomass above the MLS at the start of the year is:

$$(7) \qquad \breve{B}_t = \sum_k N_{k,t} P_{k,t} w_k$$

or, if the commercial selectivity is used instead of the MLS:

$$(8) \qquad \breve{B}_t = \sum_k N_{k,t} V_k^s w_k$$

where

$$(9) \qquad V_k^s = \frac{1}{1+19^{-\left(\left(l_k - D_{50}\right)/D_{95-50}\right)}}$$

The observed catch is then used to calculate exploitation rate, constrained for all values above U^{max} with the *posfun* function of AD Model Builder™. If the ratio of catch to available biomass exceeds U^{max}, then exploitation rate is constrained and a penalty is added to the total negative log-likelihood function. Let minimum survival rate A_{min} be 1-U^{max}, and survival rate A_t be 1-U_t:

$$(10) \qquad A_t = 1 - \frac{C_t}{\breve{B}_t} \qquad \text{for } \frac{C_t}{\breve{B}_t} \le U^{\max}$$

$$(11) \qquad A_t = 0.5A_{\min}\left[1+\left[3-\frac{2\left(1-\frac{C_t}{\breve{B}_t}\right)}{A_{\min}}\right]^{-1}\right] \quad \text{for} \quad \frac{C_t}{\breve{B}_t} > U^{\max}$$

The penalty invoked when the exploitation rate exceeds U^{max} is:

$$(12) \qquad 1000000\left(A_{\min}-\left(1-\frac{C_t}{\breve{B}_t}\right)\right)^2$$

This has no effect on the final estimates, but it prevents the model from exploring parameter combinations that give unrealistically high exploitation rates. Survival from fishing is calculated as:

$$(13) \qquad SF_{k,t} = 1-(1-A_t)P_{k,t}$$

or

$$(14) \qquad SF_{k,t} = 1-(1-A_t)V_k^s$$

The vector of numbers-at-length in the following year is calculated from:

$$(15) \qquad \mathbf{N}_t = \left(\mathbf{SF}_{t-1} \otimes \left(\mathbf{N}_{t-1}\, e^{-M}\right)\right) \bullet \mathbf{G} + \mathbf{R}_t$$

where $\otimes$ denotes the element-by-element vector product. The vector of recruitment, $\mathbf{R}_t$ is determined from *R0* and the estimated recruitment deviations:

$$(16) \qquad R_{k,t} = 0.2R0e^{\left(\varepsilon_t - 0.5\sigma_\varepsilon^2\right)} \qquad \text{for} 1 \le k \le 5$$

$$(17) \qquad R_{k,t} = 0 \qquad \text{for} k > 5$$

2.2.8 Model predictions

The model predicts CPUE in year t from recruited biomass, the scaling coefficient and the shape parameter:

$$(18) \qquad \hat{I}_t = q^I\left(B_{t+0.5}-\frac{C_t}{2}\right)^h$$

Available biomass $B_{t+0.5}$ is calculated as in equation (7) or (8), but using the mid-year numbers, $N_{k,t+0.5}$:

$$(19) \qquad N_{k,t+0.5} = N_{k,t}\left(1-A_t/2\right)P_{k,t}$$

or if commercial selectivity is used instead of MLS:

$$(20) \qquad N_{k,t+0.5} = N_{k,t}\left(1-A_t/2\right)V_k^s$$

The predicted research diver survey index is calculated from model numbers in bins greater than 90 mm length, taking into account research diver selectivity-at-length:

$$\hat{J}_t = q^J \sum_{k=11}^{51} N_{k,t+0.5} V_k^r \quad (21)$$

where V_k^r is calculated from:

$$V_k^r = \frac{1}{1+19^{-\left((l_k - T_{50})/T_{95-50}\right)}} \quad (22)$$

The model predicts proportions-at-length for the research diver survey from numbers in each length class for lengths greater than 90 mm:

$$\hat{p}_{k,t}^r = \frac{N_{k,t+0.5} V_k^r}{\sum_{k=11}^{51} N_{k,t+0.5} V_k^r} \qquad \text{for } k \geq 11 \quad (23)$$

Predicted proportions-at-length for commercial catch sampling are similar. If it is assumed that all fishing is above the MLS:

$$\hat{p}_{k,t}^s = \frac{N_{k,t+0.5} P_{k,t}}{\sum_k N_{k,t+0.5} P_{k,t}} \quad (24)$$

or alternatively, if fishing is controlled by the commercial selectivity:

$$\hat{p}_{k,t}^s = \frac{N_{k,t+0.5} V_k^s}{\sum_k N_{k,t+0.5} V_k^s} \quad (25)$$

The predicted increment for the *j*th tag-recapture record, using the linear model, is

$$\hat{d}_j = \left(\frac{\beta g_\alpha - \alpha g_\beta}{g_\alpha - g_\beta} - L_j \right) \left[1 - \left(1 + \frac{g_\alpha - g_\beta}{\alpha - \beta} \right)^{\Delta t_j} \right] \quad (26)$$

where Δt_j is in years. For the exponential model the expected increment is

$$\hat{d}_j = \Delta t_j g_\alpha \left(g_\beta / g_\alpha \right)^{\left[L_j/(\beta-\alpha) - 1/(\beta/\alpha - 1) \right]} \quad (27)$$

and the error around this expected increment is

$$\sigma_j^d = \left(\hat{d}_j \phi - \sigma_{MIN} \right) \left(\frac{1}{\pi} \tan^{-1} \left(10^6 \left(\hat{d}_j \phi - \sigma_{MIN} \right) \right) + 0.5 \right) + \sigma_{MIN} \quad (28)$$

Predicted maturity-at-length is

$$(29) \qquad \hat{p}_k^{mat} = \frac{1}{1+19^{-\left((l_k - L_{50})/L_{95-50}\right)}}$$

2.2.9 Fitting

2.2.9.1 Likelihoods

The distribution of CPUE is assumed to be normal-log, so the negative log-likelihood is:

$$-\ln(\mathbf{L})\left(\hat{I}_t \mid \theta\right) = \frac{\left(\ln(I_t) - \ln(\hat{I}_t)\right)^2}{2\left(\sigma_t^I \tilde{\sigma} / \varpi^I\right)^2} + \ln\left(\sigma_t^I \tilde{\sigma} / \varpi^I\right) + 0.5\ln(2\pi)$$

The distribution of the research diver survey index is also assumed to be normal-log, so negative log-likelihood is:

$$(30) \qquad -\ln(\mathbf{L})\left(\hat{J}_t \mid \theta\right) = \frac{\left(\ln(J_t) - \ln(\hat{J}_t)\right)^2}{2\left(\sigma_t^J \tilde{\sigma} / \varpi^J\right)^2} + \ln\left(\sigma_t^J \tilde{\sigma} / \varpi^J\right) + 0.5\ln(2\pi)$$

The proportions-at-length from commercial catch sampling are assumed to be normally distributed, with a standard deviation that depends on the proportion, the number measured and the weight assigned to the data:

$$(31) \qquad \sigma_{k,t}^s = \frac{\tilde{\sigma}}{\kappa_t^s \varpi^s \sqrt{p_{k,t}^s + 0.1}}$$

The negative log-likelihood is:

$$(32) \qquad -\ln(\mathbf{L})\left(\hat{p}_{k,t}^s \mid \theta\right) = \frac{\left(p_{k,t}^s - \hat{p}_{k,t}^s\right)^2}{2\sigma_{k,t}^{s\,2}} + \ln\left(\sigma_{k,t}^s\right) + 0.5\ln(2\pi)$$

The likelihood for research diver sampling is analogous.

Errors in the tag-recapture dataset were also assumed to be normal. For the *j*th record, the total error is a function of the predicted standard deviation (equation (28)), and the observation error:

$$(33) \qquad \sigma_j^{tag} = \sqrt{\sigma_{obs}^{\,2} + \left(\sigma_j^d\right)^2}$$

and the negative log-likelihood is:

$$(34) \qquad -\ln(\mathbf{L})\left(\hat{d}_j \mid \theta\right) = \frac{\left(d_j - \hat{d}_j\right)^2}{2\sigma_j^{tag\,2}} + \ln\left(\sigma_j^{tag}\right) + 0.5\ln(2\pi)$$

The proportion mature-at-length was assumed to be normally distributed, with standard deviation analogous to proportions-at-length:

$$\sigma_k^{mat} = \frac{\tilde{\sigma}}{\varpi^{mat}\sqrt{p_k^{mat}+0.1}} \quad (35)$$

The negative log-likelihood is:

$$-\ln(\mathbf{L})\left(\hat{p}_k^{mat} \mid \theta\right) = \frac{\left(p_k^{mat}-\hat{p}_k^{mat}\right)^2}{2\left(\sigma_k^{mat}\right)^2} + \ln\left(\sigma_k^{mat}\right) + 0.5\ln(2\pi) \quad (36)$$

2.2.9.2 Normalised residuals

These are calculated as the residual divided by the relevant σ term used in the likelihood. For CPUE, the normalised residual is

$$\frac{\ln(I_t)-\ln\left(\hat{I}_t\right)}{\left(\sigma_t^I \tilde{\sigma}/\varpi^I\right)} \quad (37)$$

and similarly for the RDSI. For the commercial sampling proportions-at-length, the residual is

$$\frac{p_{k,t}^s - \hat{p}_{k,t}^s}{\sigma_{k,t}^s} \quad (38)$$

and similarly for proportions-at-length from the research diver surveys. Because the vectors of observed proportions contain many empty bins (e.g., the bins for large and very small paua), the residuals for proportions-at-length include large numbers of very small residuals, and these distort the frequency distribution of residuals. When presenting normalised residuals from proportions-at-length, we arbitrarily ignore normalised residuals less than 0.05.

For tag-recapture data, the residual is

$$\frac{d_j - \hat{d}_j}{\sigma_j^{tag}} \quad (39)$$

and for the maturity-at-length data the residual is

$$\frac{p_k^{mat} - \hat{p}_k^{mat}}{\sigma_k^{mat}} \quad (40)$$

2.2.9.3 Dataset weights

The relative weights used for each dataset, ϖ, are relative to the tagging dataset, which is unweighted. Weights were chosen experimentally in choosing a base case, iteratively changing them to obtain standard deviations of the normalised residuals (sdnrs) close to unity for each dataset. Table 1 shows the weights chosen and the resulting sdnrs.

2.2.9.4 Priors and bounds

Bayesian priors were established for all parameters. Most were incorporated simply as uniform distributions with upper and lower bounds arbitrarily set wide so as not to restrict the estimation. The prior probability density for M was a normal-log distribution with mean μ_M and "standard deviation" σ_M. The contribution to the objective function of estimated M = x is:

$$(41) \qquad -\ln(\mathbf{L})(x \mid \mu_M, \sigma_M) = \frac{\left(\ln(M) - \ln(\mu_M)\right)^2}{2\sigma_M^{\,2}} + \ln\left(\sigma_M \sqrt{2\pi}\right)$$

The prior probability density for the vector of estimated recruitment deviations, ε, was assumed to be normal with a mean of zero. The contribution to the objective function for the whole vector is:

$$(42) \qquad -\ln(\mathbf{L})(\varepsilon \mid \mu_\varepsilon, \sigma_\varepsilon) = \frac{\sum_{i=1}^{n_\varepsilon} (\varepsilon_i)^2}{2\sigma_\varepsilon^{\,2}} + \ln\left(\sigma_\varepsilon\right) + 0.5\ln(2\pi).$$

Table 2 shows the values for each parameter used in the base case for PAU 7.

2.2.9.5 Penalties

Explicit penalties are the penalty applied to exploitation rates higher than the assumed maximum (equation (12)) and a penalty that prevents unrealistic estimates in the Francis growth equation (3). These are added to the objective function after being multiplied by arbitrary weights determined by experiment. The penalty on exploitation rate was set to make the discrepancy between observed and model catches reasonable (maximum of 15 kg) - lower values allowed a larger discrepancy and higher values tended to affect the Hessian matrix.

AD ModelBuilder™ also has internal penalties that keep estimated parameters within their specified bounds, but these should have no effect on the final outcome, because choice of a base case excludes the situations where parameters are estimated at or near a bound.

2.2.10 Fishery indicators

To compare runs by means of their MPDs in finding a base case and looking at sensitivity to modelling options, we use mid-year recruited and spawning biomass from 2003 (current biomass) and from a reference period, 1985–87. This was a period when the biomass was stable, production was good and there was a long subsequent period when the fishery flourished. The means of values from the three years were called S_{av} and B_{av}. We also used annual exploitation rate in 2003, and the minimum and maximum recruitment deviations in arithmetic space.

The assessment is based on the following indicators calculated from their posterior distributions: mid-year recruited and spawning biomass from 2003, 2008 and the reference period 1985–87, and ratios of those (e.g., $B_{2008.5} / B_{2003.5}$), exploitation rates in 2003 and 2008, the ratio of actual catch to specified catch in projections (this indicates how much of the specified catch could actually be caught). Four additional indicators are calculated as the percentage of runs in which:

- spawning biomass in 2008 had decreased from 2003
- spawning biomass in 2008 was less than the reference level
- recruited biomass in 2008 had decreased from 2003
- recruited biomass in 2008 was less than the reference level

2.2.11 Markov chain Monte Carlo (McMC) procedures

AD ModelBuilder™ uses the Metropolis-Hastings algorithm. The step size is based on the standard errors of the parameters and their covariance relationships, estimated from the Hessian matrix, and the overall step size is adjusted during the first few thousand iterations to make the acceptance rate close to 0.3.

We ran five chains of 3 million simulations each, and saved *1000* regularly spaced samples from each chain, for a total of 15 million simulations and 5000 samples. The chains were each started from the parameter vector associated with a point on the likelihood profile for M: we used the vectors from the mode and from plus and minus 1.5 and 3.5 estimated standard deviations along the profile. The MPD parameter vector does not appear anywhere in the McMC chain.

After examining the diagnostics from each chain, we discarded one chain that showed high autocorrelation and other bad diagnostics, then concatenated the other four chains into one chain and used it to generate posteriors of the parameters and other quantities of interest.

2.2.12 Projections

Projections were made through 2008 by running the dynamics forward in time with each parameter vector, driving the model with a specified catch (assumed in the first instance to be the 2003 catch). The sequence of operations is as described for the main dynamics.

Recruitment in projections is obtained by re-sampling the estimated recruitment from the years 1993 to 2002. Because the 2003 recruitment deviation is poorly determined by the data (it has no effect on any of the quantities being fitted in 2003), the estimated value is inappropriate for projections. We over-write the value for 2003 with a value obtained by re-sampling the deviations from 1993 through 2002.

In the years for which parameters are estimated, 1974 to 2003, exploitation rate is limited with *posfun*, which allows the rate to exceed the specified maximum slightly (equation 11). Projected exploitation rate is limited by simply truncating it at the specified maximum. An indicator is calculated to show, for each projection, the mean of actual catches (exploitation rate times available biomass) as a percentage of the specified catch.

3. DATA

3.1 Catch data

3.1.1 Commercial catch

The catch history was estimated by Murray & Akroyd (1984) for 1974–83, who stated that landings before 1974 were unreliable. Schiel (1989) presented estimates for 1984–1988. Schiel (1992) revisited the estimates for 1981–85, and previous PAU 7 assessments have used the Schiel (1992) estimates as a base case. The effect of this change (affecting mostly the 1981 and 1982 catches) was explored by Andrew et al. (2000a) and found to be small.

Catches from 1989 onwards were captured on QMR forms and reported in Plenary documents (eg. Annala et. al. 2002). These were cross-checked for this assessment by obtaining a new extract from the QMR reports (O'Brien, MFish, pers. comm.), which differed only slightly from the estimates published in the 2002 Plenary Report. We used the most recent extract. Data for 2001 and 2002 were supplied by MFish on 17 February 2003. For the 2003 catch we assumed the TACC.

The 1986 catch appears suspiciously low, and as in previous years we used the average of 1985 and 1987 catches (Table 3).

3.1.1.1 Commercial catch in areas 17 and 38

Nearly all the catch in 1990 and 1991 came from areas 17 and 38 (Table 3; see Figure 1 for areas). These are the areas in which all but the most recent research diver surveys have been made, and the previous assessment (Breen et al. 2001) limited the assessment to those two areas.

Figure 2 shows estimated catch from Catch and Effort Landing Returns (CELRs) for all vessels and 5-yr vessels (vessels that fished for 5 years and longer) in all areas and areas 17 and 38. Area 17 had the most catch with area 38 next. We calculated catch proportions of areas 17 and 38 from records from all vessels.

To estimate the PAU 7 catch from areas 17 and 38 catch, we examined the annual percentage of the PAU 7 catch reported from these two areas on the CELR forms. Before 1990, the percentage of the total catch reported on CELR forms was too low to support this method, but the percentage of catch from outside areas 17 and 38 appeared to be very low. For 1990 and subsequent years we applied the proportion of catches from areas 17 and 38 catch to the total PAU 7 catch reported to the Quota Management System (QMS). For the 2003 catch we used the mean proportion from the previous five years.

Table 3 shows the catch data and Figure 3 shows commercial catch in all areas, commercial catch in areas 17 and 38 only and all catches including recreational and illegal catches.

3.1.1.2 TACC

The TACC was set at 250 t when paua entered the QMS in 1987. This increased to a peak of 266.5 t in 1996 after quota appeals. For 2001, the industry agreed to shelve 20% of their quota, and for 2002 the TACC was reduced to 240.7 t, then reduced again for the 2003 season to 187.24 t (Table 3).

3.1.2 Recreational catch

In 2000, the National Recreational Fishing Survey (Boyd & O'Reilly, unpublished results) estimated 15.8 t for PAU 7. We assumed that recreational catch increased linearly from an arbitrary 5 t in 1974 to 16 t in 2000 (Table 3), and that this increase continued after 2000.

3.1.3 Illegal catch

Illegal catch was estimated by the Ministry of Fisheries to be 3 t (Paul Cresswell, MFish, pers. comm.). No historical estimates are available so we have assumed this catch to have been constant since 1974. We added this estimate to the areas 17 and 38 commercial catches used to drive the model (Table 3).

3.1.4 Customary catches

Customary catch was incorporated by the Minister of Fisheries into the PAU 7 TAC as an allowance of 15 t (Paul Cresswell, MFish, pers. comm.). No historical estimates are available, so we assumed this catch to be constant since 1974 and we added this to the commercial catches used to drive the model (Table 3).

3.2 CPUE

Catch and effort data reported on CELRs were standardised with the method of Vignaux (1993) as described by Kendrick & Andrew (2000), then changed into canonical form as described by Francis (1999), giving estimates that are independent of the reference year.

The standardisation was done on the natural logarithm of catch per diver day. The diver-hours field on the CELR forms included a high proportion of obvious errors, and as in previous assessments was not used. For the standardisation we used records only from vessels that fished for 5 years or more. Two sets of standardisation were done: for all PAU 7 areas (12 083 records involving 65 vessels) and for the main fishing areas, 17 and 38 (10 781 records involving 65 vessels), as for the 2001 assessment for PAU 7. As a sensitivity test, a standardisation was done with all vessels in areas 17 and 38 (19 359 records, 376 vessels).

Records with information missing from the fields of interest were automatically excluded from the analyses. These included records with zero catch (14 records in all PAU 7 records), which cannot be used in the logarithmic model, missing the number of divers (244 records), and missing the vessel identifier (45 records). When the fishstock and new statistical area were contradictory, the QMA was identified from the latter. A number of divers greater than nine (5 records from 2001–02 data and 25 records from older data) and diving hours per diver greater than 10 hours (20 records from 2001–02 data and 39 records from old data) were considered to be out-of-range errors and the records were deleted. So 2% of all data (392 records) were removed from all PAU 7 data because of errors, then 44% of data remaining (9426 records) were removed because they were from vessels that fished for less than 5 years.

The raw CPUE and the geometric means for each statistical area are shown in Figure 4. All areas had similar level of CPUE after 1993. The raw CPUE and the geometrical means are similar in all areas.

The variables offered to the model were vessel, fishing year, month, and statistical area. The order in which variables were selected into the model and their effect on the model r^2 are shown in Table 4. In both standardisations, month and statistical area did not increase the r^2 substantially and were not used. The model explained 40% and 42% of the variation in CPUE for all statistical areas and for areas 17 and 38 respectively.

Fits and residuals are shown in Figure 5 to Figure 7. Figure 5 and Figure 6 show fits and residuals to the data with vessels that fished for 5 years or more. Both fits show small numbers of outliers. Fits and residuals to the data with all vessels in area 17 and 38 are shown in Figure 7. There are more data observed in this plot, and the range of predicted ln(CPUE) is wider. There is a small number of outliers. The Q-Q plot shows outliers from all three fits are outside the 90% range of data (Figure 8).

The year effect, relative to the 1983 fishing year, was made canonical by multiplying each year effect by the geometric mean of the indices. Because the canonical indices do not depend on a reference year, standard errors can be calculated using the covariance matrix from the analysis. The year effects in canonical form and their relative standard errors in log space are shown in Table 5. The model uses year effect indices in natural space and standard errors in log space. For more details, see Francis (1999). The standardised CPUE is calculated as the product of the mean of the raw CPUE and year effect.

Raw and standardised CPUE with 5-yr vessels in all areas and in areas 17 and 38 only, with confidence intervals, are shown in Figure 9 and Figure 10. Both figures show little difference in raw and standardised CPUE and the confidence intervals are tight, especially in recent years. There is little difference between all areas and areas 17 and 18 only. The raw and standardised CPUE with all vessels in areas 17 and 38 are shown in Figure 11. Generally the CPUE is lower than using 5-year vessels, but the decrease over years is not as steep. The standardised CPUE fits better to the raw CPUE in early years with all vessel data.

The comparisons in CPUE indices from different datasets are shown in Figure 12 and Figure 13. CPUE index using all areas is similar to the CPUE index using areas 17 and 38 only (Figure 12). Using all vessels gives a similar shape of the CPUE trend as using 5-year vessels (Figure 13).

For the assessment, we used standardised CPUE from the 5-year vessels in areas 17 and 38 only (Table 5, middle column, and Figure 10). CPUE from areas 17 and 38 only is similar to the CPUE from all areas (Figure 12). Although there were twice as many data when using all vessels, vessel effects from vessels that fished for less than 5 years may not be precise; in any case the standardised CPUEs from all vessels and the 5-year vessels were similar (Figure 13).

3.3 Research diver survey index (RDSI)

Fishery-independent research diver survey estimates of relative abundance (RDSI) have been made since 1993 (Andrew et al. (2000b). The previous assessment for PAU 7 used a standardisation using the method of Vignaux (1993). For this year's assessment, we used the same approach as for CPUE. The standardisation was done on the natural log of the abundance index from each swim, which in turn was based on the number and size of paua patches seen in 10 minutes. The standardised result was then changed into canonical form as described by Francis (1999), giving estimates that are independent of the reference year.

There were six years of data (1993 data includes as 1994 data), five strata (Figure 14) and eight research divers. Fifteen records out of 664 with zero catches had "1" added to the index, based on inspection of the remaining data, in which the index varied from 1.3 to 806.1 (mean 59.0). The December to February 2003 survey were included in this analysis and used for the assessment. The new stratum surveyed, Cape Campbell, was not included in the analysis because this area was surveyed only for 2003. Summaries of data are shown in Table 6.

Variables offered to the model were fishing year, stratum, and diver. The order in which variables were selected into the model and their effect on the model r^2 are shown in Table 7. The model explained 18% of the variation in RDSI.

Fits and residuals are shown in Figure 15 and show no problems with outliers. The Q-Q plot shows that negative residuals do not follow the theoretical pattern (Figure 15), but the positive residuals follow the theoretical pattern well.

The year effect, relative to the 1993 fishing year, was made canonical by multiplying each year effect by the geometric mean of the raw indices. The year effects in canonical form and relative standard errors in log space are shown in Table 8. The model uses year effect indices in natural space and standard errors in log space (For more details, see Francis (1999)). The standardised diver survey index is calculated as the product of the mean of the raw diver survey index and year effect.

Raw and standardised diver survey indices with confidence intervals are shown in Figure 16. There is only a small difference in raw and standardised research diver survey indices and the confidence intervals are wide. The raw and standardised research diver survey index for each research diver are shown in Figure 17. Raw and standardised RDSI are very different for diver 5, but the confidence interval almost covers the raw RDSI. Diver 5 did the survey only in the early years when the RDSIs were higher. Divers 2 and 4 had low diver effects but were only part of one or two years of surveys.

The raw and standardised RDSI for each stratum are shown in Figure 18. D'Urville Island and Staircase had higher indices than other strata. Figure 19 shows trends of raw dive survey index for each stratum. In some strata, it shows a small increase in trends, but the average is still lower than early years.

3.4 Commercial catch sampling length frequency data (CSLF)

Length frequencies were measured in samples of shells from the commercial fishery from 1990 to 1994 and 1998 to 2003 (Table 9). As for the commercial length frequency data used for the previous PAU 7 assessment (Breen et al. 2001), the samples were simply added together for each year. It is not possible to stratify the data by catch, because only very coarse area information is available for catches in all but the most recent years.

Data without the area recorded were eliminated from the dataset (all 1998 data were eliminated because of this). Paua from the Cape Campbell (area 18) and West Coast (area 36) strata (Figure 20) tended to be larger than those from the other strata in areas 17 and 38. Because there is no research diver survey sampling in these strata (except for the 2003 fishing year), because historical catches were low in areas 18 and 36, and because the proportions-at-length are very different, the previous assessment was done with data from areas 17 and 38 only, and we have followed that course.

Data from the remaining five strata are consistent with each other (Figure 20), and all have median distributions within a few mm of the MLS, indicating a probable high exploitation rate.

After removal of the data from areas 18 and 36, the data are shown aggregated across strata for each year as cumulative frequencies in Figure 21. The 2001 to 2003 fishing years showed the smallest abundance of large paua.

Data from years within the CSLF dataset were weighted by the square root of numbers greater than MLS measured:

$$w_i^s = \frac{\sqrt{n_i^{paua \geq MLS}}}{\min_i\left(\sqrt{n_i^{paua \geq MLS}}\right)}$$

and this weight was then normalised by the lowest value.

3.5 Research diver survey length frequency data (RDLF)

Length frequencies from diver surveys of paua populations, described by Andrew et al. (2000b), are available from a number of years (Table 10). Sizes varied among strata (Figure 22), so the uneven coverage of strata seen in Table 10 may have contributed to variability in length frequencies between years, as discussed by Andrew et al. (2000b). Years in which the coverage was too sparse to be used are shown in grey in Table 10.

The upper plots of Figure 22 and Figure 23 show that the D'Urville and Northern Faces strata have similar patterns of proportions-at-length, and Perano, Runander, and Staircase strata have similar patterns among themselves. Figure 24 shows that Durville and Northern Faces have higher proportions of lengths below the MLS than the other three strata.

Figure 25 and Figure 26 show markedly fewer large paua in the surveys in 1999, 2001, and 2003 compared with previous surveys. Proportions of paua above the MLS fall rapidly within a few mm of the MLS, indicating strong exploitation rate.

For years with both commercial catch sampling and research diver surveys, Figure 27 and Figure 28 compare the proportions-at-length for the paua above the MLS. There are differences in some years between the patterns seen in the two types of data, especially obvious in the cumulative plots: the research diver surveys tended to find fewer small and more large paua. There is little difference in the 2003 data.

3.6 Growth increment data

This section describes tag-recapture data used for the assessment and describes explorations of the tagging data made outside the model. We describe the raw data, grooming, and experimental fitting with two different growth models.

3.6.1 Methods for tagging

Paua were tagged and recaptured at several sites in PAU 7 at different times by the paua team, and also in PAU 6. Methods are beyond the scope of this report, but basically they were:

- to collect paua with underwater breathing apparatus (UBA) and take them to the surface,
- to tag them with a small numbered plastic tag glued to the shell, to measure the paua to the nearest millimetres,
- to return the paua to the bottom with UBA,
- to place them carefully on the rock surface and ensure they had reattached, then
- to collect the paua as close to the anniversary of tagging as possible and
- to measure them again in the same way as during tagging.

Sites for tagging were chosen for reasons not associated with the assessment, and were probably not a random sample of possible sites.

3.6.2 Raw data

Data were available on spreadsheets of various forms obtained from the paua diving team in four datasets. These are summarised in Table 11.

PAU 6 data were considered because the total PAU 7 dataset is small, it is restricted to areas 17 and 18, there are no data from south of Farewell Spit or Cape Campbell, and PAU 6 is adjacent to PAU 7

on the west coast of the South Island. PAU 6 was thus considered to increase the representativeness of the dataset.

We rejected all recoveries that did not have the dates and lengths at both tagging and recapture, and any with notes indicating they were broken or dead on recapture. We deleted four records with negative increments between -15 and -36 mm, but left other negative increments in the data. We corrected one obvious typo.

Because the model does not represent paua less than 70 mm in length, we removed all records for paua tagged at smaller sizes (176 records, nearly all from D'Urville).

3.6.3 Growth models

For each of the four datasets, we fitted the model of Francis (1988) to the increment data alone, using the two models described in equations (3) and (4) and the likelihoods described in equations (33) and (34).

Both models give the same expected increments for lengths α and β (Figure 29), but the exponential model gives greater expected increments for lengths less than α and greater than β, and smaller increments for lengths between α and β.

We explored two assumptions with respect to the variability of growth. For the first, we assumed normally distributed variation, decreasing as the expected increment decreases but with a minimum value as in equation (5). This was fitted with equations (33) and (34).

The alternative was to assume lognormal variability, again with a c.v. described by the parameter φ. Under this assumption we minimised the negative log-likelihood:

$$-\ln(\mathbf{L}) = \sum \left[\ln\left(\sigma_j^{tag}\right) + 0.5 \left(\frac{\ln\left(d_j / \hat{d}_j\right)}{\sigma_j^{tag}} + 0.5\sigma_j^{tag} \right)^2 \right]$$

where

$$\sigma_j^{tag} = \sqrt{\sigma_{obs}^2 + \left(\sigma_j^d\right)^2}$$

When fitting this model we removed the negative and zero observed increments from the dataset.

3.6.3.1 Methods

We used the simple linear model and assumed normal error to compare the four individual datasets, and to compare two subsets of the D'Urville dataset. Then we developed a combined PAU 7 dataset and made fits with both growth models and both error assumptions and compared these four fits. Parameters estimated from the four datasets, using the linear growth model under the assumption of normally distributed errors, are summarised in Table 13 for each of the four individual datasets, with the total negative log-likelihood.

3.6.3.2 D'Urville

The fit of the simple model to the data was generally good (Figure 30). Two records had large observed increments, leading to normalised residuals of 4 or larger, but after experimentally removing

the record with the largest residual and observing only a small effect on the results, we left these two records in the data.

The data were obtained from three "bay" sites, thought to have stunted paua, and three "headland" sites, thought not to be stunted. We tested whether this idea was correct by fitting to the two sets of sites independently. The results (Table 12) show relatively small differences between the two sets of sites, although the bay sites indeed had smaller growth. The differences are smaller than between-dataset differences (Table 13).

3.6.3.3 Staircase

The Staircase dataset was unusual in that tagged paua were left in the water for nearly two years. The linear model fitted this small dataset well (Figure 31). Two records from paua between 100 and 110 mm had little growth and one normalised residual approached 4, but we considered there was no case to remove them.

3.6.3.4 2001 data

This dataset showed some large increments at small sizes, and one larger than predicted increment at large size that gave a normalised residual of 7. However, the increment does not appear to be so out of pattern as to be called an outlier (Figure 32) and we retained it. Estimated parameters were considerably higher from this dataset (see Table 13) than from the others.

3.6.3.5 PAU 6

We removed an outlier with a negative increment of 9 mm after observing its large effect on results. The increments from PAU 6 were generally smaller than those from the other datasets (Figure 33), reflected in the smaller growth estimates (Table 13). After examining these results we chose not to include these data in the PAU 7 assessment.

3.6.3.6 Combined data

The fit of the simple model to the combined PAU 7 dataset is shown in Figure 34, and the fit of the exponential model in Figure 35. Both figures show the fit when using normal error. The two fits are little different, although with both error structures the linear model fits slightly better, and no outliers are obvious. The growth parameters are similar (Table 14) except that g_a was larger in the exponential fit. Predicted increments for paua larger than 130 mm, i.e. outside the range of the re-capture data, are larger when the exponential model is used.

The fits when using lognormal error rather than normal error were slightly different for each model (Table 14). Lognormal error gave a steeper relation in each case, with larger increments at 75 mm and smaller increments at 120 mm. Distributions of residuals (Figure 36) show reasonable fits for each of the four combinations, and there is little difference in the quality of the q-q plots (Table 14).

3.6.3.7 Discussion of growth explorations

We were cautious in removing suspected outliers. Records with impossibly large negative outliers were removed summarily. We deleted one with an apparent decrease of 9 mm only after inspecting the fit, retained the remaining three negative increments (largest -3 mm), and deleted no large increments. Although some increments seemed unusually large or small on inspection of normalised

residuals in the fits to individual datasets, there was no compelling reason to remove the records, and in the fit to the combined data there was no normalised residual greater than 4.7.

The various datasets show considerable variation in estimated growth parameters (see Table 13). This is much greater than the differences between bays and headlands within the D'Urville dataset (Table 12). Records from PAU 6 were considered, as this area adjoins the western side of PAU 7, but the growth parameters from PAU 6 were clearly smaller than those from any PAU 7 dataset.

The data unfortunately contain few individuals tagged at lengths greater than the minimum legal size (there are few such individuals in PAU 7). Length frequencies from areas 17 and 18 in PAU 7 extend to about 150 mm, so growth of recruited individuals is of high importance to the assessment.

The exercise described above suggested that normal and lognormal error assumptions are both valid, although lognormal error may create a bias because negative and zero observed increments cannot be used. In the assessment, only normal error was used.

3.7 Maturity data

Maturity affects only the model's estimate and projections of spawning biomass. Data were obtained from the paua team in spreadsheet form from one site at Staircase and six sites at D'Urville in March and May 1994. Paua were checked for maturity and for sex if mature. Data were collated in this study as the number examined and the number mature at each 1 mm of length. In all, 178 paua were examined.

The maturity ogive was fitted to the data using equation (29). The best fit is shown in Figure 37. The two maturity parameters were 90.7 and 11.8 mm. The *L50* parameter is well determined by the data.

4. MODEL RESULTS

This section first shows the MPD results from the base case, which was chosen by altering the relative weights for each dataset until the standard deviations of standardised residuals were close to 1.0 for each dataset. Sensitivities to datasets and modelling options were explored by comparing MPD runs.

Next we show diagnostics from each of five McMC chains, each obtained by starting the McMC run at a parameter vector obtained from the likelihood profile on *M*. Then we show the Bayesian fits and residuals from these fits. The MPD does not appear in the chain used to estimate posterior distributions.

The assessment is obtained from the posterior distributions of a set of indicators based on biomass and exploitation rate at three times: the present, at the end of five-year projections, and a reference period, 1985–87. Values are given in a table showing, for each relevant indicator, the minimum and maximum, the 5th and 95th percentiles, and the mean and median.

4.1 MPD results

The base case was obtained with the exponential growth model and after iterative re-weighting (see Table 1). The MPD estimate of *M* was 0.121, slightly larger than the assumed mean of the prior distribution, 0.10. The profile likelihood and the posterior distribution were very similar (Figure 38), and both were much narrower than the prior. This result suggests that the model finds some information about *M* in the data. Probably this information comes from the length distributions: the model estimates growth rates and exploitation rates, and length frequencies are well determined if growth and total mortality are known.

The model fits the observed CPUE reasonably well for the recent years (Figure 39), but shows some pattern, under-estimating a series of data in the late 1980s. The model fits the middle four of the six RDSI data well (Figure 39), and cannot fit the first and last points. This leads to a pattern in the residuals (Figure 40), both over time and against the predicted value.

The model estimated h as 0.62, giving a relation between CPUE and biomass with some hyperstability (Figure 41). This is what one would expect from abalone populations, where divers can maintain high catch rates as the stock is fished down.

Fits to proportions-at-length were reasonably good (Figure 42), and there was no consistent relation between the residuals and length (Figure 43), although there are some patterns near MLS for the commercial catch sampling data. The q-q plot is generally better from the research diver data (Figure 44).

The fit to growth increment data (Figure 45) is generally similar to that obtained when fitting to the tag data only: using the proportions-at-length data causes g_α to increase slightly, g_β to decrease slightly and the c.v. to increase very slightly. There are a few large positive residuals (near 4, Figure 45) but no large negative ones. There are more positive residuals than expected above 1.5 – more animals grew more than expected than grew less.

The fit to maturity data (Figure 46) is also similar to that seen when fitting the maturity data alone.

The q-q plot from all model residuals from all data (Figure 47) is generally good except for positive residuals above 1.5, which are caused by the pattern seen in the tagging increment data (Figure 45).

The expected annual growth increment (Figure 48 top) is curved because the non-linear growth model was used, in turn because it gave a better fit than the linear model. The standard deviation shown is the one predicted from the growth model alone and used in the growth transition matrix. The MPD c.v. of the expected annual growth increment was 0.58.

The midpoint of the research diver selectivity ogive (Figure 48 middle) was 104 mm, and the ogive was broad. The midpoint of the commercial selectivity (Figure 48 bottom) was 123.77 mm, just under the MLS, and this ogive was very narrow.

Sections of the growth transition matrix, based on the expected increments seen in Figure 48, are shown in Figure 49. All individuals remain in the last bin when they reach it.

The model's MPD estimates of recruitment (Figure 50) show a higher than average period in the late 1980s, and a lower than average trend in the late 1990s. The estimate for 2003 is near the average because there is no information in the data about the 2003 recruitment (this value is over-written in projections).

Exploitation rate (Figure 50) increased steadily over the history of the fishery, reached the upper bound of 80% in 2000, decreased slightly, and then hit the bound again in 2003.

The virgin length frequency (Figure 51) has a mode at 131 mm, and a considerable accumulation of individuals in the 171-mm plus group. Recent proportions-at-length have far fewer large paua.

When plotted against the model's spawning biomass two years earlier (Figure 52), recruitment appears to be positively related with spawning biomass. In recent years, both have declined, so this is not good evidence of a stock-recruit relation, but the possible relation should be of concern to managers and stakeholders.

4.2 MPD sensitivity trials

Sensitivity trials on the MPD results are shown in Table 15. Only the MPD results are compared in this table; these must be treated with caution because the shape of posterior distributions could differ among trials despite the MPDs being similar, and conversely. All sensitivity trials had positive definite Hessian matrices.

Removing the RDSI dataset from fitting had almost no effect on anything except the scalar for this index. Removing CPUE data had a larger effect, but parameters and indicators changed very little. The most dramatic effect on indicators occurred when the research diver proportions-at-length were removed. This caused current biomass relative to reference biomass to increase from 14.6% in the base case to 21.4%. Removing the tag data changed the growth parameters considerably: g_α reduced from 16.1 mm in the base case to 6.4 mm; the growth c.v. decreased from 0.575 to 0.156. These changes increased the biomass estimates but not the ratio indicators.

In general, the effects of removing single datasets were not substantial, a result that indicates the assessment is not dependent on any single dataset. The single most influential dataset is probably the tag-recapture dataset, without which the model chooses a quite different growth curve.

Fixing the h parameter to 1.0 resulted in a smaller estimate of B_{av} but a similar estimate for current biomass, so that the ratio of these two increased to 20%. Using the linear growth model gave a lower g_α (13.5 compared with 16.1 mm in the base case), but had little effect on the indicators.

Few of the remaining sensitivity trials had much effect on the MPD results. Using the MLS to control the commercial fishery led to an estimate of M on its upper bound of 0.5, an unrealistic result. Using a lower value for $U^{\max}$ gave more optimistic biomass estimates. Using a contrived vector of illegal catches (from 3 t in 1974 to 25 000 t in 1990) also gave increased biomass estimates and a more optimistic ratio of current to reference biomass.

4.3 McMC results

We examined the chains for each parameter from each of the five McMC runs. Five tests – Raftery and Lewis (1992), Geweke (1992), Heidelberger and Welch (1983), the single chain Gelman, and the Brooks, Gelman & Rubin test (see Gelman & Rubin, 1992 and Brooks & Gelman, 1998) – were used to test the single chains for stationarity and convergence (*see* Brooks & Roberts 1998). The fifth chain, started from minus 3.5 standard deviations from the mode of likelihood profile for M, failed many more tests than the other four chains (Table 16).

Sets of diagnostic plots for the five parameters that failed the Gelman test are shown in Figure 53, Figure 54, Figure 55, Figure 56, and Figure 57. In each figure, the traces look good and the autocorrelation is low after the first few samples except for the fifth chain, and the other diagnostic plots look good except for the fifth chain.

As a result of these various tests we discarded the fifth chain, concatenated the other four chains into a single chain, and based the assessment on those 4000 samples from the joint posterior distribution. No parameter was near its bounds. In Figure 58 we compare the posterior distributions for some indicators from each of the five chains plotted separately. The discarded fifth chain gives posterior distributions that are not substantially different from those of the other four chains, even though the diagnostics suggest that the chain was not converged.

4.4 Marginal posterior distributions and the Bayesian fit

Posterior distributions from the combined chain of 4000 samples are shown in Figure 59 and summarised in Table 17. For all posteriors for which we had an MPD estimate, that estimate fell near the centre of the posterior distribution. The posterior distributions of the standard deviations of the normalised residuals lay between 0.9 and 1.10. This indicates that the relative dataset weights assigned to the MPD remained valid through the McMC procedure.

The posterior distribution of the fit to CPUE shows a some pattern of misfitting (Figure 60): for five years – 1985, 1987, 1989, 1992, and 1999 – the predicted CPUE has a distribution that excludes the observed CPUE. The posterior distributions of normalised residuals (Figure 60) reflect this pattern. The model fits the overall trend in CPUE but cannot track the fine-scale variation, leading to runs of first positive and then negative residuals.

In the posterior distribution of the fit to the RDSI (Figure 61), the model fits the central four data, but posterior distributions of predicted *RDSI* exclude the first and last observed *RDSI* point.

We show the posterior distributions of fits and normalised residuals for only one year's proportion-at-length data. Although the fit to commercial catch sampling data is generally good (Figure 62), the model always over-estimates the proportion immediately below the MLS, and under-estimates the proportion above the MLS. This leads to a strongly persistent pattern in the posterior distributions of normalised residuals (Figure 62, Figure 63).

The fit to the research diver survey data is generally better than the fit to commercial catch sampling data (Figure 64). There is some systematic trend in the posteriors of residuals (Figure 65) for sizes of 130 mm and larger: the model persistently under-estimated the proportions of paua from 130 to 138 mm, and consistently over-estimated the proportions of paua larger than 150 mm. Differences between the proportions from the two types of sampling were seen in the data, especially from earlier years. The model cannot fit both datasets equally well.

The posterior distribution of the Q-Q plot from the tag-recapture residuals (Figure 66) shows that the fit varies little in the McMC simulations. The fit to maturity data (Figure 67) shows considerable uncertainty; this affects only the model's estimated spawning biomass.

The posterior distributions of biomass trajectories (Figure 68) show the most uncertainty in the earliest years, least uncertainty from the 1990s to the present, and increasing uncertainty in the projections. These are generally very tight posteriors. The trajectory for recruited biomass is shown in Figure 69 from 1995 onwards to show the variation on an appropriate scale. The uncertainty is least in 2001–03, and remains low in the early projections, because the exploitation rate jams itself against the upper bound of 80% (Figure 70). That exploitation rate is against the assumed upper bound causes uncertainty for this variable parameter to be under-estimated, and has downstream effects on uncertainty in other quantities.

The exploitation rate trajectory is also tight (upper part of Figure 70) and pressed against the upper bound for 2000 and 2003. In projections, the exploitation rate was squeezed tightly against the upper bound of 80%, indicating that the current catch cannot be taken from the projected future biomass.

The recruitment trajectory (lower part of Figure 70) shows high uncertainty, especially before the 1990s, and an overall trend similar to that seen in the MPD, with a decline in the 1990s.

Surplus production shows a trend that increased to a maximum in 1990 and then declined; this is a tight trajectory (Figure 71). The uncertainty is restricted because of the exploitation rate being against its upper bound: the exploitation rate is thus constrained to a tiny range, in turn biomass is constrained, with catch fixed the production estimate is also constrained. Surplus production was plotted against recruited biomass for a subsample of the parameter vector samples (Figure 72) and shows that maximum productivity may occur between 500 and 1000 t recruited biomass, which corresponds

roughly with the reference level (Table 17). Uncertainty is least at the lowest biomass levels, probably because of the same mechanism that reduced uncertainty around recruited biomass discussed above.

4.5 Assessment of PAU 7

The assessment is summarised in Table 17. It suggests that current mid-season biomass has a median of 98 t, with 5% to 95% intervals of 95–105 t. This range is tight because of the limit on exploitation rate considered possible: for current exploitation rate the model goes to the upper bound of 80% (median 79.9%, 76.7% to 81.2%), so with catch and exploitation rate both fixed, the recruited biomass must be known within a small range. Because 50% of paua are mature at 80–90 mm, well below the MLS, current spawning biomass is much larger, with a median of 604 t, with 5% to 95% intervals of 565–652 t.

The reference biomasses from the period 1985–87 were 664 t (580–753 t) for recruited biomass and 1412 t (1339–1502 t) for spawning biomass. The current recruited biomass has a median of only 15% of the reference biomass (13%–17%). Current spawning biomass has a median of 42.7% of the reference biomass (40%–46%). Thus current biomass is well below reference levels for both recruited and spawning biomass.

In five-year projections using the current catch, the median exploitation rate is 80% (75.1% to 80%). In projections the model truncates the exploitation rate to the assumed maximum of 80%. The median catch actually taken in projections was only 84.9% (77.1%–93.6%) of the current catch. These results suggest that the current TAC will not be caught in the near future.

Recruited biomass in projections declined in 92% of runs, and after five years showed a median value of 80% of current biomass (64.5%–105.4%). Spawning biomass was more optimistic: it increased 59% of the time, and showed a median of 103.1% (81.4–130.9%). In the projections, recruited biomass after five years was lower than the reference level in 100% of runs, and had a median of 12% of the reference level (9%–16%). Projected spawning biomass also remained below reference levels in 100% of runs, with a median of 44% (35%–56%).

4.6 Retrospective analysis

We compared four retrospective analyses: the first used the full dataset, the next eliminated data from 2002, and so on. Only abundance indices and length frequencies were eliminated; we did not eliminate the growth increment data (see Breen et al. 2001). Table 18 shows the summary of data used for this analysis.

We first compared the MPD trajectories of recruited biomass and exploitation rate from each of the four fits (Figure 73). The recruited biomass lay close together after 1990 fishing year. The recruited biomass in early years becomes lower as we remove one year of data from the original dataset, but the pattern of decrease remains the same. The exploitation rate gets higher as we remove one year of data from the original dataset except for the last year of each dataset and the overall trend of the exploitation rate is very similar.

We then compared the posteriors of trajectories (5th, 25th, 50th, 75th, and 95th percentiles) from 3 million McMC simulations made from the MPD from each dataset including the base case (Figure 74 to Figure 76). For recruited biomass, the posterior trajectories lay close together from the late 1980s to the late 1990s (Figure 74). The 2001 to 2003 runs were all similar in their fit through 2000. the last year common to all four. The biomass projections from the 2000 run were then considerably more optimistic than the those from the other three runs.

For the exploitation rate, the 2000 run gave a much lower estimate than the other three runs. Projections differed for all runs, becoming dramatically less optimistic with each additional year of data (Figure 75).

For recruitment, trajectories lay close together except for the 2000 run, which lay well above the others (Figure 76). The pattern of recruitments was similar for all runs.

The retrospectives suggest that the assessment of the state of the stocks is not sensitive to the data, in turn suggesting that bias or model mis-specification are not problems with this assessment. They do, however, suggest that forward projections are sensitive to the last year of data, and that these should therefore be treated with caution.

4.7 McMC sensitivity analysis

We conducted a sensitivity analysis to the value for U_{max} by comparing posteriors from McMCs. As for the retrospectives, we used 3 million simulations started from the MPD for each trial. We compared the base case value for Umax, 80%, with 65% and 95%.

There was no dramatic difference in recruited biomass trajectories using the three values, at least after the mid 1980s (Figure 77). With U_{max} = 65%, a higher function value shows that the model fits the data worse, and it estimates high *ln(R0)* and *M*. Both the spawning and recruited biomass were higher than the base case and the ratios of B_{03} and B_{08} to B_{av} was higher than the base case (Table 19).

The exploitation rate always hit U_{max} in the projection years and the general pattern of the trajectories trend was the same in all three trials (Figure 78).

With U_{max} = 65%, the recruitment in all years was doubled with increased uncertainty and the general trends stayed the same as for U_{max} = 80% or 95% (Figure 79).

4.8 Comparison with previous assessment

When recruited biomass from the base case MPD is converted to biomass at the beginning of the year, it can be compared with the base case MPD biomass trajectory from the 2001 assessment (Figure 80). The two trajectories are very similar, but the current assessment has 20–30% lower recruited biomass for 2000 and 2001. Exploitations rates are similar for the whole period modelled (Figure 81).

Recruitment (Figure 82) is more variable in the 2003 assessment and shows a somewhat steeper recent downward trend. Surplus production curves are similar (Figure 83) (these are both based on start of the year biomass) although somewhat higher in two periods from the current assessment and lower for the most recent years in the current assessment.

The different definitions for spawning and recruited biomass make it difficult to compare McMC results between the 2001 and 2003 assessments. However, both summaries of the posterior distributions (Table 20) suggested that current (2001 or 2003) exploitation rate was very high in both assessments. In both, current biomass estimates were less than the reference biomass estimates, more so in the 2003 assessment. Projections cannot be compared because the starting points are different.

Reasons for the differences are difficult to pinpoint because of the number of changes made to the model and data since 2001. The 2001 decline in CPUE and the recent shifts in length frequencies from both sources towards smaller paua are probably important factors.

4.9 Model projections with alternative catches

At the request of MFish, we made stochastic projections with 11 alternative total catch levels, from the full TACC to 100% reduction in the commercial catch, in 10% reduction increments. It was assumed that other catches would remain at their 2003 values. Medians and 5th and 95th percentiles are shown in Table 21, Table 22 and Table 23 respectively.

Projected exploitation rate decreased as catch level decreased: Figure 84 shows the mean and the 5th and 95th percentiles from the posterior distributions at each level. Exploitation rate at the current catch level has a median value of 80% in 2008 (5th and 95th percentiles 75.1–80%); this diminishes to 12% after an 80% reduction in commercial catch (Table 21).

Projected spawning biomass, compared with current spawning biomass, increased as catch level decreased. Only a slight increase to 103% (81–131%) is expected at the current catch. The percentage of runs with decreased spawning biomass is 41% at the current catch level, decreasing to 6.5% at a 40% reduction in commercial catch. The risk of further declines in recruited biomass drops with decreasing catch at a higher rate than for spawning biomass.

Table 21 shows other indicators, such as projected biomass compared with the reference period, 1985–87. These suggest that rebuilding to the reference levels would take longer than 5 years, even with very severe catch reductions.

These results should allow stakeholders and managers to choose management action.

5. DISCUSSION

The diagnostics for this assessment were mostly favourable. The base case obtained from iterative re-weighting appeared to be a good fit to the various data, and the standardised normal residuals (sdnrs) remained near 1 during the McMCs. The posteriors of fits to proportions-at-length suggest that these data could nonetheless be over-weighted – future assessments should choose their base case from trial McMCs rather than from MPDs.

After fixing the over-parameterised growth model, we experienced no further problems with the Hessian matrix. Sensitivity trials with the MPD indicated no single data set upon which the assessment results depended strongly. The tagging data set was the major basis for the growth parameter estimates, as shown by different estimates when it was removed, but the indicators did not change dramatically when this dataset was removed. McMC runs appeared to be converged except for one chain, which was then discarded, but the posteriors even from that chain were similar to those from the other chains.

The assessment is not an optimistic one, and indicates that the current level of catch is unsustainable. The current exploitation rate is very high (91% if the model is allowed to estimate it; otherwise at the assumed upper bound); consequently the estimated current biomass is very low. [The McMC sensitivity trial on maximum exploitation rate suggested that the assessment results are not dependent on the assumed maximum.] In model projections the current catch is unlikely to be fully caught in the near future, recruited biomass is likely to decline with a high probability, and spawning biomass has a 40% chance of declining further.

The main differences between this assessment and the previous assessment for PAU 7 (Breen et al. unpublished results) are in the behaviour of projections rather than in the way the model assesses the current state of the stock. When results from this assessment and the previous assessment were plotted together, biomass and exploitation rate were very similar through 2000, recruitment showed roughly the same trend in both but was more variable in the current assessment. This may result from better fits to the length frequency data than were obtained in the previous assessment.

These results and the retrospective analysis point to the data, rather than the model, as the source of the difference in the two assessments. Changes to the model appear to result in better fits and perhaps better diagnostics, but would not be expected to cause major differences in the assessment results, and the direct comparisons support this.

The projections from the two assessments cannot be compared directly in the way that biomass trajectories can be compared; they started from different years and were driven by different catches. Retrospective analysis, however, starting from the 2000 data set, shows that adding data causes little change to biomass and exploitation rate trajectories, but causes large changes to projected biomass. Each successive year of data causes projections to be less optimistic, and with the current year's data there is almost no chance that exploitation rate will decrease or that recruited biomass will increase. The major features of the data, possibly accounting for this behaviour, are: a decline in CPUE between 2000 and 2001, a decline in the RDSI between 1999 and 2001, and shifts in both sets of proportion-at-length data towards relatively smaller paua and relatively fewer large paua.

Projections made with alternative total catches suggest that small decreases in catch are likely to have little effect, because the current catch level and slightly reduced catch levels cannot be fully caught in the projections. Stakeholders and managers should be able to determine, from the projection results, what level of catch to permit in light of the risks they identify as important.

As in previous assessments, some cautions must be expressed about the assessment. The model assumptions are simple ones, in light of the limited experimental data, and reality is demonstrably much more complex. Abalone have different population characteristics in populations short distances apart (e.g., Day & Fleming 1992, McShane & Naylor 1995, Worthington & Andrew 1998). Variation in growth is addressed to some extent by having a stochastic growth transition matrix based on increments observed in several different places; similarly the length frequency data are integrated across samples from many places. An open question is whether a model fitted to data aggregated from a large area, within which are smaller populations with different responses to fishing, can make credible estimates of the response of the aggregated sub-populations. The model assumes a unit stock in which abalones have the same growth and mortality characteristics in all parts of the stock, and assumes that abundance indices respond instantly to changes in biomass anywhere in the stock. These are obviously over-simplifications; their consequences could be studied with future simulation testing.

An obvious danger, and a large source of uncertainty in this assessment, is that fishing may cause spatial contraction of populations (e.g., Shepherd & Partington 1995), or that some populations become relatively unproductive after initial fishing (Gorfine & Dixon 2000). Depending on when data have been collected, the model could over-estimate productivity in the population as a whole. Past recruitments estimated by the model might instead have been the result of serial depletion.

In this assessment, estimated recruitment and spawning biomass both decline with time, so that a plot of recruitment against spawning biomass shows a positive relation. Because of the "one-way trip", this is not good evidence for a stock-recruit relation, but the possibility should be of great concern to stakeholders and managers. The result, if there is a relation, is that projections presented here may be too optimistic with respect to future recruitments.

Another large uncertainty comes from the non-commercial catches. Customary and recreational catches are not well estimated, and their historical trends are unknown. The illegal catch estimate of 3 t is certain to be an underestimate. Industry express the concern that commercial catch cuts may simply transfer catch to other sectors. If this happens, model projections are too optimistic.

Previous projections may have been overly optimistic, and the retrospective analysis suggests that projections from this model-data system must be treated with caution, and management decisions made with great care.

Model results point towards a need for more maturity-at-length data and for growth increment data from paua larger than the MLS. The estimated errors around the RDSI are large and thought might be given to how these could be reduced effectively.

6. ACKNOWLEDGMENTS

This work was supported by a contract from the Ministry of Fisheries (PAU2002-01). Thanks to the paua team, Neil Andrew for his support, Vivian Haist for her suggestions, and to David Gilbert, Andre Punt, and an anonymous reviewer for their helpful suggestions on the 2001 assessment publication. Thanks to Andy McKenzie for comments on an earlier version of this report.

7. REFERENCES

Andrew, N.L.; Naylor, J.R.; Kim, S.W. (2002). Fishery independent surveys of paua (*Haliotis iris*) in PAU 5B and PAU 5D. *New Zealand Fisheries Assessment Report 2002/41.* 24 p.

Andrew, N.L.; Breen, P.A.; Naylor, J.R.; Kendrick, T.H.; Gerring, P. (2000a). Stock assessment of paua (*Haliotis iris*) in PAU 7 in 1998-99. *New Zealand Fisheries Assessment Research Report 2000/49.* 40 p.

Andrew, N.L.; Naylor, J.R.; Gerring, P.; Notman, P.R. (2000b). Fishery independent surveys of paua (*Haliotis iris*) in PAU 5B and PAU 5D. *New Zealand Fisheries Assessment Report 2000/3.* 21 p.

Annala, J.H.; Sullivan, K.J.; O'Brien, C.J.; Smith, N.W.McL.; Varian, S.J.A (comps.) (2002). Report from the Fishery Assessment Plenary, May 2002: Stock assessments and yield estimates. Ministry of Fisheries, Wellington. 640 p. (Unpublished report held in NIWA library, Wellington, New Zealand.)

Breen, P.A.; Andrew, N.L.; Kendrick, T.H. (2000a). Stock assessment of paua (*Haliotis iris*) in PAU 5B and PAU 5D using a new length-based model. *New Zealand Fisheries Assessment Report 2000/33.* 37 p.

Breen, P.A.; Andrew, N.L.; Kendrick, T.H. (2000b). The 2000 stock assessment of paua (*Haliotis iris*) in PAU 5B using an improved Bayesian length-based model. *New Zealand Fisheries Assessment Report 2000/48.* 36 p.

Breen, P.A.; Andrew, N.L.; Kim, S.W. (2001). The 2001 stock assessment of paua (*Haliotis iris*) in PAU 7. *New Zealand Fisheries Assessment Report 2001/55.* 53 p.

Breen, P.A.; Kim, S.W.; Starr, P.J.; Bentley, N. (2002). Assessment of the red rock lobsters (*Jasus edwardsii*) in area CRA 3 in 2001. *New Zealand Fisheries Assessment Report 2002/27.* 82 p.

Brooks, S.P.; Gelman, A. (1998). General methods for monitoring convergence of iterative simulations. *Journal of Computational and Graphical Statistics 7 (4)*: 434–455.

Brooks, S.P.; Roberts, G.O. (1998). Convergence assessment techniques for Markov chain Monte Carlo. *Statistics and Computing 8 (4)*: 319–335.

Day, R.W., Fleming, A.E. (1992). The determinants and measurement of abalone growth. *In* 'Abalone of the world: Biology, fisheries and culture'. (Shepherd, S.A.; Tegner, M.J.; Guzman del Proo, S. eds.) pp. 141–168. (Blackwell Scientific: Oxford.)

Francis, R.I.C.C. (1999). The impact of correlations in standardised CPUE indices. New Zealand Fisheries Assessment Research Document 99/42. 30 p. (Unpublished report held in NIWA library, Wellington.)

Francis, R.I.C.C. (1988). Maximum likelihood estimation of growth and growth variability from tagging data. *New Zealand Journal of Marine and Freshwater Research 22*: 42–51.

Gelman, A.; Rubin, D.B. (1992). Inference from iterative simulation using multiple sequences. *Statistical Science 7*: 457–511.

Geweke, J. (1992). Evaluating the accuracy of sampling-based approaches to calculating posterior moments. *In* Bayesian Statistics 4, (Bernardo, J.M.; Berger, J.O.; Dawid, A.P.; Smith, A.F.M. eds.). Clarendon Press, Oxford, UK.

Gorfine, H.K.; Dixon, C.D. (2000). A behavioural rather than resource-focused approach may be needed to ensure sustainability of quota managed abalone fisheries. *Journal of Shellfish Research 19*: 515–516.

Heidelberger, P.; Welch, P. (1983). Simulation run length control in the presence of an initial transient. *Operations Research 31*: 1109–1144.

Kendrick, T.H.; Andrew, N.L. (2000). Catch and effort statistics and a summary of standardised CPUE indices for paua (*Haliotis iris*) in PAU 5A, 5B, and 5D. *New Zealand Fisheries Assessment Report 2000/47.* 25 p.

McShane, P.E.; Mercer, S.F.; Naylor, J.R. (1994). Spatial variation and commercial fishing of the New Zealand abalone (*Haliotis iris* and *H. australis*). *New Zealand Journal of Marine and Freshwater Research 28*: 345–355.

McShane, P.E.; Mercer, S.; Naylor, J.R.; Notman, P.R. (1996): Paua (*Haliotis iris*) fishery assessment in PAU 5, 6, and 7. New Zealand Fisheries Assessment Research Document 96/11. 35 p. (Unpublished report held in NIWA library, Wellington.)

McShane, P.E.; Naylor, J R. (1995). Small-scale spatial variation in growth, size at maturity, and yield- and egg-per-recruit relations in the New Zealand abalone *Haliotis iris*. *New Zealand Journal of Marine and Freshwater Research 29:* 603–612.

Murray, T.; Akroyd, J. (1984). The New Zealand paua fishery: An update and review of biological considerations to be reconciled with management goals. N.Z. Min. Agric. Fisheries Research Centre Internal Report 5. 25 p. (Unpublished report held in NIWA library, Wellington.).

Raftery, A.L.; Lewis, S. (1992). How many iterations in the Gibbs sampler? *In* Bayesian Statistics 4, (Bernardo, J.M.; Berger, J.O.; Dawid, A.P.; Smith, A.F.M. eds.). Clarendon Press, Oxford, UK.

Schiel, D.R. (1989). Paua fishery assessment 1989. NZ Fishery Assessment Research Document 89/9: 20 p. (Unpublished report held in NIWA library, Wellington, New Zealand.)

Schiel, D.R.; Breen, P.A. (1991). Population structure, ageing and fishing mortality of the New Zealand abalone *Haliotis iris*. *Fishery Bulletin 89*: 681–691.

Schiel, D.R. (1992). The paua (abalone) fishery of New Zealand. *In* 'Abalone of the world: Biology, fisheries and culture'. (Shepherd, S.A.; Tegner, M.J.; Guzman del Proo, S. eds.) pp. 427–437 (Blackwell Scientific: Oxford.)

Shepherd, S.A.; Partington, D. (1995). Studies on Southern Australian abalone (genus *Haliotis*). XVI. Recruitment, habitat and stock relations. *Marine and Freshwater Research 46:* 669–680.

Vignaux, M. (1993). Catch per unit of effort (CPUE) analysis of the hoki fishery, 1987–92. New Zealand Fisheries Assessment Research Document 93/14: 23 p. (Unpublished report held in NIWA library, Wellington.)

Worthington, D.G., and Andrew, N.L. (1998). Small-scale variation in demography and its implications for an alternative size limit in the fishery for blacklip abalone (*Haliotis rubra*) in New South Wales, Australia. *In* 'Proceedings of the North Pacific Symposium on Invertebrate Stock Assessment and Management'. (Jamieson, G.S.; Campbell, A. eds.) pp. 341–348. *Canadian Special Publication of Fisheries and Aquatic Sciences 125.*

Table 1: Relative dataset weights and the standard deviations of normalised residuals in the base case. CSLF: catch sampling length frequencies; RDLF: research diver survey length frequencies.

			proportions-at-length			
data	**CPUE**	**RDSI**	**CSLF**	**RDLF**	**tags**	**maturity**
weights	0.056	0.083	36.4	59	-	1.734
sdnrs	0.997	0.998	0.997	1.002	1.068	0.999

Table 2: The lower and upper bounds, prior type (0 - uniform, 1- normal, 2 - lognormal), mean and standard deviation of the prior for each parameter in the base case.

Parameter	**lower bound**	**upper bound**	**prior type**	**prior mean**	**standard deviation**
$\tilde{\sigma}$	0.01	1	0	-	-
$\ln(R0)$	5	50	0	-	-
M	0.01	0.5	2	0.1	0.35
T_{50}	70	125	0	-	-
T_{95-50}	0.001	50	0	-	-
D_{50}	70	145	0	-	-
D_{95-50}	0.01	50	0	-	-
L_{50}	70	145	0	-	-
L_{95-50}	1	50	0	-	-
$\ln(q^I)$	-30	0	0	-	-
$\ln(q^J)$	-30	0	0	-	-
g_α	1	50	0	-	-
g_β	0.01	50	0	-	-
ϕ	0.001	1	0	-	-
h	0.01	2	0	-	-
ε	-2.3	2.3	1	0	0.4

Table 3: Catch data (kg) used in the PAU 7 assessment. "Source" gives the source for the commercial catch estimates ("Comm."). "Rec.": recreational catch; "Custom.": customary catch. The shaded area shows the years for which all catch in PAU 7 was assumed to be from areas 17 and 38. The percentage of catch in areas 17 and 38 was estimated for 2003 as the mean of the previous five years.

Source	Fishing year	PAU 7 Comm.	CELR/ QMR	% 17+38	Comm. 17 & 38	Rec.	Illegal	Custom.	Total
Murray & Akroyd	1974	147440		100.0%	147440	5000	3000	15000	170440
(1984)	1975	197910		100.0%	197910	5423	3000	15000	221333
	1976	141880		100.0%	141880	5846	3000	15000	165726
	1977	242730		100.0%	242730	6269	3000	15000	266999
	1978	201170		100.0%	201170	6692	3000	15000	225862
	1979	304570		100.0%	304570	7115	3000	15000	329685
	1980	223430		100.0%	223430	7538	3000	15000	248968
Schiel	1981	490000		100.0%	490000	7962	3000	15000	515962
(1992)	1982	370000		100.0%	370000	8385	3000	15000	396385
	1983	400000	52.4%	100.0%	400000	8808	3000	15000	426808
	1984	330000	82.9%	100.0%	330000	9231	3000	15000	357231
	1985	230000	75.3%	100.0%	230000	9654	3000	15000	257654
Averaged	1986	236090	38.0%	100.0%	236090	10077	3000	15000	264167
Schiel	1987	242180	45.3%	100.0%	242180	10500	3000	15000	270680
(1992)	1988	248530	25.1%	100.0%	248530	10923	3000	15000	277453
MFish	1989	246029	24.6%	100.0%	246029	11346	3000	15000	275375
	1990	267052	80.2%	99.8%	266509	11769	3000	15000	296279
	1991	273253	82.9%	98.4%	268782	12192	3000	15000	298975
	1992	268309	93.2%	93.1%	249789	12615	3000	15000	280404
	1993	264802	90.8%	96.3%	255045	13038	3000	15000	286084
	1994	255472	100.5%	97.2%	248285	13462	3000	15000	279746
	1995	247108	103.5%	96.1%	237571	13885	3000	15000	269456
	1996	268742	91.9%	90.1%	242057	14308	3000	15000	274365
	1997	267594	91.4%	86.2%	230570	14731	3000	15000	263300
	1998	266655	89.1%	81.9%	218479	15154	3000	15000	251633
	1999	265050	86.9%	86.5%	229198	15577	3000	15000	262775
	2000	264642	110.6%	75.0%	198419	16000	3000	15000	232419
	2001	215920	120.4%	65.2%	140731	16423	3000	15000	175154
	2002	187152	98.4%	74.1%	138721	16846	3000	15000	173567
TACC	2003	187240		76.5%	143307	17269	3000	15000	178576

Table 4: The order in which variables were selected into the GLM model of CPUE and their cumulative effect on the model r^2 for PAU 7.

5-year vessels all areas		5-year vessels areas 17 & 38		All vessels areas 17 & 38	
Variable	**Model r^2**	**Variable**	**Model r^2**	**Variable**	**Model r^2**
Vessel	0.317	Vessel	0.333	Vessel	0.426
Year	**0.396**	Year	**0.420**	Year	**0.476**
Area	0.404	Month	0.425	Month	0.478
Month	0.410	Area	0.427	Area	0.479

Table 5: Standardised CPUE indices for all areas and for areas 17 & 38.

	5-year vessels all areas		5-year vessels areas 17 & 38		All vessels areas 17 & 38	
Year	**Year effect**	**SE**	**Year effect**	**SE**	**Year effect**	**SE**
1983	1.753	0.038	1.780	0.037	1.707	0.031
1984	1.580	0.033	1.606	0.033	1.693	0.028
1985	1.640	0.037	1.667	0.036	1.678	0.031
1986	1.371	0.044	1.397	0.043	1.493	0.038
1987	1.556	0.045	1.589	0.044	1.381	0.037
1988	1.262	0.053	1.376	0.053	1.478	0.047
1989	1.224	0.049	1.256	0.048	1.210	0.041
1990	0.977	0.027	1.000	0.026	1.035	0.024
1991	0.988	0.024	1.000	0.024	1.012	0.022
1992	0.865	0.024	0.860	0.024	0.858	0.021
1993	1.017	0.026	1.026	0.025	1.000	0.022
1994	0.978	0.027	0.992	0.027	0.999	0.024
1995	0.919	0.026	0.920	0.026	0.943	0.023
1996	0.949	0.025	0.950	0.026	0.926	0.023
1997	0.838	0.025	0.828	0.026	0.824	0.023
1998	0.834	0.025	0.812	0.026	0.811	0.024
1999	0.881	0.026	0.868	0.028	0.864	0.025
2000	0.630	0.025	0.604	0.027	0.603	0.023
2001	0.495	0.026	0.443	0.029	0.462	0.024
2002	0.480	0.025	0.458	0.027	0.443	0.023

Table 6: Summary of research diver survey data - showing the number of timed swim surveys made in each stratum in each year (a) and each month in each year (b). The shaded area shows data from Cape Campbell that was not used, and which do not appear in the lower tables. The mean of ln(index) is shown by diver in (c) and by stratum in (d).

(a)

Count	Stratum						
Real fishing year	**D'Urville**	**Northern Faces**	**Perano**	**Runnunder**	**Staircase**	**Campbell**	
1993	29	28					
1994			30	32			
1995		30		4	4		
1996	24		30	44	6		
1999	40	38	40	40	10		
2001	40	32	32	32	9		
2003	30	30	30	30	12	30	

(b)

Count	Month									
Fishing year	**10**	**11**	**12**	**1**	**2**	**3**	**4**	**5**	**6**	**8**
1993							57			
1994	62									
1995								38		
1996		30				30			44	
1999		40		78				42		8
2001			85		60					
2003			40	50	42					

(c)

Average	Divers							
Fishing year	**1**	**2**	**3**	**4**	**5**	**6**	**7**	**8**
1993					3.67		3.57	3.28
1995					3.93		4.19	3.93
1996		2.52		2.47	4.49		3.95	3.63
1999			3.73	3.50		3.31	3.11	4.20
2001						3.39	3.18	3.62
2003	3.54		3.42			3.84	3.73	3.55

(d)

Average	Stratum				
Fishing year	**D'Urville**	**Northern Faces**	**Perano**	**Runnunder**	**Staircase**
1993	4.3	3.3	2.9	3.8	
1995		4.3		3.3	2.8
1996	5.0		3.3	2.7	4.6
1999	4.0	3.9	2.9	2.4	4.1
2001	3.7	3.7	2.9	3.0	3.9
2003	4.0	3.6	3.3	3.7	3.8

Table 7: The order in which variables were selected into the GLM model of RDSI and their cumulative effect on the model r^2 for PAU 7.

Variable	Model r^2
Stratum	0.1404
Diver	0.1663
Fishing year	0.1846

Table 8: Standardised RDSI.

Fishing year	Index	SE
1993	0.943	0.112
1995	1.211	0.172
1996	1.225	0.123
1999	0.829	0.099
2001	0.756	0.098
2003	1.140	0.116

Table 9: Numbers of paua measured in commercial catch sampling, by year and stratum.

Stratum	1990	1991	1992	1993	1994	1999	2000	2001	2002	2003
Cape Campbell		2837	655	1623	924	95	424	773	618	792
D'Urville	2990	4861	1988	2475	1715	1055	218	299	170	445
Northern Faces	1736	4716	6771	1879	322	3295	634	875	244	1003
Perano					2490	143	1027	710	1533	826
Runander				642	1696	705	3073	1582	1916	1870
Staircase				2342	2529		218		931	239
West Coast			643				409	705		189

Table 10: Numbers of paua measured in research diver surveys, by year and stratum. Years shown in grey have coverage too sparse to be used in the assessment.

Stratum	1983	1990	1992	1993	1995	1996	1999	2001	2003
Durville	20	335		1717		1623	2078	1679	1620
Northern Faces		526		63	2829		1716	1162	1019
Perano			616	694		677	663	583	747
Runander		53	786	1135	106	785	693	657	858
Staircase		128			492	491	530	432	438
Cape Campbell									178

Table 11: Summary of tag-recapture datasets discussed in this report.

Dataset	Tagged between	and	Tagged	Recovered	Retained after grooming	Sites
D'Urville	12-Jul-93	17-Jul-93	?	508	331	6
Staircase	?	?	?	48	45	?
2000 series	13-Apr-00	26-May-00	2864	342	341	5
PAU 6	14-Feb-95	30-Jan-96	979	155	143	2
all PAU 7					718	

Table 12: Growth estimates from the linear growth model to the two sets of sites within the D'Urville dataset.

	g_α	g_β	φ	-ln(L)
All sites	13.98	6.86	0.48	620.24
Bays	13.09	6.29	0.56	372.12
Headlands	15.13	7.87	0.37	237.70

Table 13: Summary of parameter estimates from the four tag-recapture datasets. Values for α and β were set at 75 and 100 mm shell length.

Dataset	g_α	g_β	φ	-ln(L)
D'Urville	14.0	6.9	0.481	620.2
2001	21.4	12.8	0.545	701.6
Staircase	14.7	7.5	0.204	91.2
PAU 6	9.6	6.0	0.800	266.0

Table 14: Estimates from fitting each of the two growth models with normal and lognormal error. r is the correlation coefficient between expected and observed quantiles of the normalised residuals .

model	error	g_α	g_β	v	-ln(L)	r
linear	**normal**	14.546	10.139	0.552	1481.4	0.98026
linear	**lognormal**	15.941	10.550	0.630	-34.0	0.97894
exponential	**normal**	15.270	9.861	0.558	1491.5	0.97537
exponential	**lognormal**	17.529	10.028	0.636	-28.1	0.97424

Table 15: MPD results from the base case (column 2) and from sensitivity trials described in the text. RDSI: research diver survey index, CSLF: commercial catch sampling length frequencies, RDLF: research diver survey length frequencies; sdnrs: standard deviations of the normalised residuals.

	Base case	No CPUE	No RDSI	No CSLF	No RDLF	No Tags	No maturity	$h = 1.0$	Linear growth
sdnrs									
CPUE	1.00	4.71	1.00	1.07	0.94	1.25	1.00	1.65	0.92
RDSI	1.00	1.01	1.01	1.02	0.50	1.14	1.00	0.96	0.96
CSLF	1.00	1.00	1.00	1.61	1.01	0.95	1.00	0.97	1.00
RDLF	1.00	1.00	1.00	0.99	3.96	1.01	1.00	0.97	1.01
tags	1.07	1.07	1.07	1.03	1.05	5.11	1.07	1.06	1.07
maturity	1.00	1.00	1.00	1.03	1.03	1.11	2.59	0.95	0.94
Parameters									
$\tilde{\sigma}$	0.188	0.188	0.188	0.182	0.182	0.170	0.188	0.197	0.200
$\ln(R0)$	14.33	14.39	14.34	14.30	14.65	14.60	14.33	14.39	14.36
M	0.121	0.129	0.122	0.120	0.155	0.104	0.121	0.136	0.114
T_{50}	104.09	104.57	104.06	102.06	103.14	110.93	104.09	105.29	102.79
T_{95-50}	31.16	31.30	31.19	25.53	0.50	28.15	31.16	30.89	23.81
D_{50}	123.77	123.77	123.77	124.27	123.73	123.98	124	123.77	123.63
D_{95-50}	2.55	2.56	2.55	2.51	2.40	2.93	3	2.56	2.41
L_{50}	88.44	88.44	88.44	88.44	88.44	88.44	107.22	88.44	88.44
L_{95-50}	15.50	15.50	15.50	15.50	15.50	15.49	25.88	15.50	15.50
$\ln(q^1)$	-8.12	-15.00	-8.12	-7.59	-8.45	-8.81	-8.12	-12.87	-8.23
$\ln(q^J)$	-15.05	-15.05	-15.00	-15.09	-15.24	-15.27	-15.05	-15.03	-15.07
g_α	16.11	16.09	16.11	15.98	15.93	6.43	16.11	16.00	13.48
g_β	5.52	5.52	5.52	5.74	5.95	4.22	5.52	5.68	5.72
φ	0.575	0.575	0.575	0.581	0.560	0.156	0.575	0.569	0.570
σ_{MIN}	1.00	1.00	1.00	1.00	1.00	1.00	1.00	1.00	1.00
σ_{obs}	0.25	0.25	0.25	0.25	0.25	0.25	0.25	0.25	0.25
h	0.62	1.01	0.62	0.58	0.65	0.66	0.62	1	0.63
****Likelihoods****									
CPUE	-16.94	4146.27	-16.90	-16.15	-18.72	-13.29	-16.93	1.23	-17.27
RDSI	0.58	0.64	0.76	0.54	-1.88	0.91	0.58	0.64	0.69
CSLF	-897.20	-897.09	-897.13	-673.73	-904.93	-939.85	-897.20	-890.92	-878.24
RDLF	-981.87	-982.87	-982.12	-993.22	810.99	-1004.10	-981.88	-977.81	-965.27
Tags	2177.89	2177.74	2177.93	2167.90	2163.91	17196.90	2177.91	2172.16	2159.15
Maturity	-5.78	-5.78	-5.78	-5.73	-5.72	-5.35	169.30	-5.73	-5.69
Prior on M	0.02	0.13	0.03	0.00	0.65	-0.12	0.02	0.26	-0.06
Prior on ε	8.07	8.19	8.14	9.06	6.75	10.75	8.07	8.88	8.12
U^{max} penalty	0.18	0.15	0.19	0.70	0.13	0.00	0.18	0.07	0.66
Total	284.96	301.11	284.36	1163.11	1240.20	-1951.04	290.74	308.79	302.09
Indicators									
maxRdev	156.5%	160.0%	156.3%	188.4%	156.8%	172.5%	156.5%	153.3%	141.3%
minRdev	47.9%	46.5%	47.6%	42.0%	45.4%	45.1%	47.9%	47.6%	38.7%
U_{03}	80.3%	80.2%	80.3%	80.3%	63.6%	71.3%	80.3%	80.1%	80.2%

B0	3273780	3111230	3263570	3368390	2963680	3472530	3273900	2855530	3112940
B_{av}	664177	583349	663593	774675	628836	765265	664224	486707	652572
$B_{2003.5}$	97178	97199	97113	106748	134336	114632	97177	98455	96416
$B_{2003.5}$/B0	3.0%	3.1%	3.0%	3.2%	4.5%	3.3%	3.0%	3.4%	3.1%
$B_{2003.5}/B_{av}$	14.6%	16.7%	14.6%	13.8%	21.4%	15.0%	14.6%	20.2%	14.8%

Table 15: ***continued.***

	Base case	beta=110	beta=130	Cauchy prior	fixed Commfish	Emax=0.7	sigmaEps 0.2	sigmaEps 0.6	increasing C illegal
sdnrs									
CPUE	1.00	1.00	1.00	1.00	1.16	1.06	0.98	1.00	1.00
RDSI	1.00	1.00	1.00	1.00	1.09	0.97	0.95	1.01	0.88
CSLF	1.00	1.00	1.00	1.00	1.04	0.99	0.99	1.00	1.00
RDLF	1.00	1.00	1.00	1.00	0.96	1.01	1.02	1.00	1.00
tags	1.07	1.07	1.07	1.07	1.02	1.08	1.07	1.07	1.06
maturity	1.00	1.00	1.00	1.00	0.89	1.00	0.99	1.00	1.00
Parameters									
$\tilde{\sigma}$	0.188	0.188	0.188	0.188	0.211	0.188	0.190	0.188	0.189
$\ln(R0)$	14.33	14.33	14.33	14.29	16.88	14.49	14.24	14.51	14.55
M	0.121	0.121	0.121	0.118	0.500	0.131	0.117	0.133	0.137
T_{50}	104.09	104.09	104.09	103.81	116.15	102.39	103.97	104.87	106.68
T_{95-50}	31.16	31.16	31.16	31.09	24.63	29.44	30.63	31.43	31.88
D_{50}	123.77	123.77	123.77	123.77	124.00	123.71	123.77	123.78	123.80
D_{95-50}	2.55	2.55	2.55	2.55	2.00	2.39	2.53	2.56	2.59
L_{50}	88.44	88.44	88.44	88.44	88.44	88.44	88.44	88.44	88.44
L_{95-50}	15.50	15.50	15.50	15.50	15.50	15.50	15.50	15.50	15.50
$\ln(q^1)$	-8.12	-8.12	-8.12	-8.10	-6.69	-8.72	-8.22	-8.00	-8.77
$\ln(q^2)$	-15.05	-15.05	-15.05	-15.05	-15.49	-15.21	-15.05	-15.05	-15.16
g_α	16.11	16.11	16.11	16.11	15.39	16.56	16.20	16.07	16.01
g_β	5.52	7.00	4.35	5.51	5.53	5.07	5.56	5.52	5.62
φ	0.575	0.575	0.575	0.575	0.614	0.592	0.568	0.576	0.572
σ_{MIN}	1.00	1.00	1.00	1.00	1.00	1.00	1.00	1.00	1.00
σ_{obs}	0.25	0.25	0.25	0.25	0.25	0.25	0.25	0.25	0.25
h	0.62	0.62	0.62	0.62	0.50	0.66	0.63	0.61	0.67
****Likelihoods****									
CPUE	-16.94	-16.94	-16.94	-16.98	-10.97	-15.72	-17.03	-16.94	-16.94
RDSI	0.58	0.58	0.58	0.57	1.85	0.43	0.39	0.65	-0.09
CSLF	-897.20	-897.20	-897.20	-897.24	-679.81	-899.71	-896.59	-897.35	-895.69
RDLF	-981.87	-981.87	-981.87	-981.99	-963.75	-981.43	-976.05	-983.45	-981.79
Tags	2177.89	2177.89	2177.89	2178.21	2173.17	2200.30	2177.23	2177.52	2174.00
Maturity	-5.78	-5.78	-5.78	-5.78	-5.41	-5.78	-5.78	-5.78	-5.78
Prior on M	0.02	0.02	0.02	0.10	10.44	0.16	-0.03	0.19	0.27
Prior on ε	8.07	8.07	8.07	8.04	31.04	9.29	0.69	16.92	6.20
U^{max} penalty	0.18	0.18	0.18	0.18	0.00	2.15	0.32	0.16	0.13
Total	284.96	284.96	284.96	285.12	556.57	309.68	283.15	291.92	280.32
Indicators									

maxRdev	156.5%	156.5%	156.5%	160.2%	591.2%	155.0%	157.0%	148.4%	147.9%											
minRdev	47.9%	47.9%	47.9%	48.9%	29.6%	43.5%	59.3%	36.9%	50.0%											
U_{03}	80.3%	80.3%	80.3%	80.3%	72.5%	70.3%	80.1%	80.3%	80.3%											
B_{av}	3273780	3273780	3273780	3323560	1133670	3143950	3236110	3308090	3289350											
$B_{2003.5}$	664177	664177	664177	667455	1126600	718557	643946	687282	703894											
$B_{2003.5}$/B0	97178	97178	97178	97145	156985	119511	97364	97197	118877											
$B_{2003.5}/B_{av}$	3.0%	3.0%	3.0%	2.9%	13.8%	3.8%	3.0%	2.9%	3.6%											
B_{av}	14.6%	14.6%	14.6%	14.6%	13.9%	16.6%	15.1%	14.1%	16.9%											

Table 16: Convergence diagnostics from five McMC chains described in the text. An asterisk indicates that the test statistic was significantly different (P=0.05) from that indicating convergence. RL: Raftery & Lewis; HW: Heidleberger & Welsh; BGR: Brooks, Gelman and Rubin tests.

	RL					Geweke					HW					Gelman				
	1	2	3	4	5	1	2	3	4	5	1	2	3	4	5	1	2	3	4	5 BGR
f						*	*		*		*	*		*	*	*			*	
ln($R0$)						*		*		*					*					*
$\tilde{\sigma}$							*													
M								*		*					*					*
g_α										*										
g_β										*					*					*
T_{50}								*		*					*					*
T_{95-50}						*									*					*
D_{50}								*		*										
D_{95-50}										*					*					
L_{50}																				
L_{95-50}								*		*										
φ															*					
$\ln(q^1)$						*														
$\ln(q^J)$															*					
h						*														
U_{08}																				
S_{av}						*		*		*					*					*
$S_{2003.5}$						*		*		*		*			*					*
$S_{2008.5}$										*										
B_{av}																				
$B_{2003.5}$								*		*		*	*							*
$B_{2008.5}$										*										
$S_{2003.5}/S_{av}$								*		*					*					*
$S_{2008.5}/S_{av}$																				
$S_{2008.5}/S_{2003.5}$							*													
$B_{2003.5}/B_{av}$								*		*										
$B_{2008.5}/B_{av}$							*			*										
$B_{2008.5}/B_{2003.5}$																				
PCatindex								*		*										

Table 17: Summary of the marginal posterior distributions from the combined four chains from the base case for PAU 7. The columns show the minimum values observed in the 4000 samples, the maxima, the 5th and 95th percentiles, and the means and medians.

	min	0.05	median	mean	0.95	max
f	284.97	300.28	307.27	307.50	315.58	327.97
$\ln(R0)$	13.88	14.09	14.33	14.33	14.58	14.82
$\tilde{\sigma}$	0.172	0.183	0.192	0.192	0.202	0.215
M	0.091	0.104	0.123	0.123	0.145	0.167
g_α	14.26	15.28	16.04	16.04	16.84	17.87
g_β	5.07	5.26	5.46	5.46	5.65	5.87
T_{50}	98.41	101.90	104.32	104.39	107.13	110.25
T_{95-50}	23.77	27.95	31.76	31.93	36.51	42.67
D_{50}	123.58	123.69	123.78	123.78	123.87	123.94
D_{95-50}	2.11	2.35	2.56	2.56	2.76	2.98
L_{50}	80.69	86.35	88.26	88.20	89.83	91.52
L_{95-50}	9.04	12.27	16.11	16.41	21.45	32.10
φ	0.53	0.56	0.59	0.59	0.62	0.66
$\ln(q^I)$	-10.30	-9.15	-8.12	-8.14	-7.17	-6.12
$\ln(q^J)$	-15.43	-15.24	-15.06	-15.06	-14.87	-14.70
h	0.466	0.550	0.624	0.625	0.704	0.795
U_{03}	71.0%	76.7%	79.9%	79.5%	81.2%	82.3%
U_{08}	52.6%	75.1%	80.0%	79.4%	80.0%	80.0%
S_{av}	1262	1339	1412	1415	1502	1643
$S_{2003.5}$	517	565	604	606	652	729
$S_{2008.5}$	365	488	624	632	797	1073
B_{av}	440	580	664	665	753	835
$B_{2003.5}$	92	95	98	99	105	118
$B_{2008.5}$	52	63	79	81	104	177
$S_{2003.5}/S_{av}$	37.8%	40.2%	42.7%	42.8%	45.7%	50.3%
$S_{2008.5}/S_{av}$	26.2%	34.6%	44.2%	44.7%	56.0%	76.1%
$S_{2008.5}/S_{2003.5}$	60.5%	81.4%	103.1%	104.4%	130.9%	176.1%
$B_{2003.5}/B_{av}$	11.4%	13.0%	14.9%	15.0%	17.3%	23.9%
$B_{2008.5}/B_{av}$	7.3%	9.3%	11.9%	12.2%	16.2%	27.2%
$B_{2008.5}/B_{2004.5}$	53.6%	64.5%	79.7%	81.6%	105.4%	173.7%
PCatindex	71.6%	77.1%	84.9%	85.1%	93.6%	100.0%
Percentage	**indicators**					
$S_{2008.5}<S_{2003.5}$	41.4%					
$S_{2008.5}<S_{av}$	100.0%					
$B_{2008.5}<B_{2003.5}$	92.1%					
$B_{2008.5}<B_{av}$	100.0%					

Table 18: Number of data in each dataset for each retrospective analysis. Each column heading represents the last year of data included.

	2003	2002	2001	2000
CPUE	20	20	19	18
RDSI	6	5	5	4
CSLF	10	9	8	7
RDLF	6	5	5	4

Table 19: Comparison of parameters and indicators based on posterior distributions from the sensitivity trial using different values for $U^{\max}$.

	Base case			65%			98%		
	0.05	**median**	**0.95**	**0.05**	**median**	**0.95**	**0.05**	**median**	**0.95**
f	299.35	305.64	313.45	346.83	353.70	362.10	295.28	301.77	310.07
$\ln(R0)$	14.13	14.32	14.54	14.49	14.99	15.36	14.03	14.25	14.49
$\tilde{\sigma}$	0.183	0.192	0.202	0.184	0.194	0.205	0.184	0.193	0.204
M	0.107	0.122	0.138	0.132	0.195	0.240	0.102	0.120	0.140
g_α	15.23	16.03	16.86	15.79	16.63	17.50	15.02	15.77	16.58
g_β	5.25	5.45	5.64	4.71	4.94	5.14	5.45	5.70	5.96
T_{50}	101.74	104.19	106.85	101.14	106.17	110.22	102.27	105.24	108.66
T_{95-50}	27.93	31.73	36.61	27.05	30.41	34.58	29.59	34.07	40.41
D_{50}	123.70	123.78	123.86	123.63	123.73	123.82	123.75	123.84	123.94
D_{95-50}	2.35	2.55	2.76	2.17	2.39	2.61	2.48	2.70	2.93
L_{50}	86.33	88.22	89.86	86.31	88.26	89.88	86.29	88.24	89.81
L_{95-50}	12.41	16.03	21.39	12.36	16.06	21.11	12.39	16.20	21.30
φ	0.56	0.59	0.62	0.58	0.61	0.64	0.55	0.58	0.62
$\ln(q^1)$	-9.12	-8.14	-7.19	-10.05	-8.88	-7.77	-8.72	-7.75	-6.83
$\ln(q^J)$	-15.25	-15.06	-14.88	-15.46	-15.27	-15.08	-15.15	-14.95	-14.75
h	0.552	0.625	0.702	0.584	0.670	0.760	0.527	0.600	0.675
U_{03}	76.7%	79.9%	81.2%	61.6%	64.9%	66.3%	84.5%	91.1%	97.1%
U_{08}	76.0%	80.0%	80.0%	61.5%	65.0%	65.0%	91.2%	98.0%	98.0%
S_{av}	1340	1412	1497	1667	1938	2237	1253	1330	1421
$S_{2003.5}$	564	602	651	716	806	904	473	522	581
$S_{2008.5}$	486	624	791	624	828	1068	416	547	727
B_{av}	585	668	751	680	781	898	552	638	728
$B_{2003.5}$	95	98	105	131	135	146	70	78	90
$B_{2008.5}$	63	79	102	91	112	140	39	50	72
$S_{2003.5}/S_{av}$	40.0%	42.6%	45.6%	38.3%	41.6%	45.3%	35.8%	39.2%	43.1%
$S_{2008.5}/S_{av}$	34.5%	44.1%	56.0%	33.2%	42.7%	54.0%	31.3%	41.1%	54.5%
$S_{2008.5}/S_{2003.5}$	81.2%	103.3%	130.2%	80.1%	102.8%	128.6%	80.3%	104.6%	137.5%
$B_{2003.5}/B_{av}$	13.1%	14.8%	17.1%	15.1%	17.4%	20.3%	10.4%	12.3%	14.8%
$B_{2008.5}/B_{av}$	9.2%	11.8%	15.8%	11.2%	14.3%	18.6%	5.8%	7.8%	11.6%
$B_{2008.5}/B_{2004.5}$	64.6%	79.8%	103.3%	67.1%	82.0%	102.3%	48.5%	63.8%	91.3%
PCatindex	76.9%	84.7%	93.3%	79.5%	87.4%	95.9%	69.7%	79.4%	91.3%
$S_{2008.5}<S_{2003.5}$	41.0%			42.7%			40.3%		
$S_{2008.5}<S_{av}$	100.0%			100.0%			100.0%		
$B_{2008.5}<B_{2003.5}$	92.9%			93.5%			97.3%		
$B_{2008.5}<B_{av}$	100.0%			100.0%			100.0%		

Table 20: Comparison of some key indicators based on posterior distributions from the 2001 and 2003 assessments. "Current" refers to 2003 for the 2003 assessment and 2001 for the 2001 assessment. Biomass is start of the year biomass for the 2001 assessment, and mid-season biomass for the 2003 assessment.

	2001			2003		
	5%	median	95%	5%	median	95%
U_{01}	54.0%	71.0%	84.0%			
U_{03}				76.7%	79.9%	79.5%
current B/B_{av}	36.7%	46.2%	60.4%	13.0%	14.9%	15.0%
current S/S_{av}	54.7%	82.4%	124.6%	40.2%	42.7%	42.8%

Table 21: Medians of posterior distributions of derived parameters generated from the base case assessment of PAU 7 for 11 alternative TACC levels for projections to 2008, including the current catch of 179t. B is recruited biomass, S is spawning biomass, U is exploitation rate. Values for the first seven indicators are the medians of 4000 samples from the McMC simulations. Percentages indicated for the last four indicators are the percentage of the 4000 samples in which the indicator was true.

TACC cut	0%	10%	20%	30%	40%	50%	60%	70%	80%	90%	100%
Projected Catch (t)	179	164	150	136	121	107	93	78	64	50	35
U_{08} (%)	80.0	80.0	76.3	54.4	39.9	29.9	22.5	16.8	12.3	8.6	5.6
$S_{2003.5}/S_{av}$(%)	42.7	42.7	42.7	42.7	42.7	42.7	42.7	42.7	42.7	42.7	42.7
$S_{2008.5}/S_{av}$	44.2	44.3	45.4	49.3	53.7	58.0	62.5	66.8	71.2	75.5	79.8
$S_{2008.5}/S_{2003.5}$(%)	103.1	103.5	106.0	114.8	125.0	135.2	145.4	155.6	165.8	175.9	186.1
$B_{2003.5}/B_{av}$(%)	14.9	14.9	14.9	14.9	14.9	14.9	14.9	14.9	14.9	14.9	14.9
$B_{2008.5}/B_{av}$(%)	11.9	11.9	13.3	21.2	29.7	38.4	47.3	56.2	65.2	74.2	83.2
$B_{2008.5}/B_{2004.5}$(%)	79.7	79.8	88.5	142.1	199.5	258.2	317.8	377.7	438.0	498.5	558.6
$\%S_{2008.5}<S_{2003.5}$	41.4	41.0	35.3	19.2	6.5	1.1	0.1	0.0	0.0	0.0	0.0
$\%S_{2008.5}<S_{av}$	100.0	100.0	100.0	100.0	100.0	100.0	100.0	99.9	99.8	99.5	98.2
$\%B_{2008.5}<B_{2003.5}$	92.1	86.2	61.5	13.8	0.2	0.0	0.0	0.0	0.0	0.0	0.0
$\%B_{2008.5}<B_{av}$	100.0	100.0	100.0	100.0	100.0	100.0	100.0	100.0	100.0	99.1	94.5

Table 22: 5th percentiles of posterior distributions of derived parameters generated from the base case assessment of PAU 7 for 11 alternative TACC levels for projections to 2008, including the current catch of 179t. Caption as for Table 21.

TACC cut	0%	10%	20%	30%	40%	50%	60%	70%	80%	90%	100%
Projected Catch (t)	179	164	150	136	121	107	93	78	64	50	35
U_{08} (%)	75.1	66.7	51.6	39.3	30.4	23.6	18.2	13.9	10.4	7.4	4.9
$S_{2003.5}/S_{av}$(%)	40.2	40.2	40.2	40.2	40.2	40.2	40.2	40.2	40.2	40.2	40.2
$S_{2008.5}/S_{av}$	34.6	34.6	34.7	37.1	41.3	45.6	49.9	54.2	58.4	62.5	66.7
$S_{2008.5}/S_{2003.5}$(%)	81.4	81.5	82.1	87.7	97.9	108.2	118.5	128.5	138.3	148.4	158.4
$B_{2003.5}/B_{av}$(%)	13.0	13.0	13.0	13.0	13.0	13.0	13.0	13.0	13.0	13.0	13.0
$B_{2008.5}/B_{av}$(%)	9.3	9.3	9.4	11.7	19.9	28.2	36.4	44.8	53.1	61.4	69.7
$B_{2008.5}/B_{2004.5}$(%)	64.5	64.6	65.6	81.3	138.1	196.5	255.1	314.1	373.5	433.1	491.9

Table 23: 95th percentiles of posterior distributions of derived parameters generated from the base case assessment of PAU 7 for 11 alternative TACC levels for projections to 2008, including the current catch of 179t. Caption as for Table 21.

TACC cut	0%	10%	20%	30%	40%	50%	60%	70%	80%	90%	100%
Projected Catch (t)	179	164	150	136	121	107	93	78	64	50	35
U_{08} (%)	80.0	80.0	80.0	77.6	53.0	37.8	27.5	20.1	14.4	10.0	6.4
$S_{2003.5}/S_{av}$(%)	45.7	45.7	45.7	45.7	45.7	45.7	45.7	45.7	45.7	45.7	45.7
$S_{2008.5}/S_{av}$	56.0	56.8	59.5	63.9	68.3	72.7	77.0	81.5	85.9	90.4	94.7
$S_{2008.5}/S_{2003.5}$(%)	130.9	132.3	137.4	147.8	158.2	168.1	178.4	188.7	199.0	209.4	219.3
$B_{2003.5}/B_{av}$(%)	17.3	17.3	17.3	17.3	17.3	17.3	17.3	17.3	17.3	17.3	17.3
$B_{2008.5}/B_{av}$(%)	16.2	18.1	25.0	33.8	42.9	52.4	61.7	71.4	81.3	90.9	100.7
$B_{2008.5}/B_{2004.5}$(%)	105.4	117.6	161.5	218.6	276.6	335.3	394.0	453.7	513.8	574.8	636.3

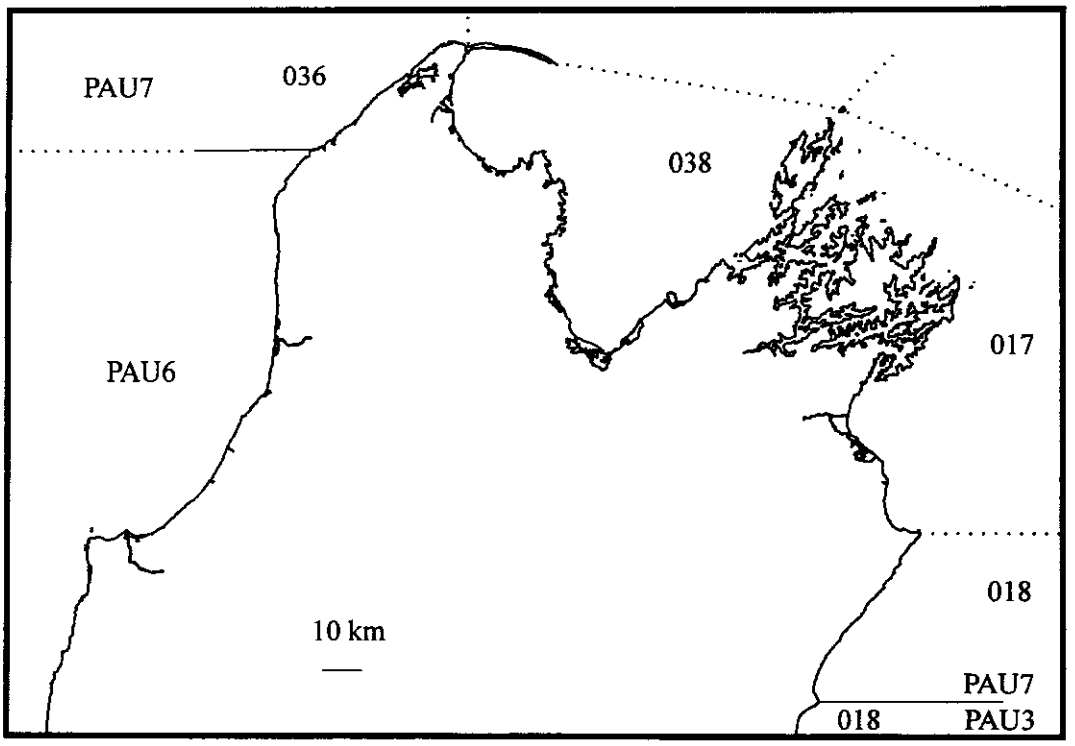

Figure 1: Boundaries of PAU 7 and its statistical areas.

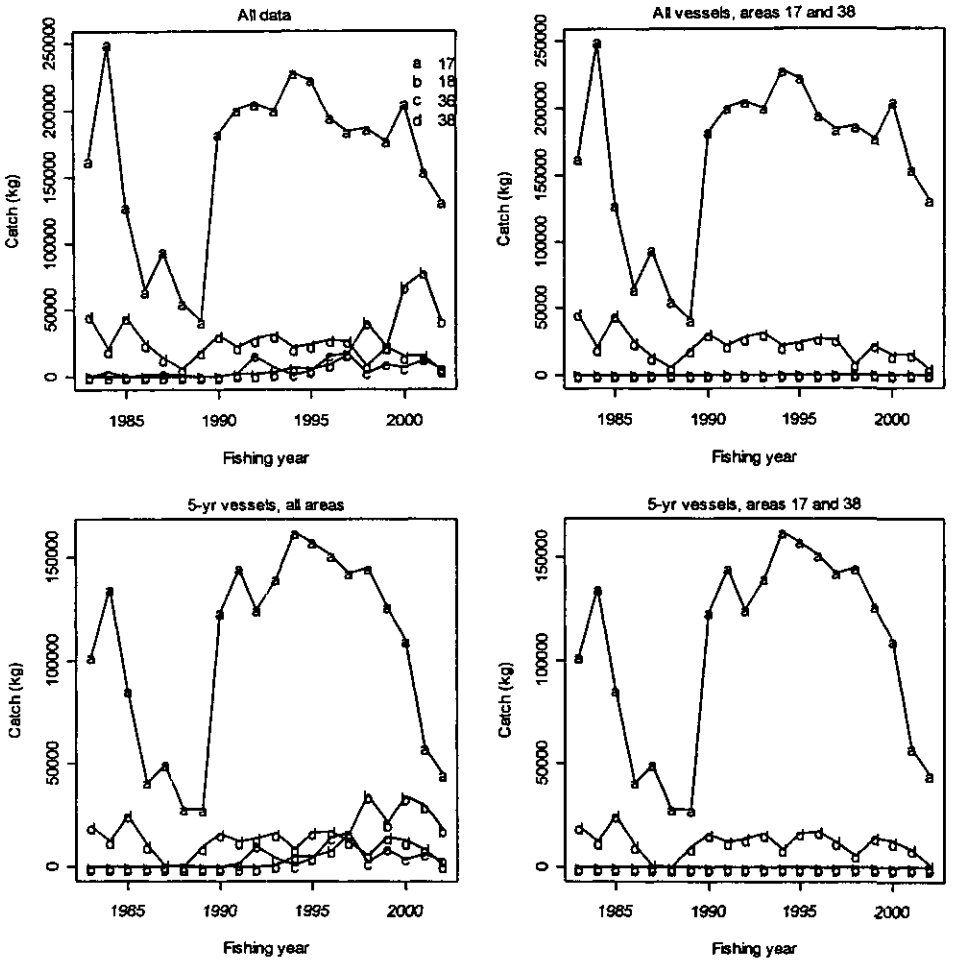

Figure 2: Estimated commercial catch (kg) by area from the CELR forms for all vessels (top) and 5-yr vessels (vessels that fished for 5 years and longer, bottom) in all areas (left) and in areas 17 and 38 only (right).

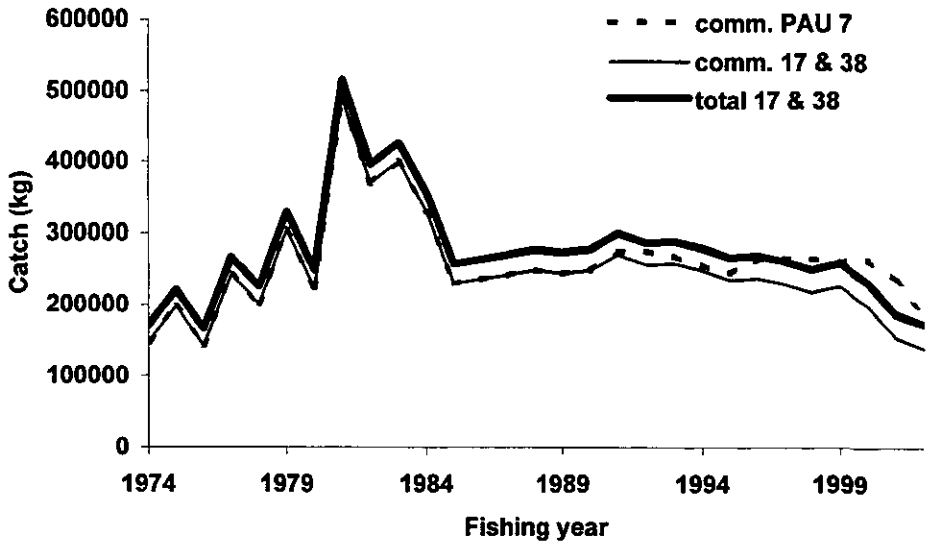

Figure 3: Commercial catch from 1974 to 2002 in all of PAU 7 (dashed line) and in areas 17 & 18 only (light solid line). The heavy line shows estimated total catches (including non-commercial catches) from areas 17 and 38 as used in the assessment (Table 3).

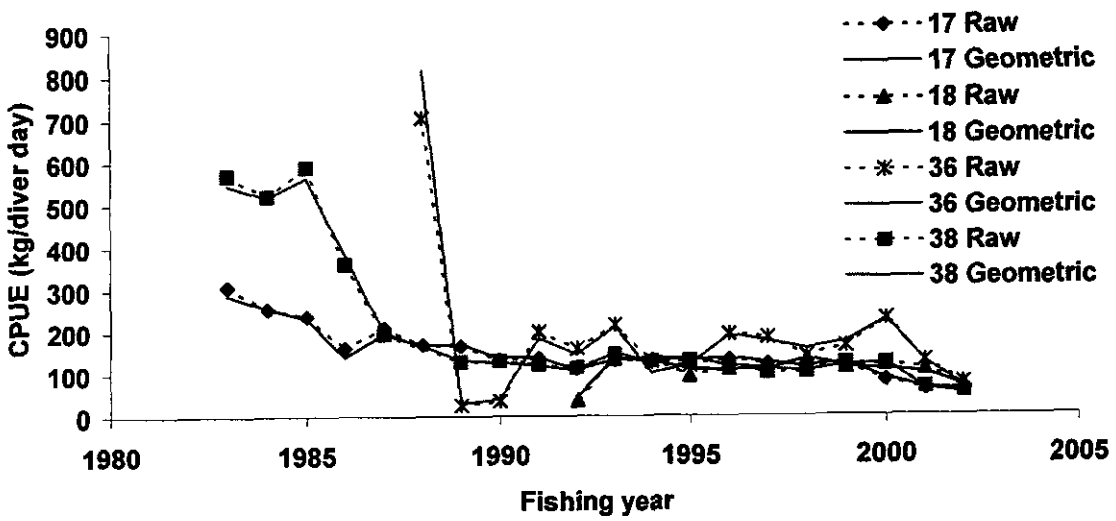

Figure 4: Raw CPUE (kg/diver day) and geometric mean of CPUE by statistical area.

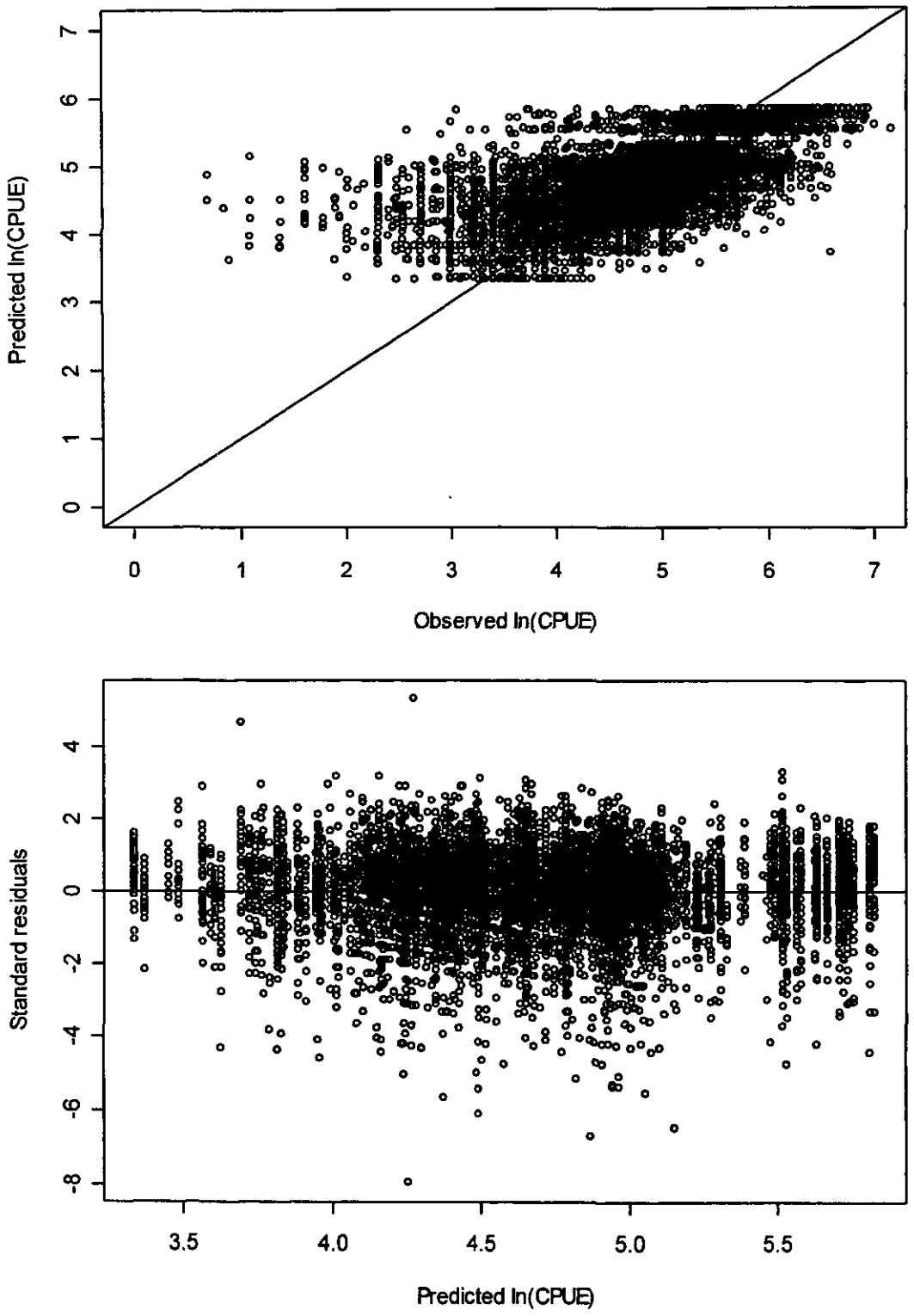

Figure 5: Fits and residuals from the GLM model of CPUE, using 5-year vessels in all areas.

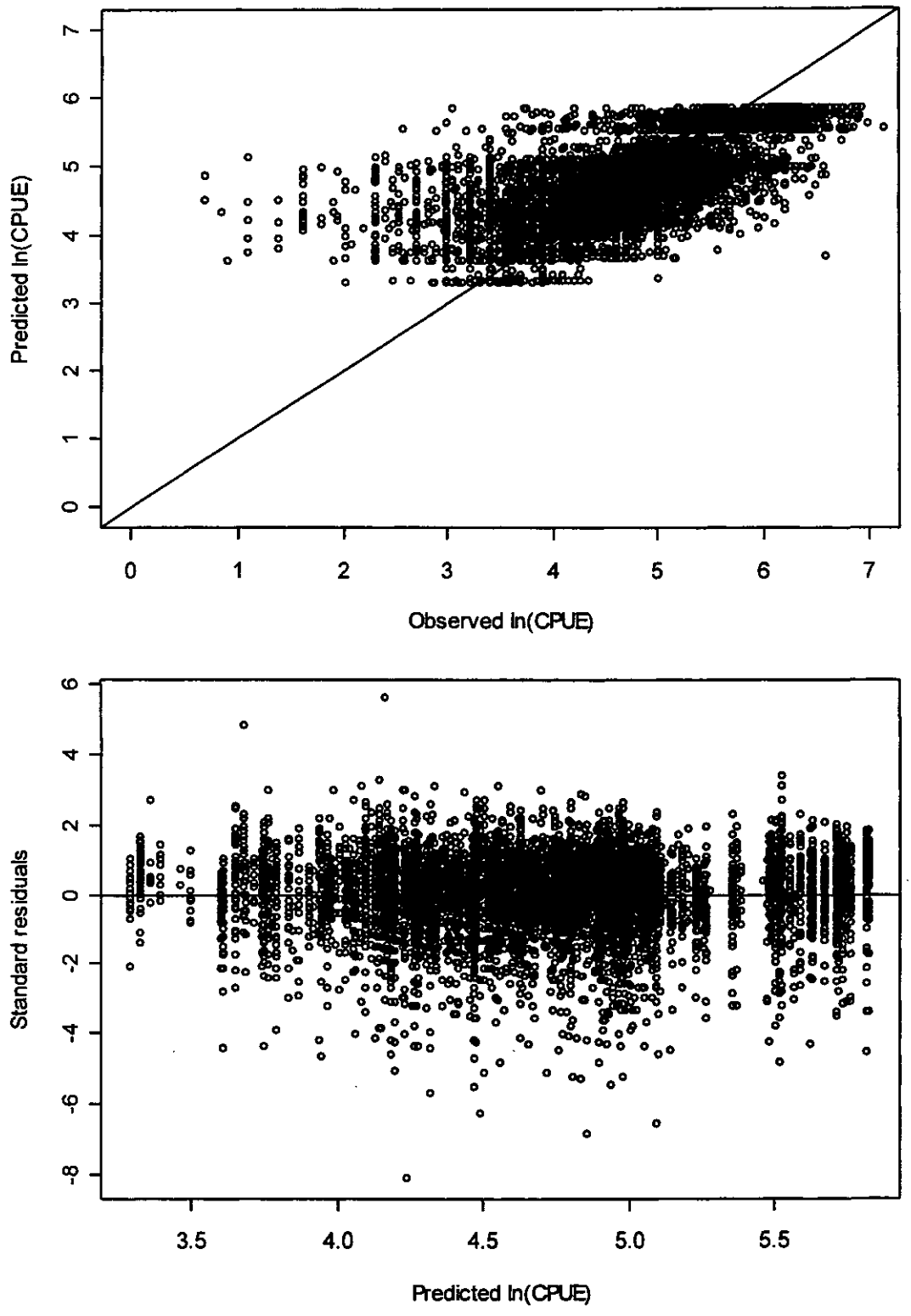

Figure 6: Fits and residuals from the GLM model of CPUE, using 5-year vessels in areas 17 and 38.

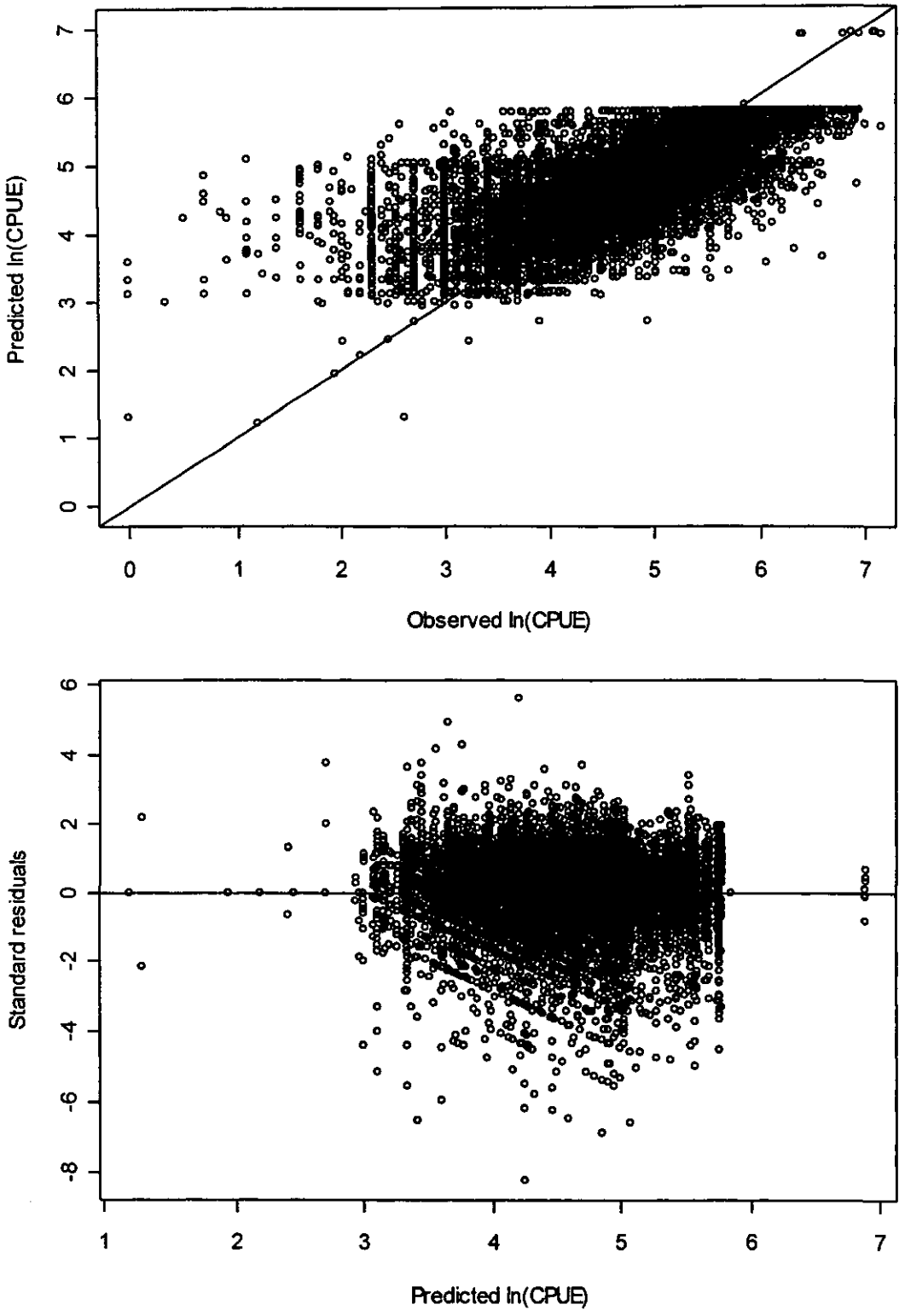

Figure 7: Fits and residuals from the GLM model of CPUE, using all vessels in areas 17 and 38.

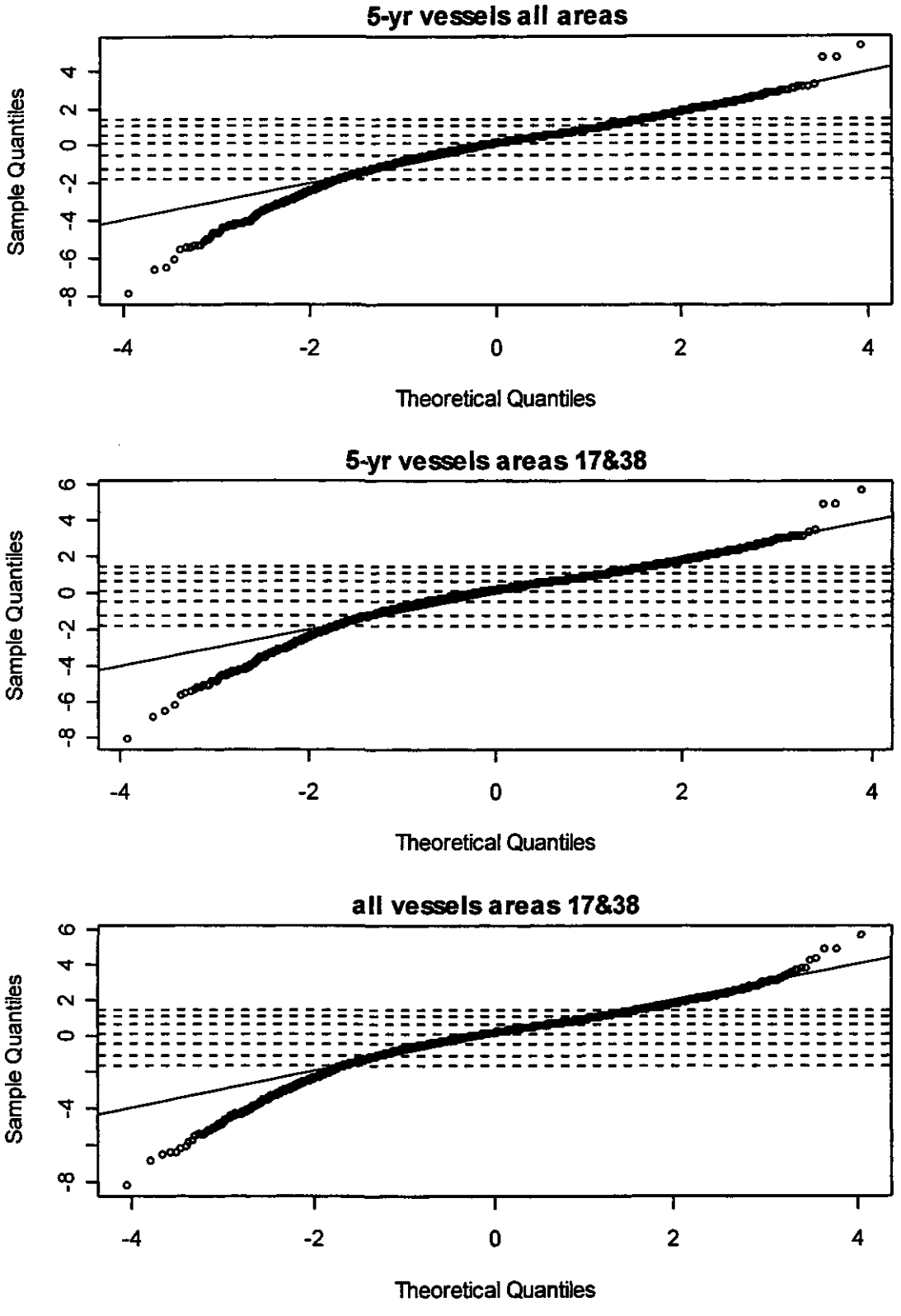

Figure 8: Q-Q plots for the residuals from the GLM model of CPUE shown in Figure 5 to Figure 7.

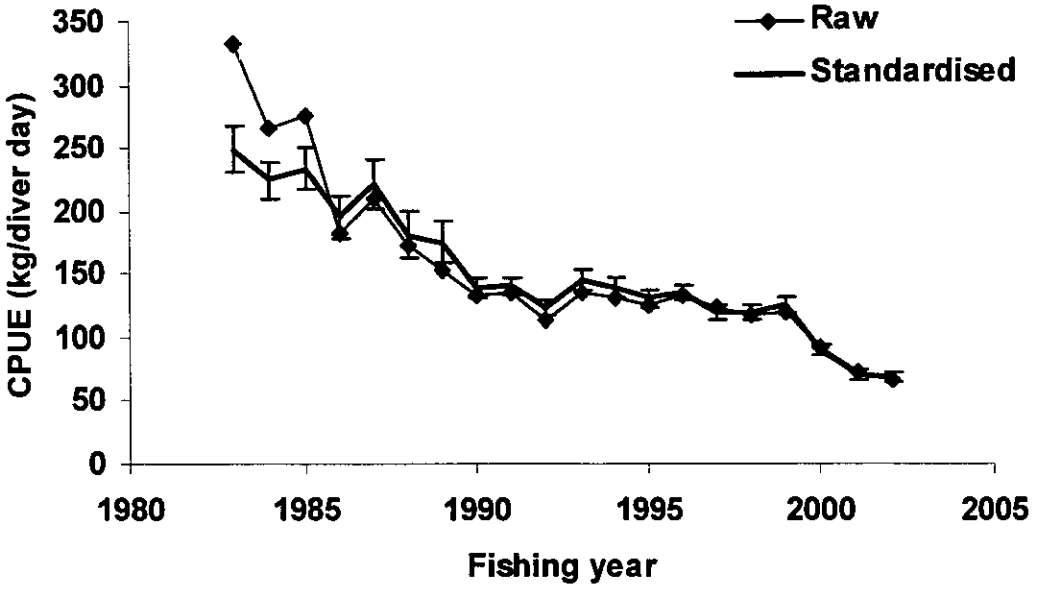

Figure 9: Raw and standardised CPUE from all statistical areas for 5-year vessels.

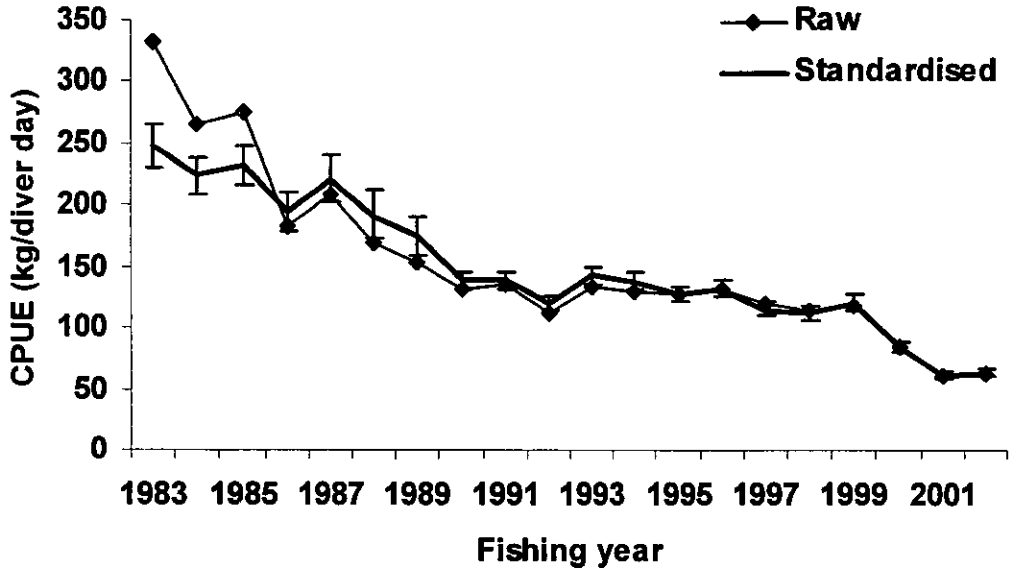

Figure 10: Raw and standardised CPUE from statistical areas 17 and 38 only for 5-year vessels.

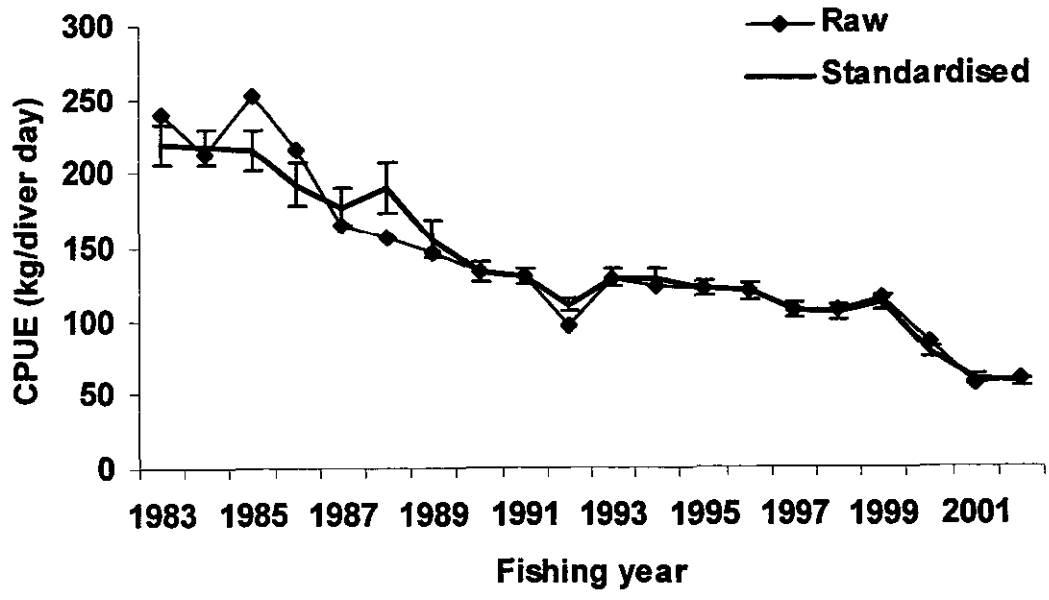

Figure 11: Raw and standardised CPUE from statistical areas 17 and 38 only for all vessels.

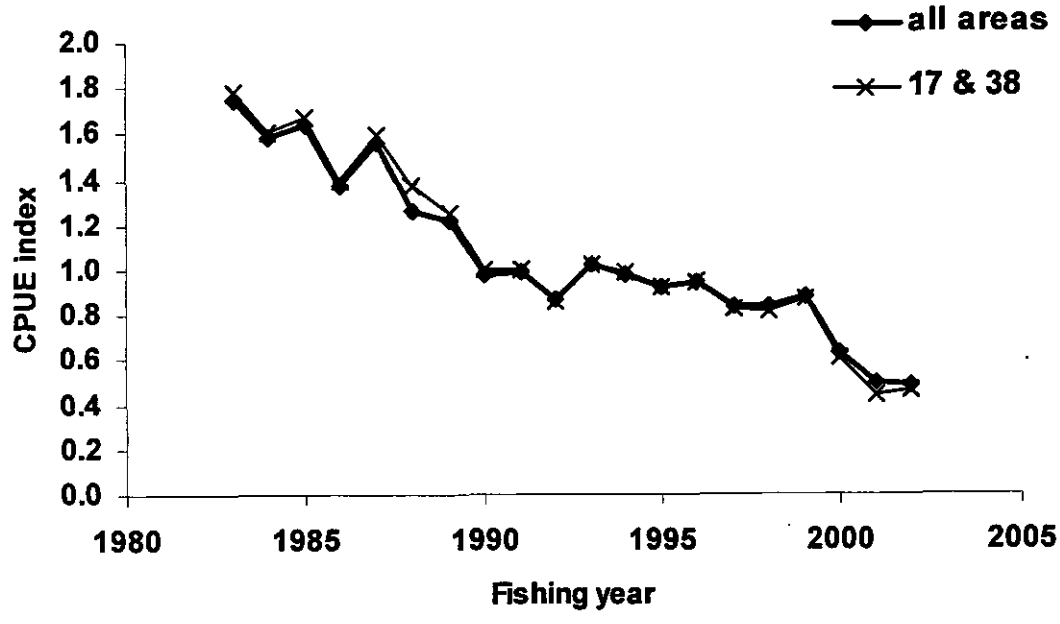

Figure 12: Comparison of CPUE indices using different datasets: all areas and areas 17 and 38 only, based on 5-year vessels.

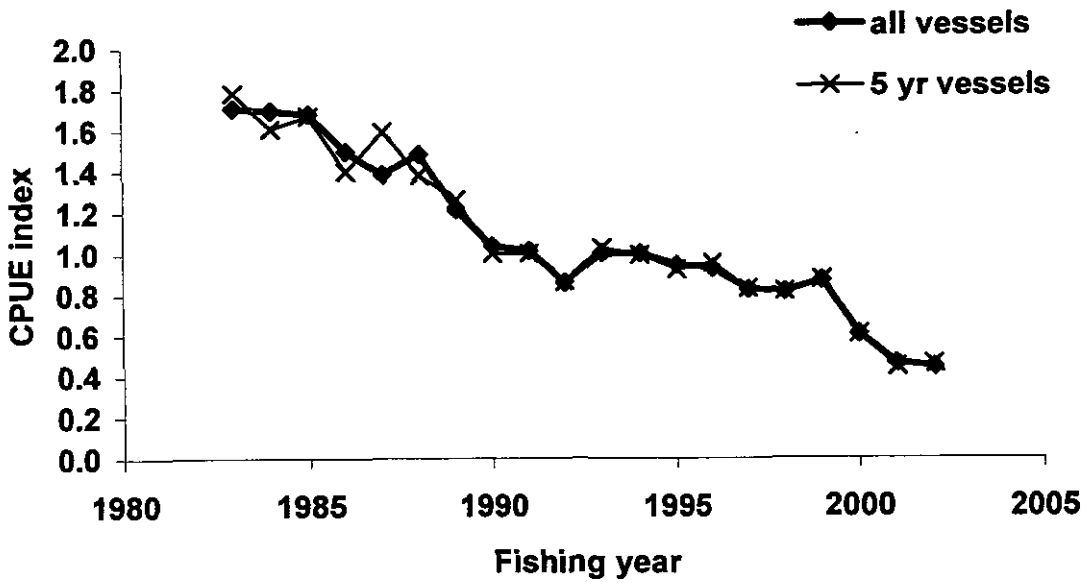

Figure 13: Comparison of CPUE indices using different datasets: all vessels and vessels that fished for 5 years or more in areas 17 and 38.

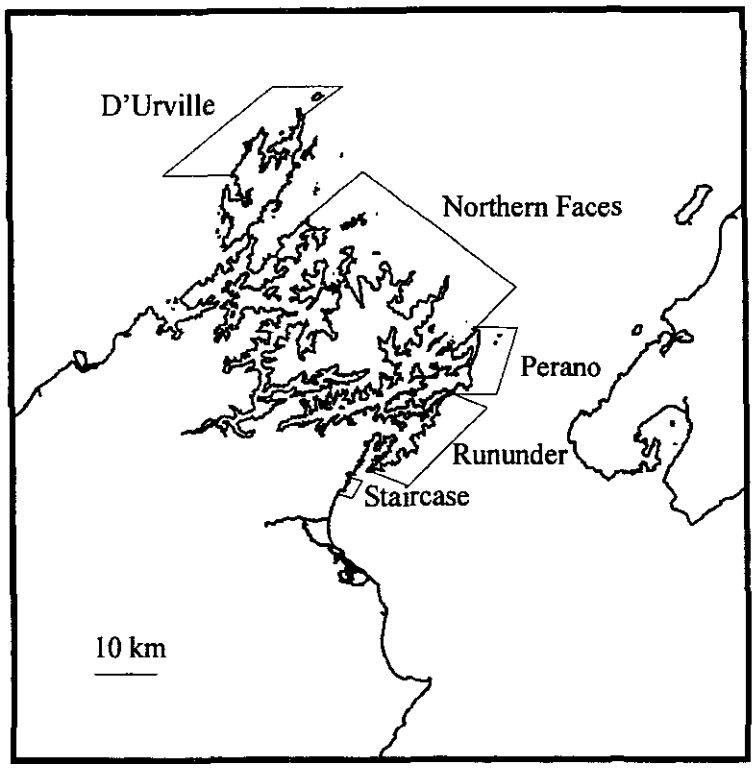

Figure 14: Research diver survey strata in PAU 7. The stratum "West Coast", not shown, comprises all of the PAU 7 area to the south and west of Cape Farewell. The stratum "Cape Campbell", not shown, comprises all of the PAU 7 area to the south and east of Cape Campbell.

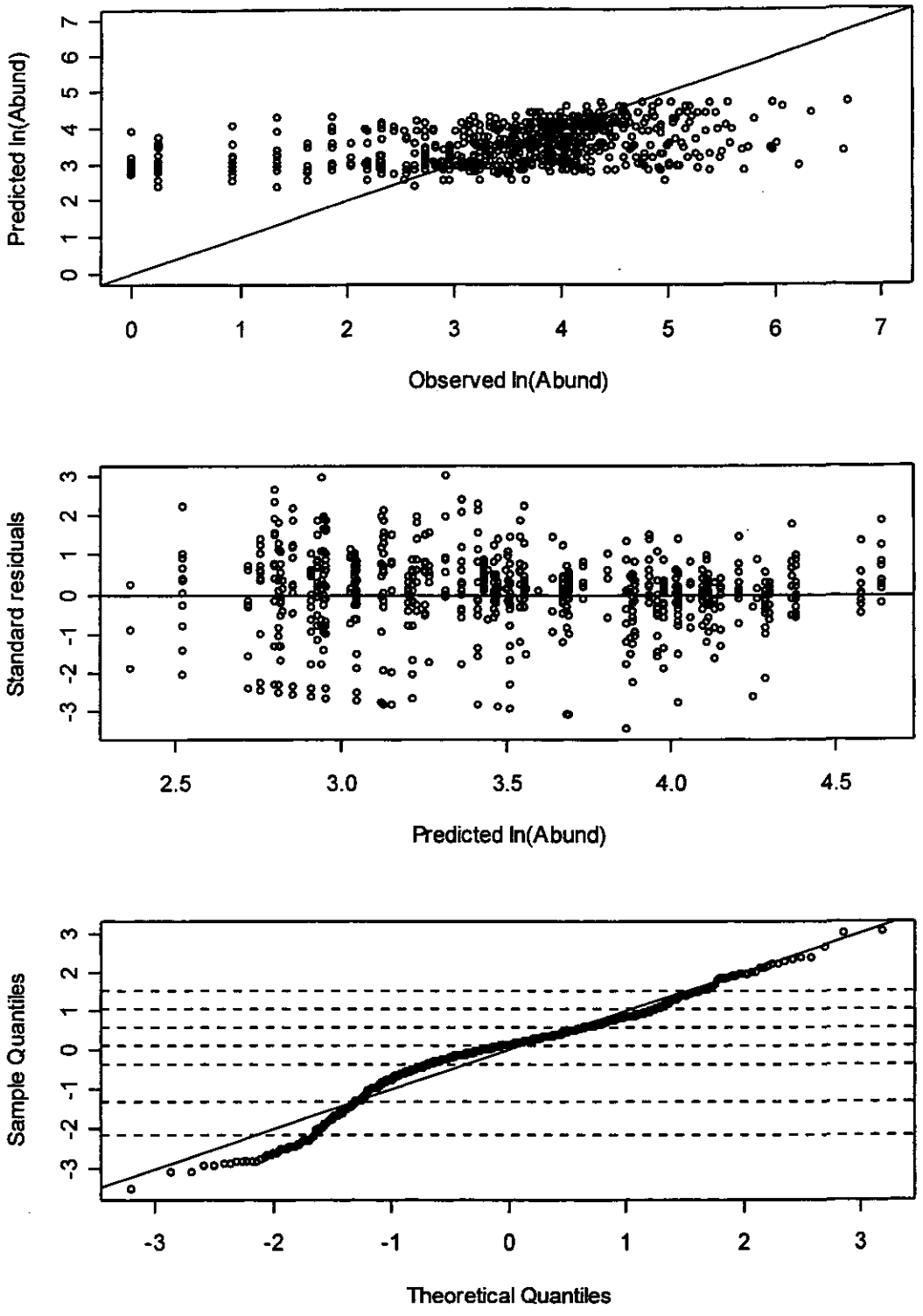

Figure 15: Fits, residuals, and Q-Q plot for the standardised RDSI.

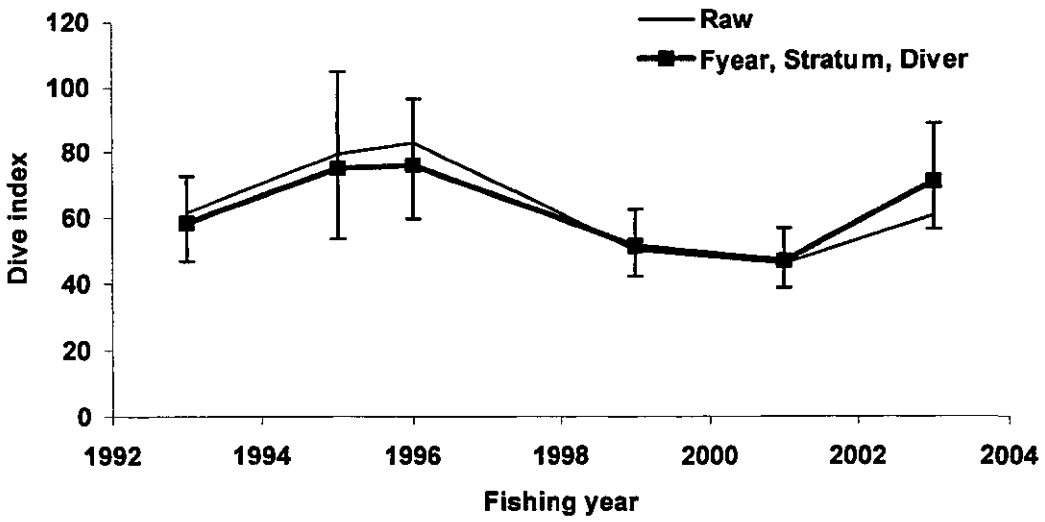

Figure 16: Raw and standardised RDSI.

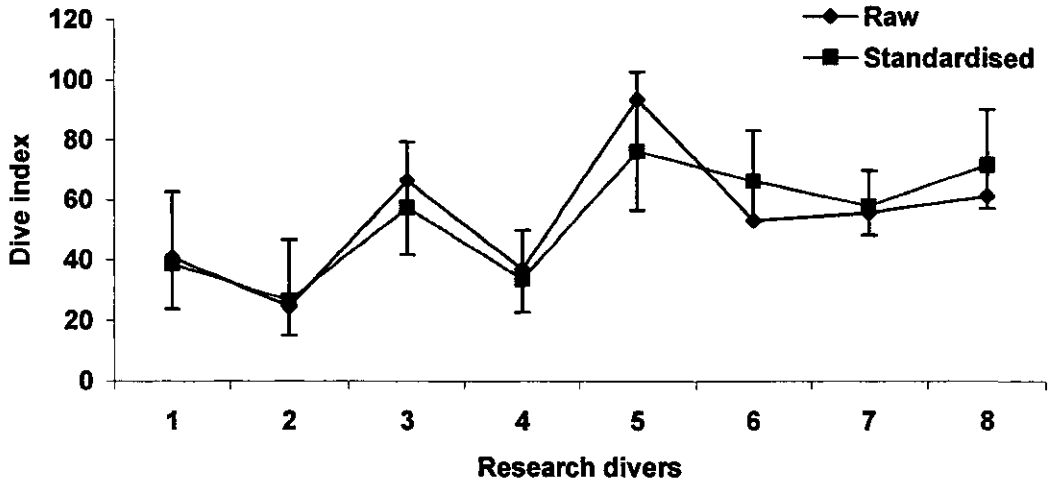

Figure 17: Raw and standardised RDSI for each research diver.

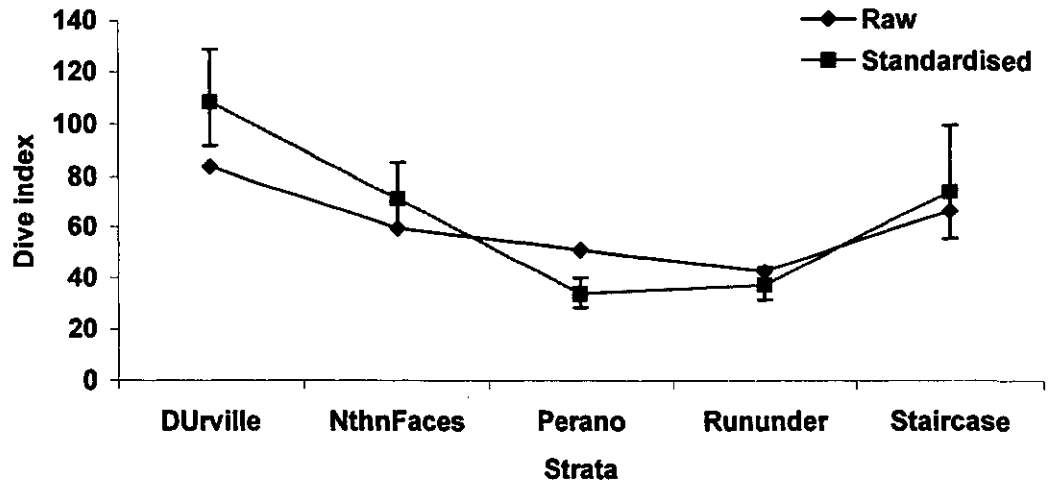

Figure 18: Raw and standardised RDSI for each survey stratum.

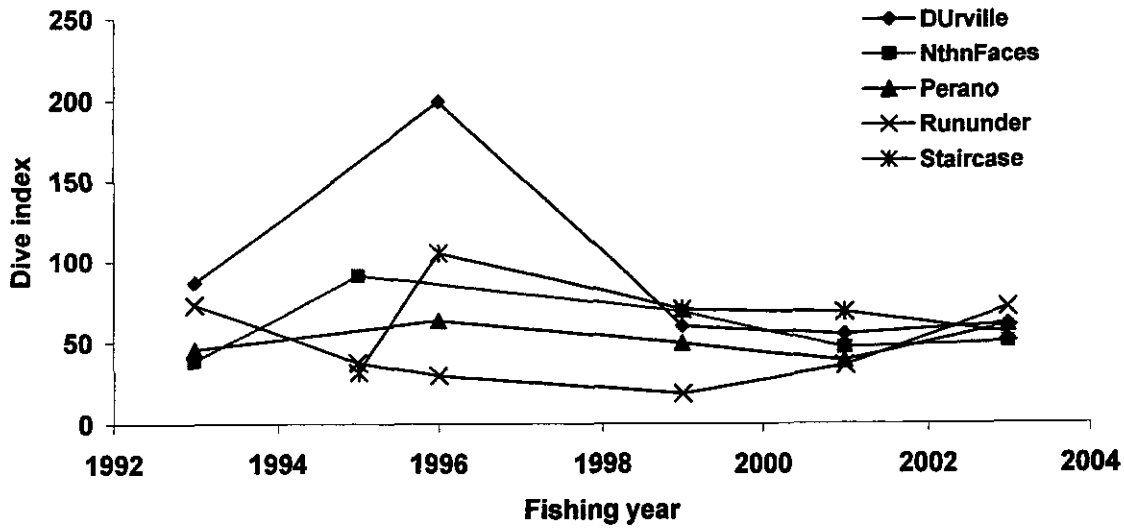

Figure 19: Average RDSI trends for each survey stratum.

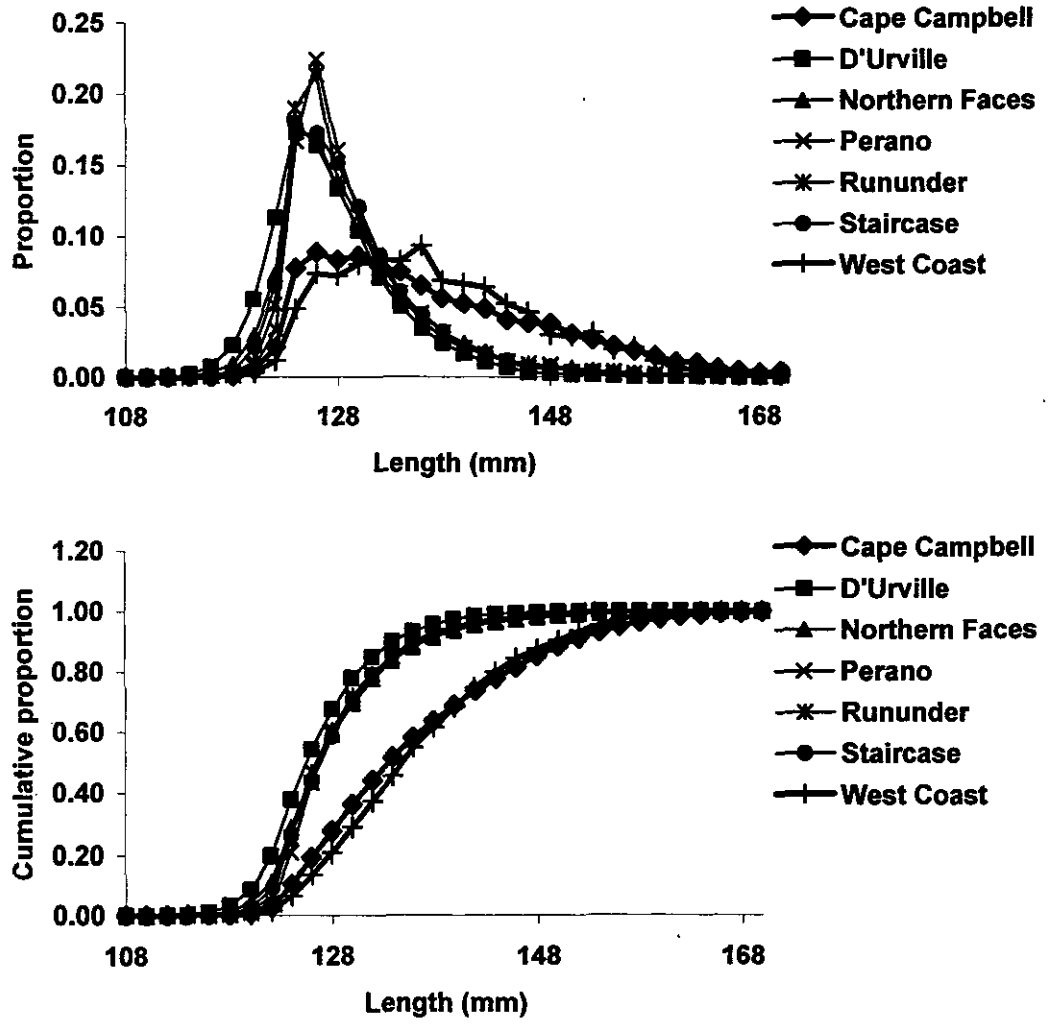

Figure 20: Commercial catch sampling length frequencies from all years, plotted as proportion-at-length (top) and cumulative proportion-at-length (bottom) for each survey stratum.

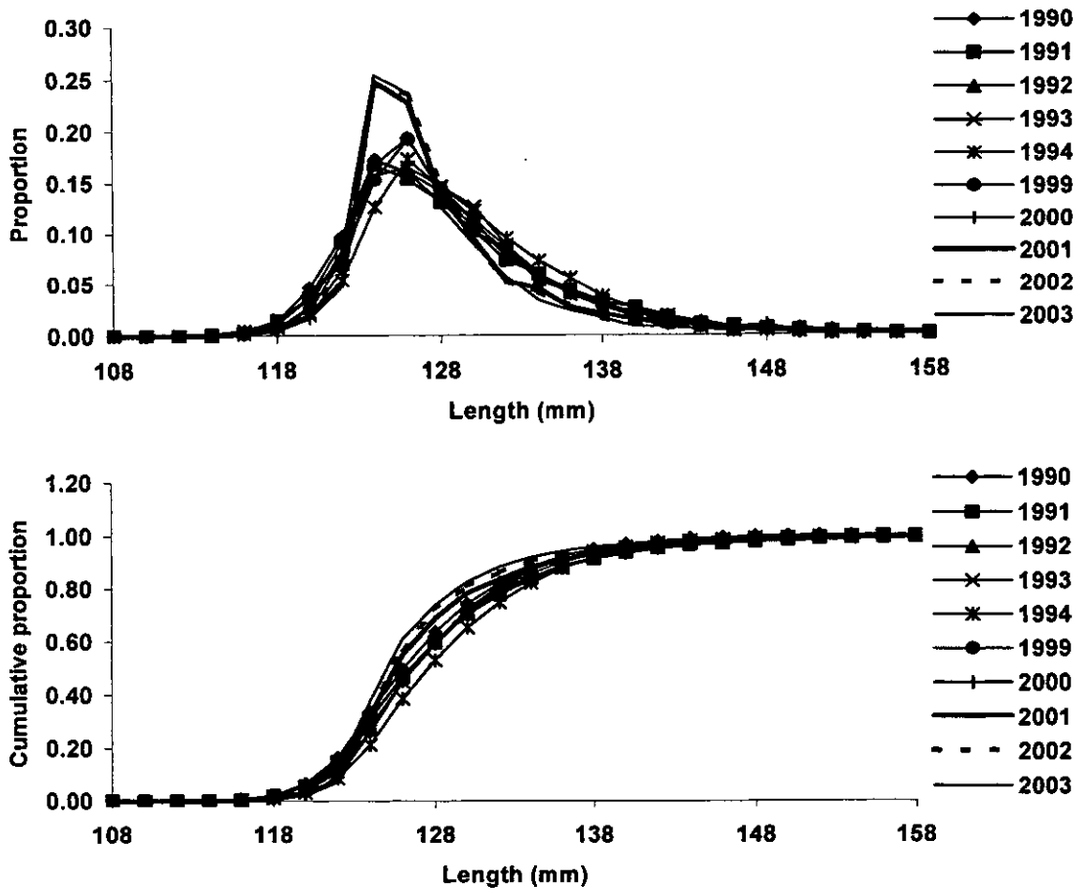

Figure 21: Commercial catch sampling length frequencies from all survey strata aggregated, but with West Coast and Cape Campbell strata omitted, plotted as proportion-at-length (top) and cumulative proportion-at-length (bottom) for each year.

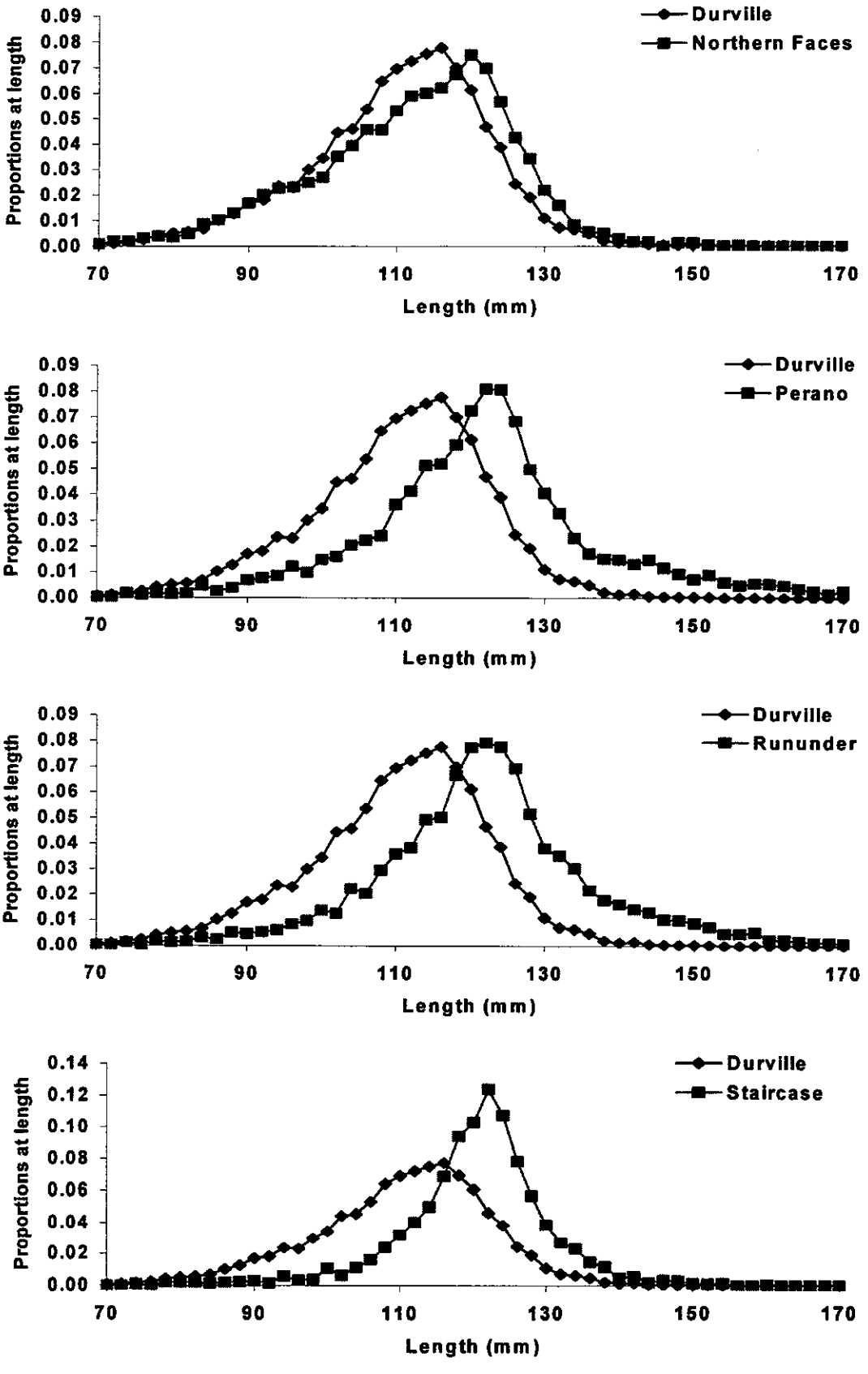

Figure 22: Comparison of research survey proportions-at-length by survey stratum, aggregated across years. Durville is shown in each figure for comparison.

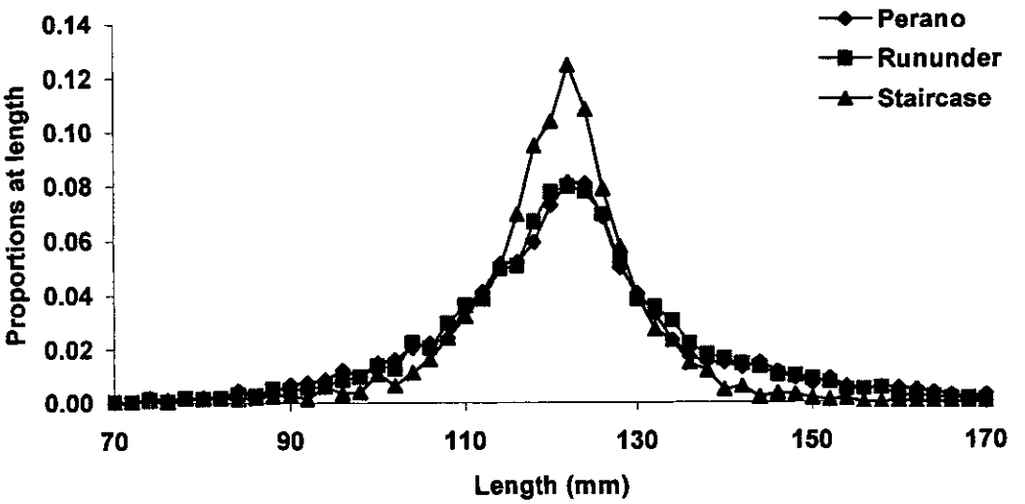

Figure 23: Comparison of research survey proportions-at-length, aggregated across years, from the three strata Perano, Runander, and Staircase.

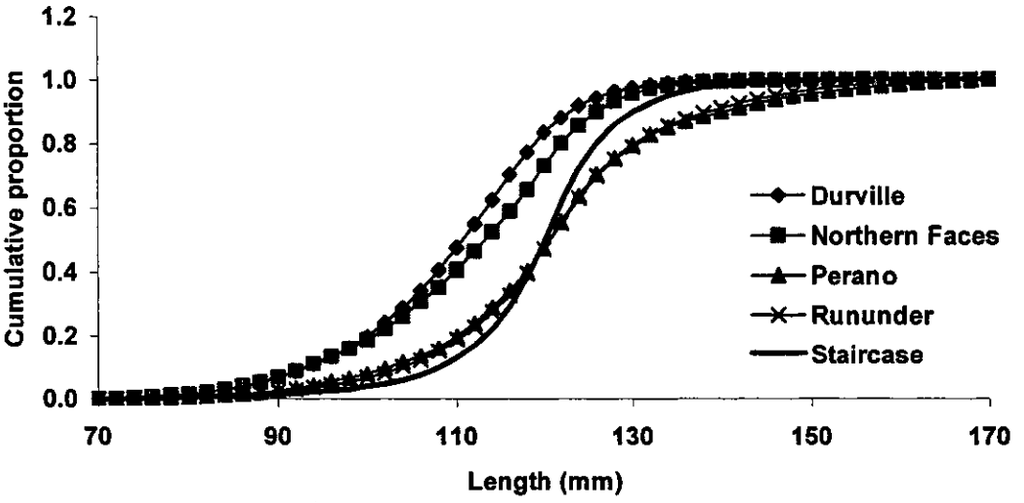

Figure 24: Comparison of cumulative research survey proportions-at-length, aggregated across years, by stratum.

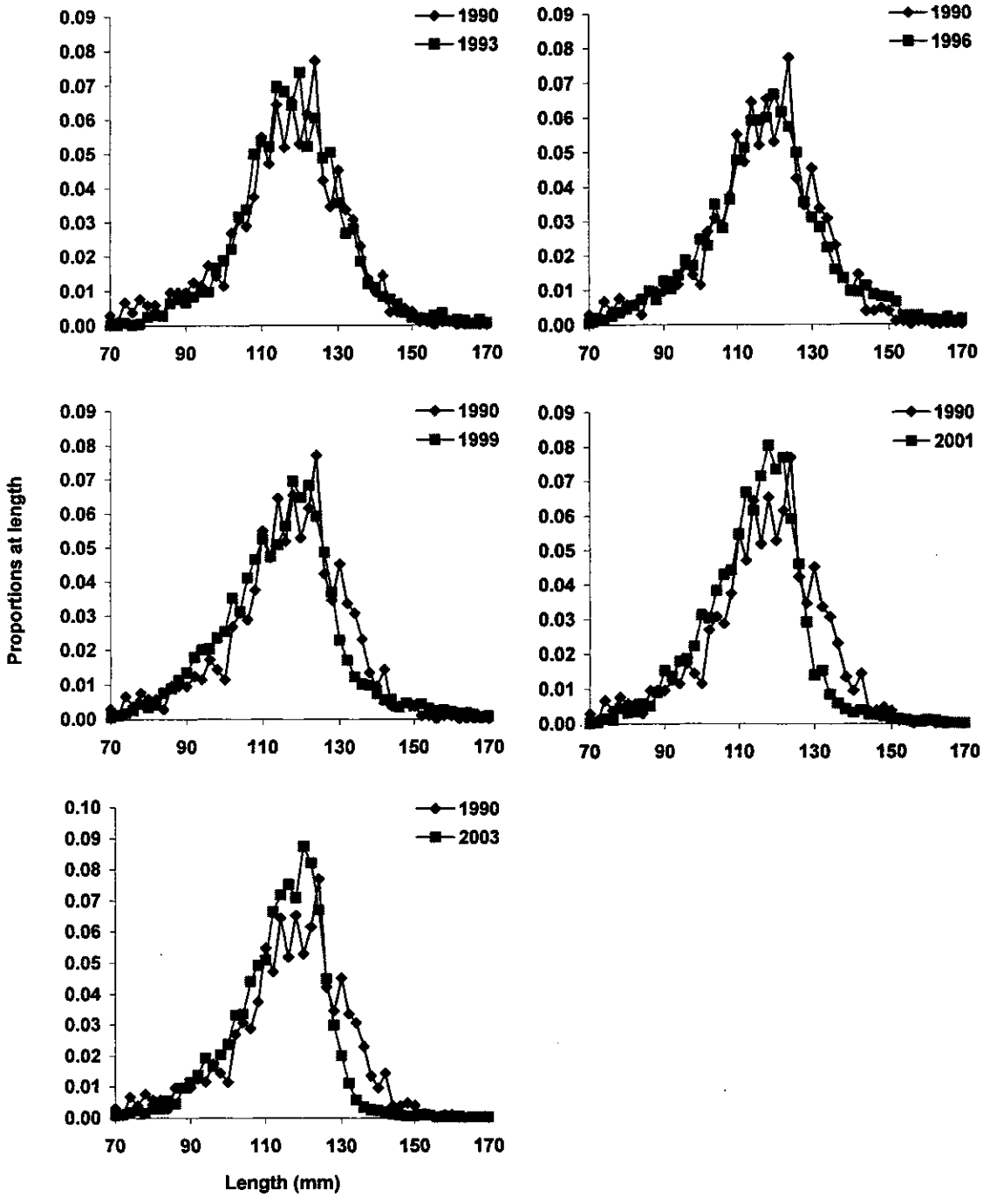

Figure 25: Comparison of research survey proportions-at-length from the research survey by year. In each figure, 1990 is given as a reference.

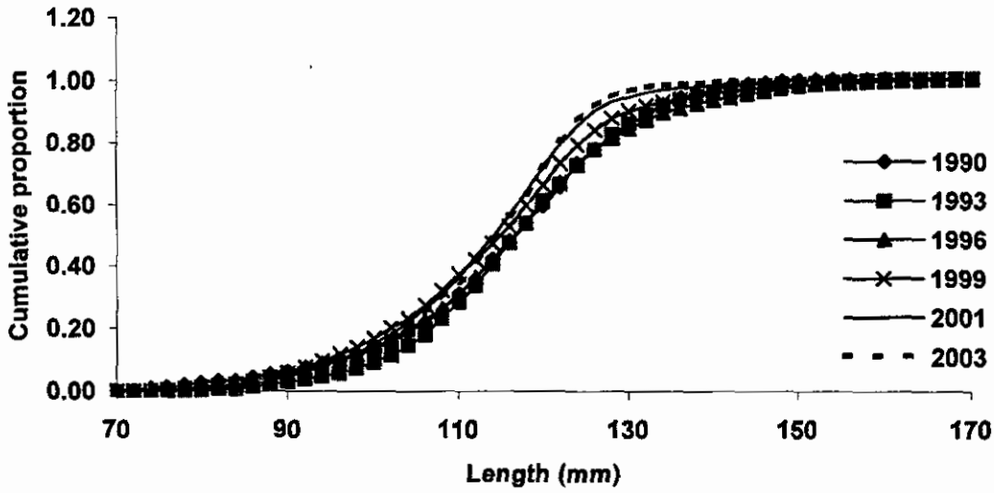

Figure 26: Comparison of cumulative research survey proportions-at-length, aggregated across strata, by year.

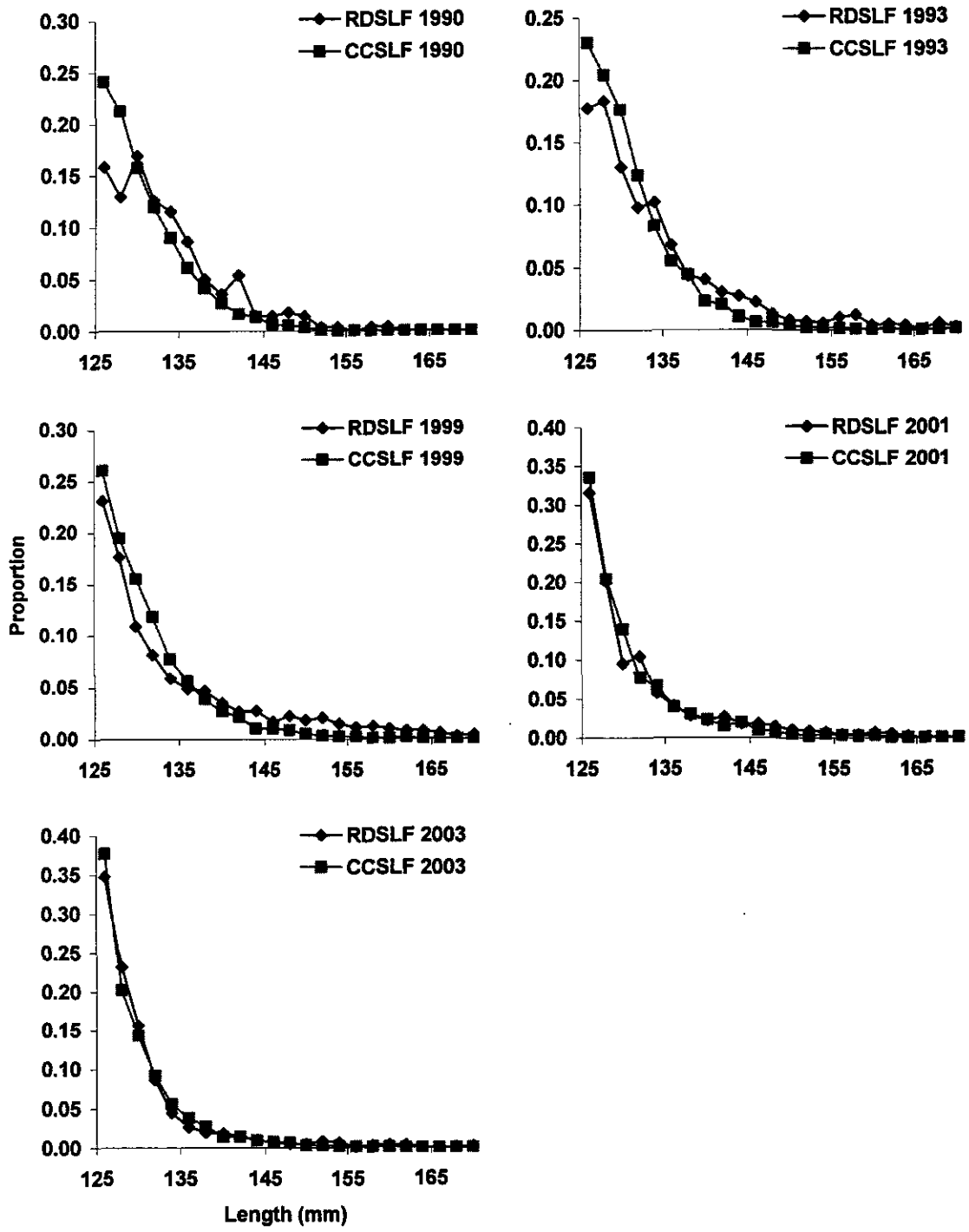

Figure 27: Comparison of proportions-at-length from commercial catch sampling (CCSLF) and research diver surveys (RDSLF) for each of the years indicated.

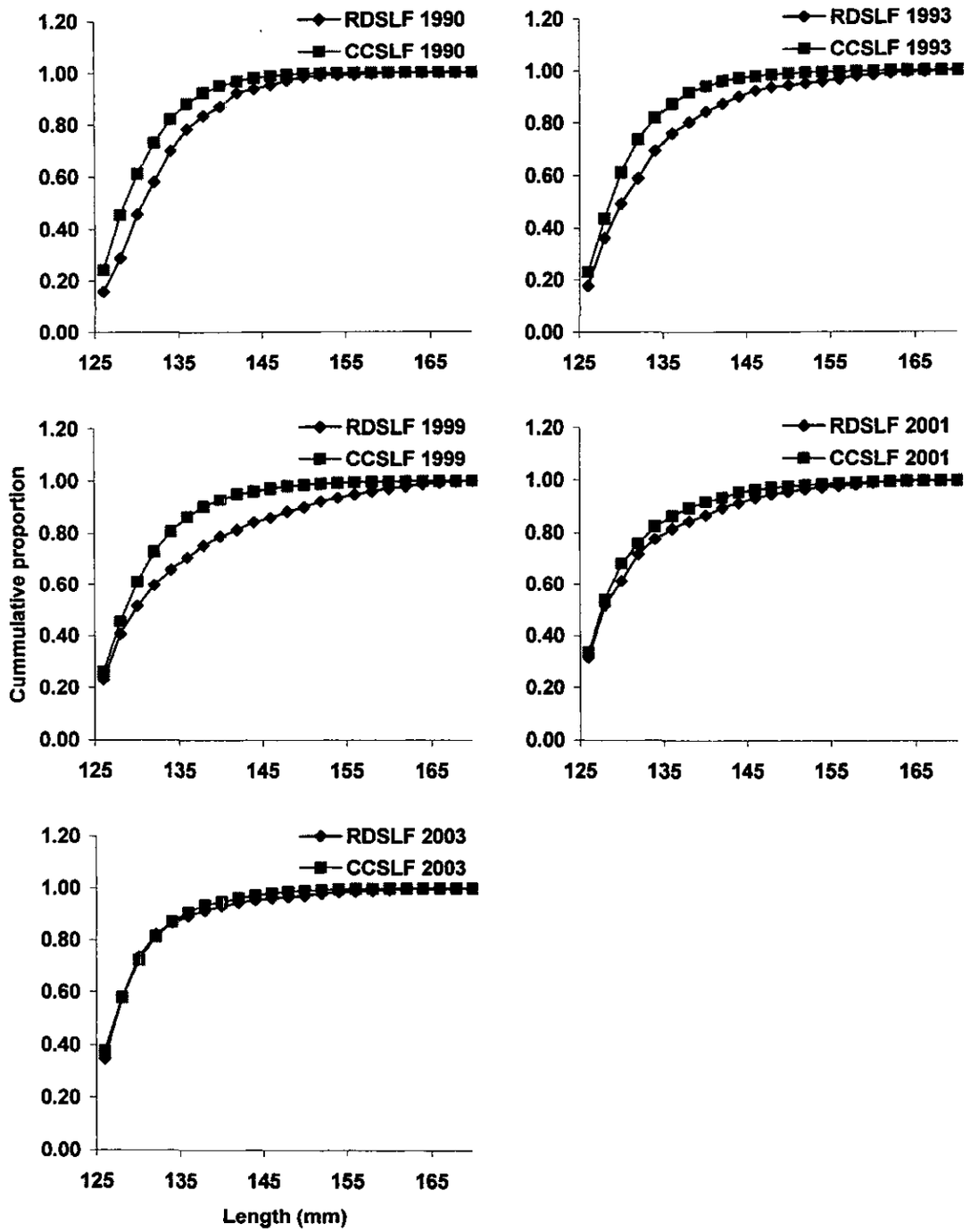

Figure 28: Comparison of cumulative proportions-at-length from commercial catch sampling (CCSLF) and research diver surveys (RDSLF) for each of the years indicated.

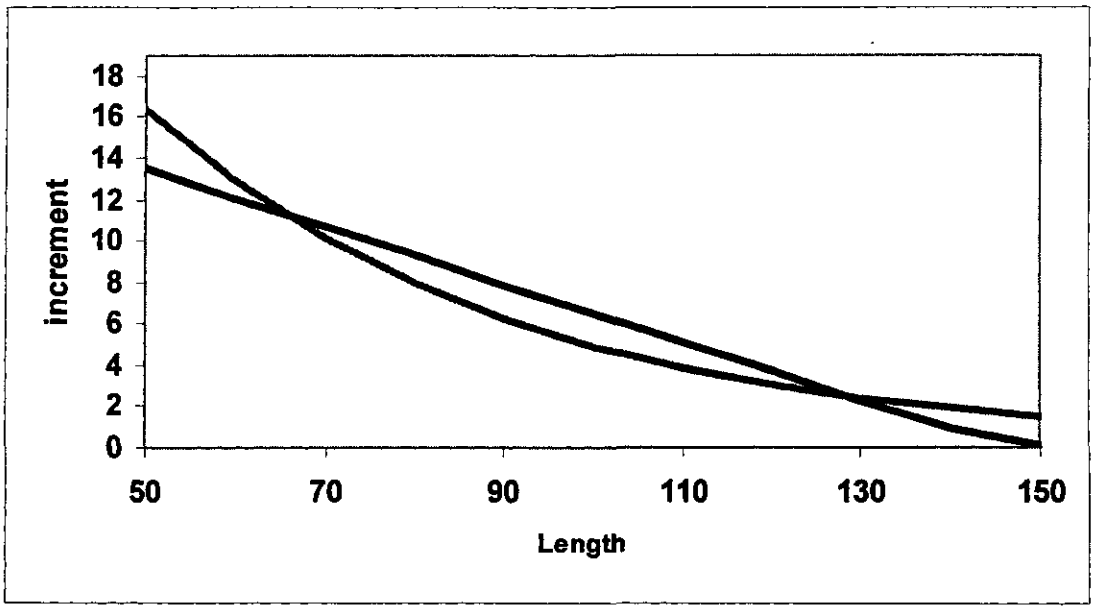

Figure 29: Showing expected increments for the two growth models described in the text, using the same parameters $g_\alpha = 10$ and $g_\beta = 3$, where α and β are 75 and 125 respectively.

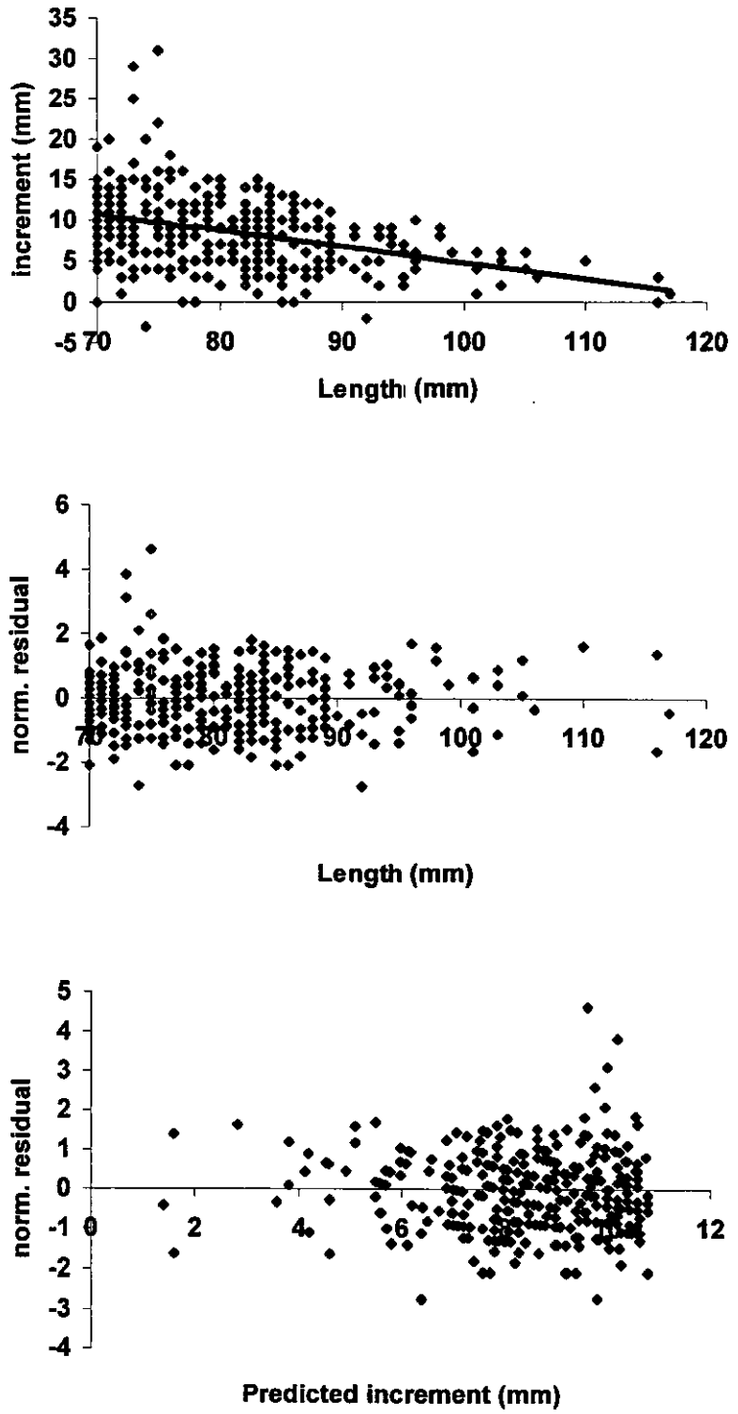

Figure 30: Fit of the linear growth model to the D'Urville stratum tag-recapture dataset. Upper: observed and predicted (grey) increments plotted against initial length; middle: normalised residuals plotted against initial length; bottom: normalised residuals plotted against predicted increment.

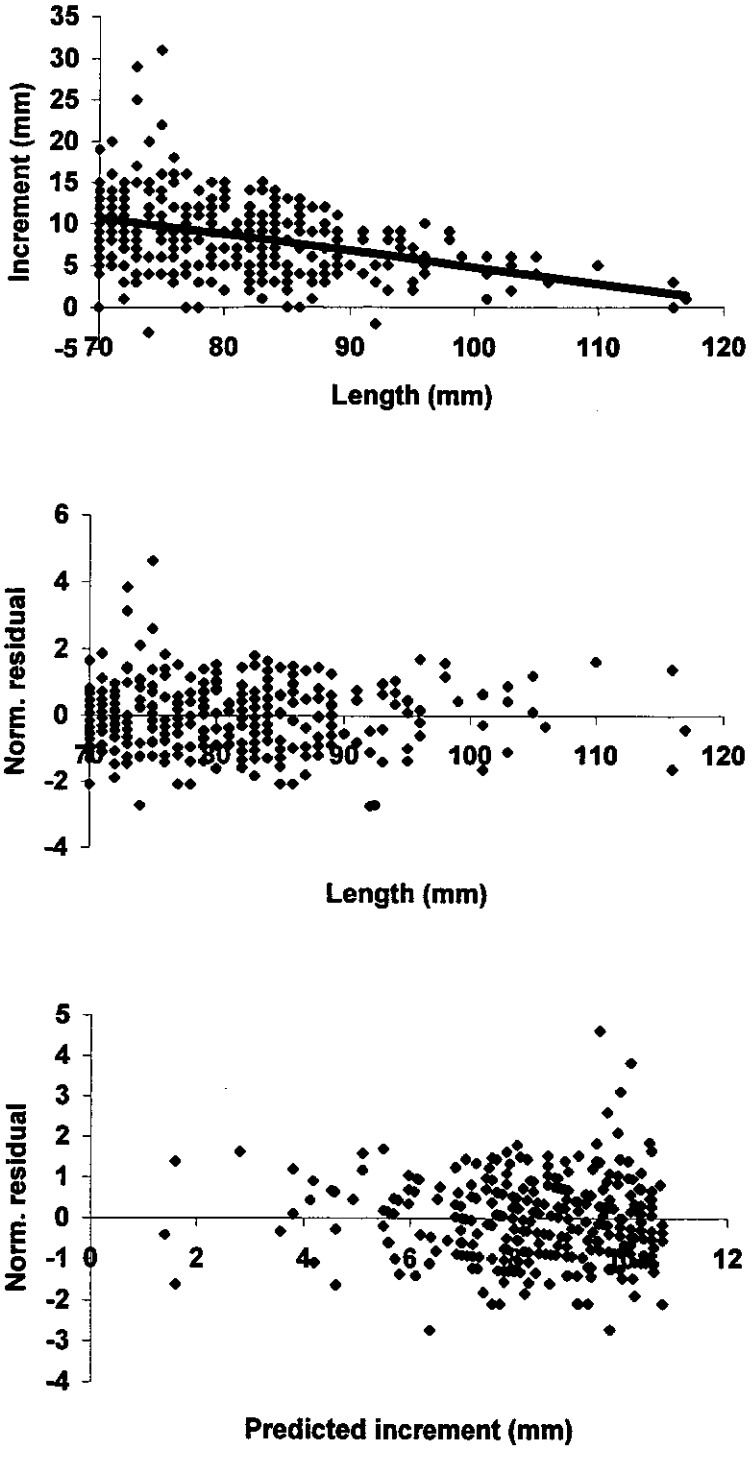

Figure 31: Fit of the linear growth model to the Staircase stratum tag-recapture dataset. Caption as for Figure 30.

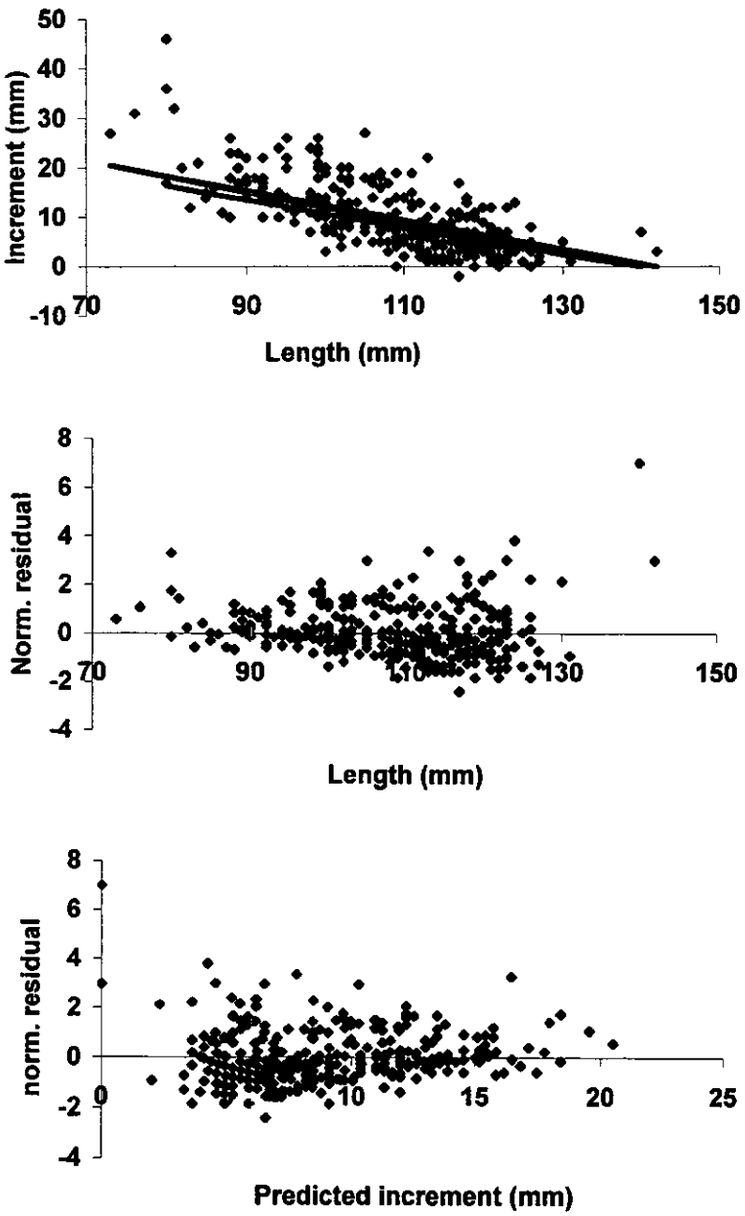

Figure 32: Fit of the linear growth model to the2001 tag-recapture dataset. Caption as for Figure 30.

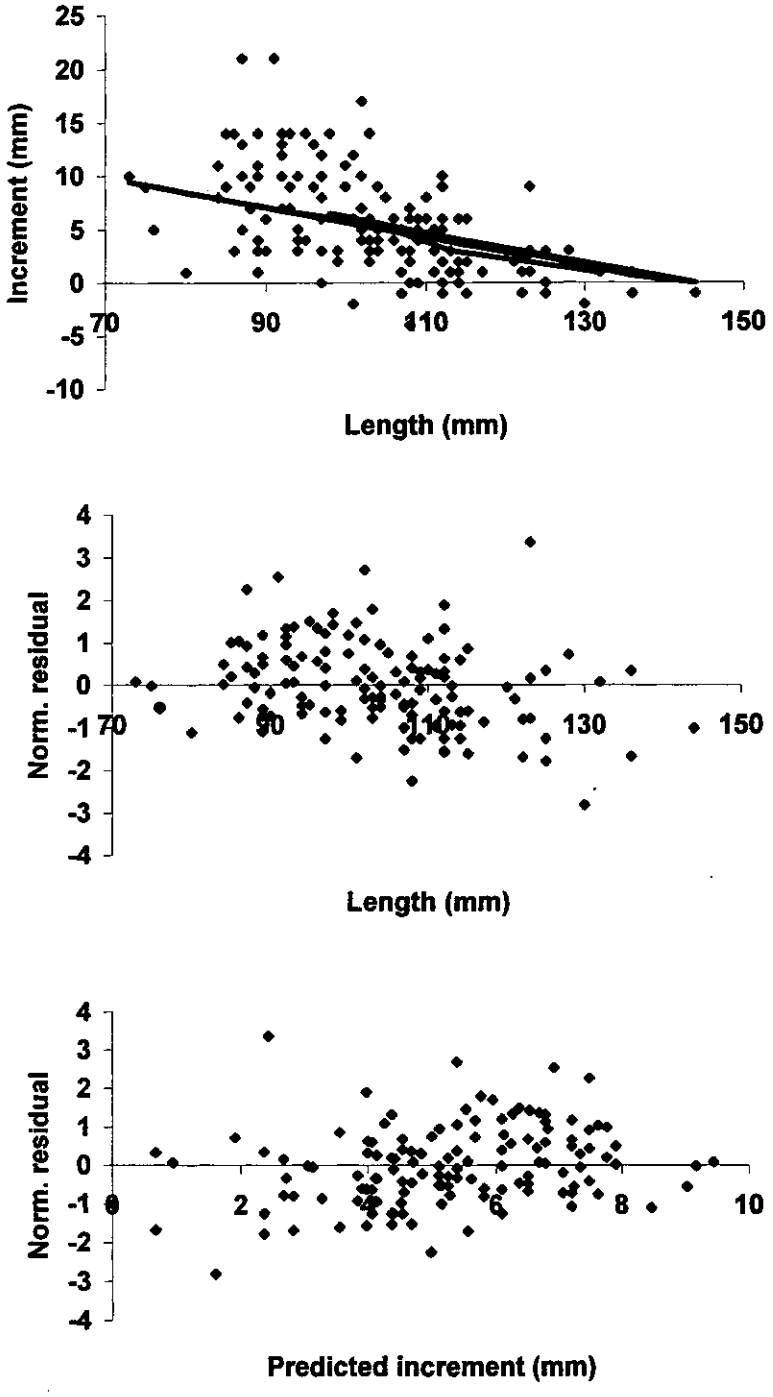

Figure 33: Fit of the linear growth model to the PAU 6 tag-recapture dataset. Caption as for Figure 30.

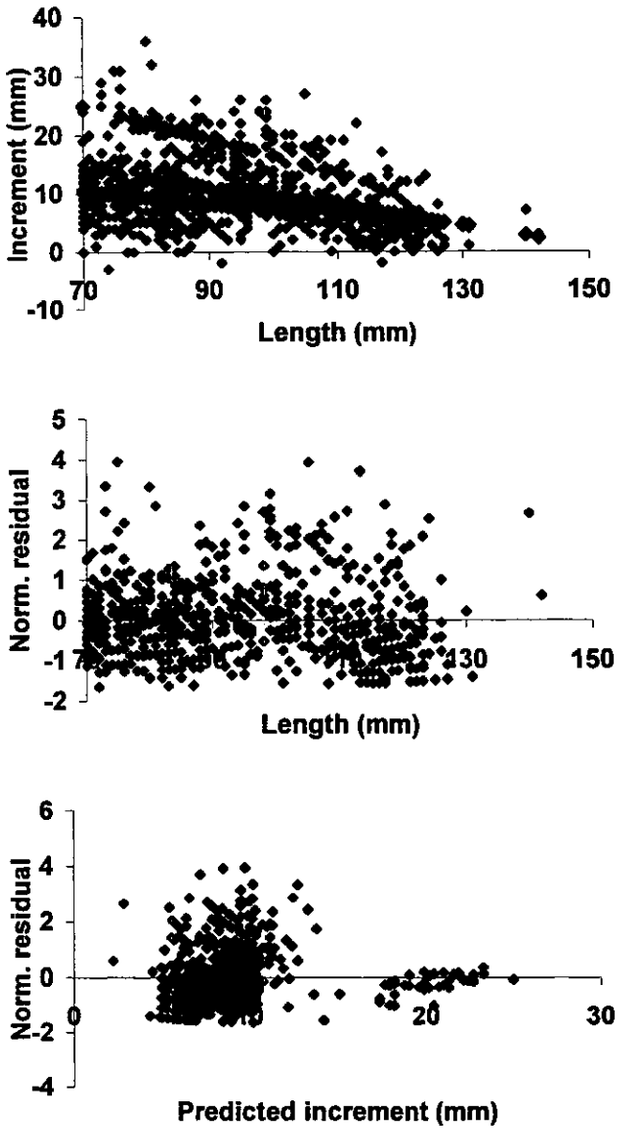

Figure 34: Fit of the linear growth model to all the PAU 7 tag-recapture data combined. Caption as for Figure 30. The different values for predicted increments reflect the different times at liberty in the various datasets.

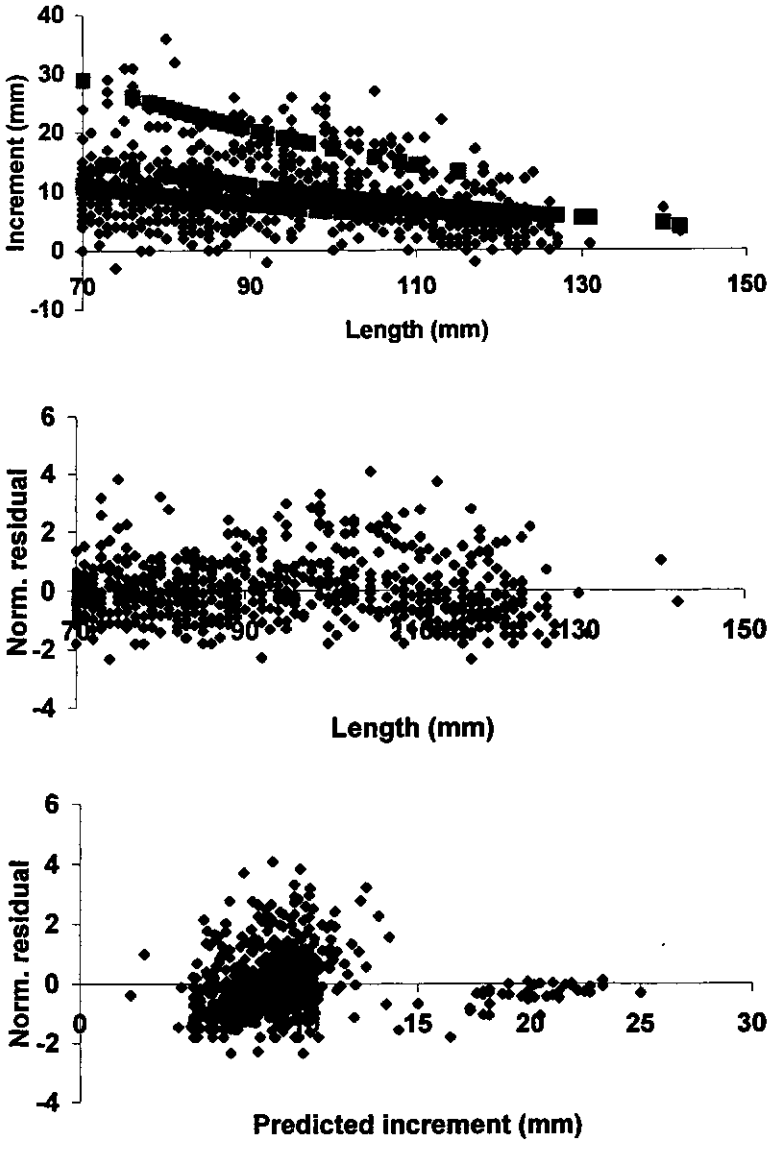

Figure 35: Fit of the exponential growth model to all the PAU 7 tag-recapture data combined. Caption as for Figure 30 except that the model is not linear.

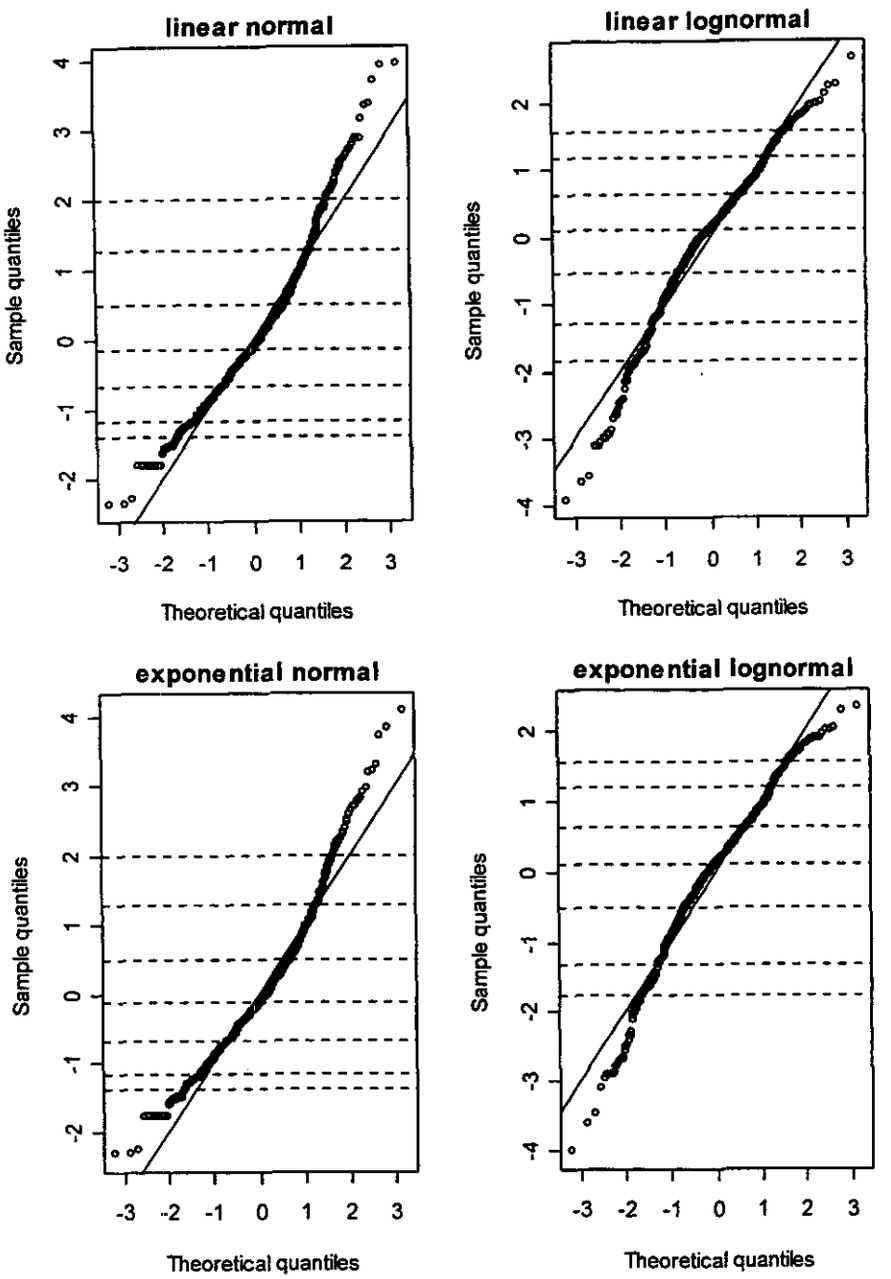

Figure 36: Quantile-quantile plots of the normalised residuals from each of the four fits to the combined PAU 7 tag-recapture data described in the text.

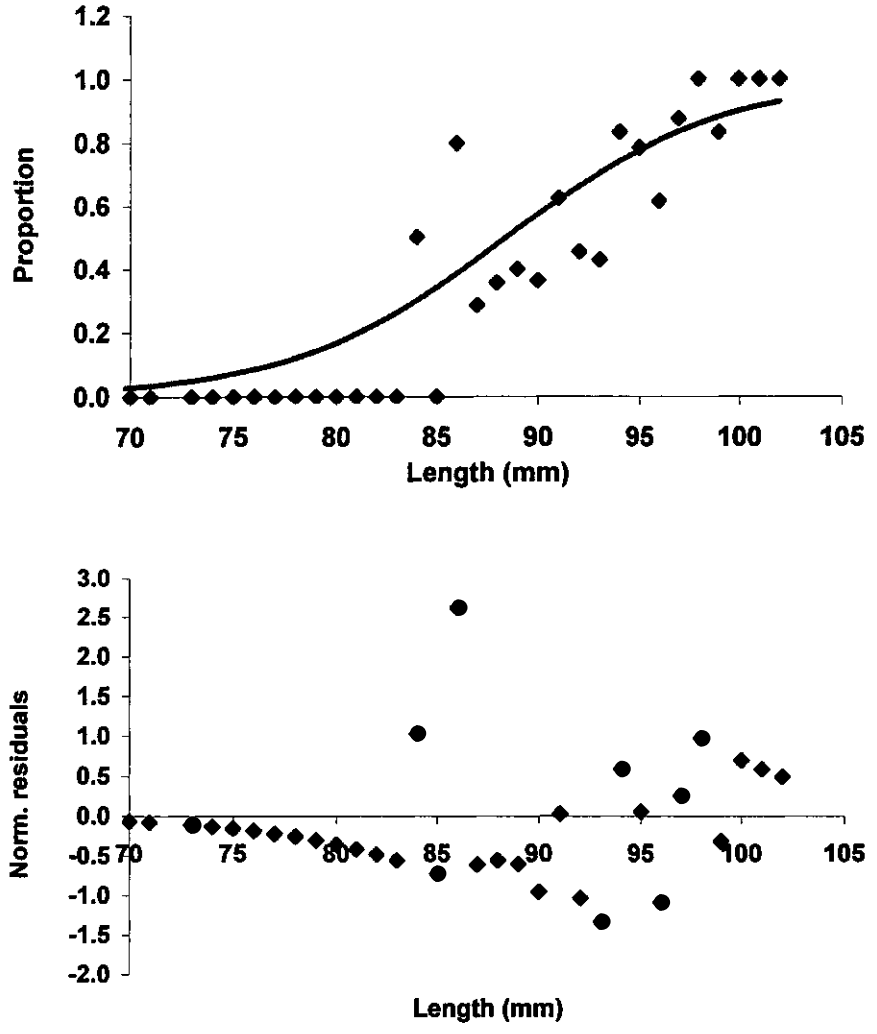

Figure 37: Fit of the model to observed proportion mature-at-length data (top) and residuals (below).

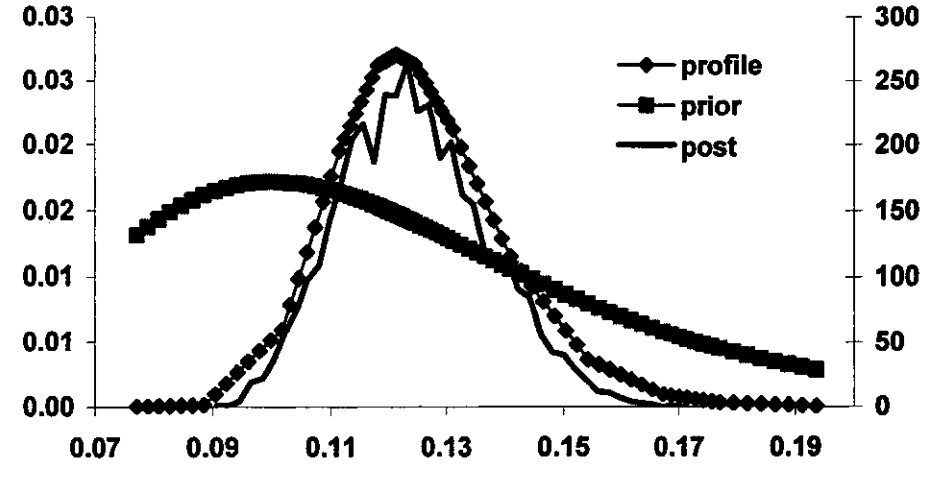

Figure 38: Comparing the prior and posterior distributions and the likelihood profile from the MPD fit for *M*.

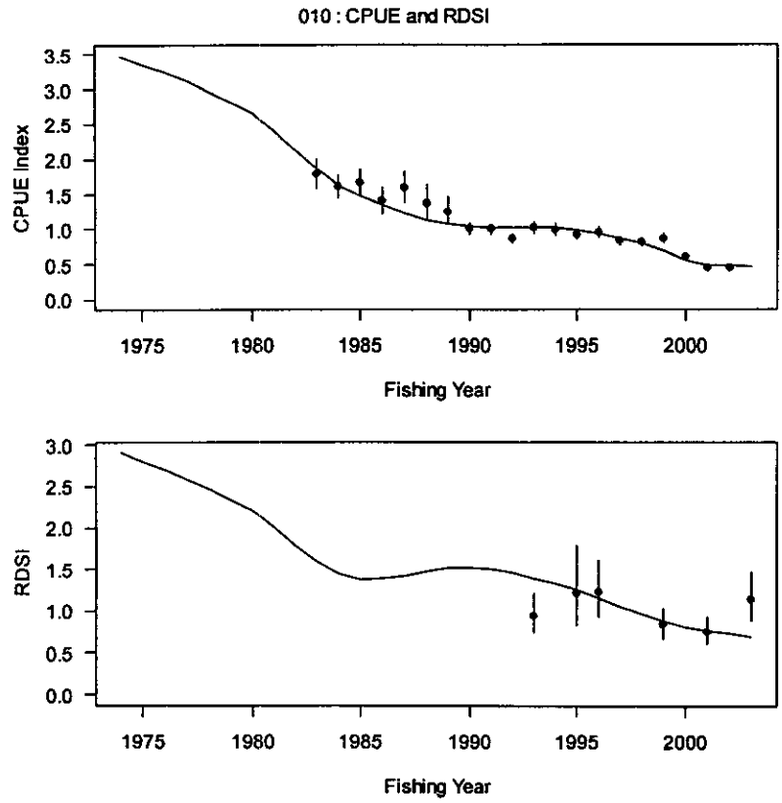

Figure 39: Observed (dots) and predicted (solid line) CPUE (top) and research diver survey indices (RDSI) (bottom) for the base case MPD fit for PAU 7. Error bars show the standard error term used by the model in fitting.

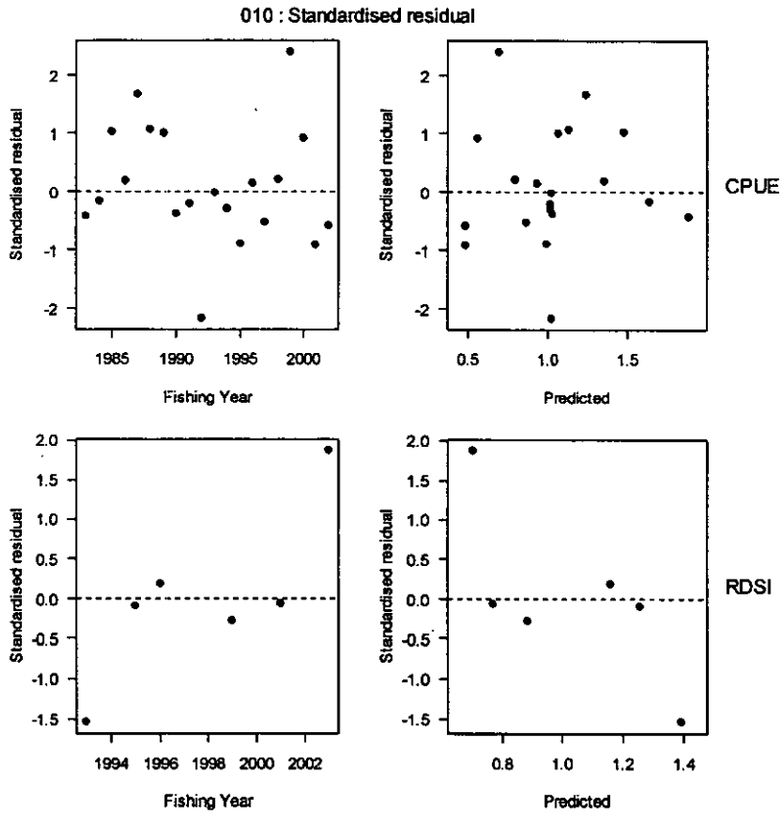

Figure 40: Standardised residuals for CPUE (top) and RDSI (bottom) for the base case MPD fit for PAU 7.

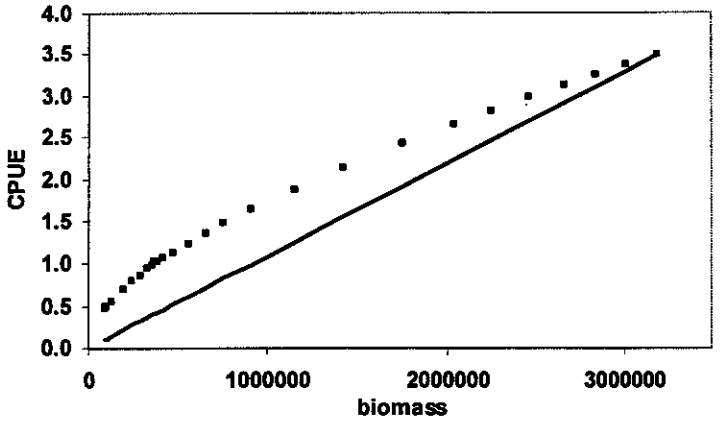

Figure 41: Showing the base case MPD relation between recruited biomass and predicted CPUE. The 45-degree line shows what would be expected with no hyperstability or hyperdepletion.

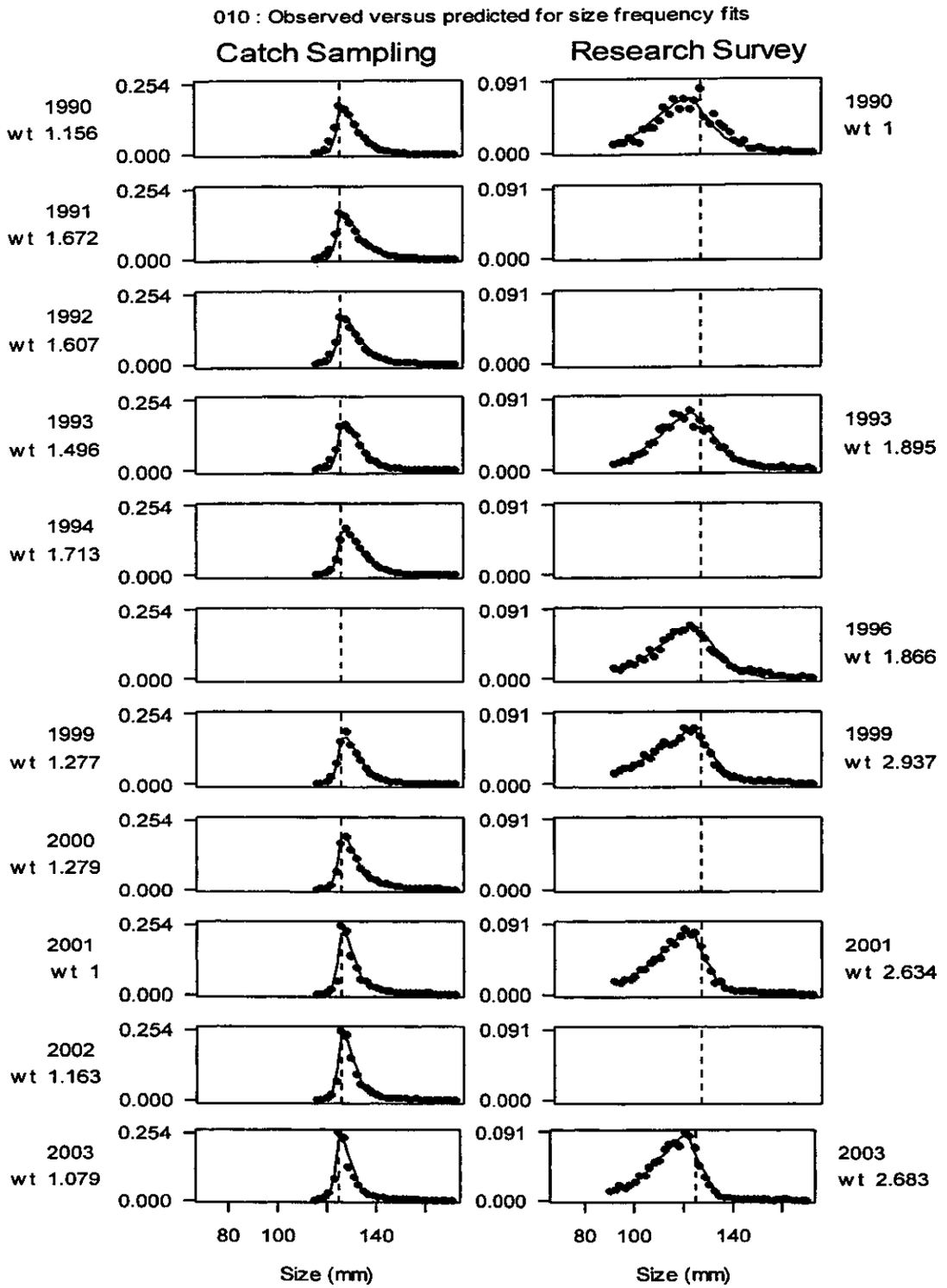

Figure 42: Observed (dots) and predicted (lines) proportions-at-length from commercial catch sampling (left) and research diver surveys (right) for the base case MPD fit for PAU 7. The number under each year is the relative weight given to the dataset, based on the number of paua measured and (for the research diver surveys) the number of strata sampled.

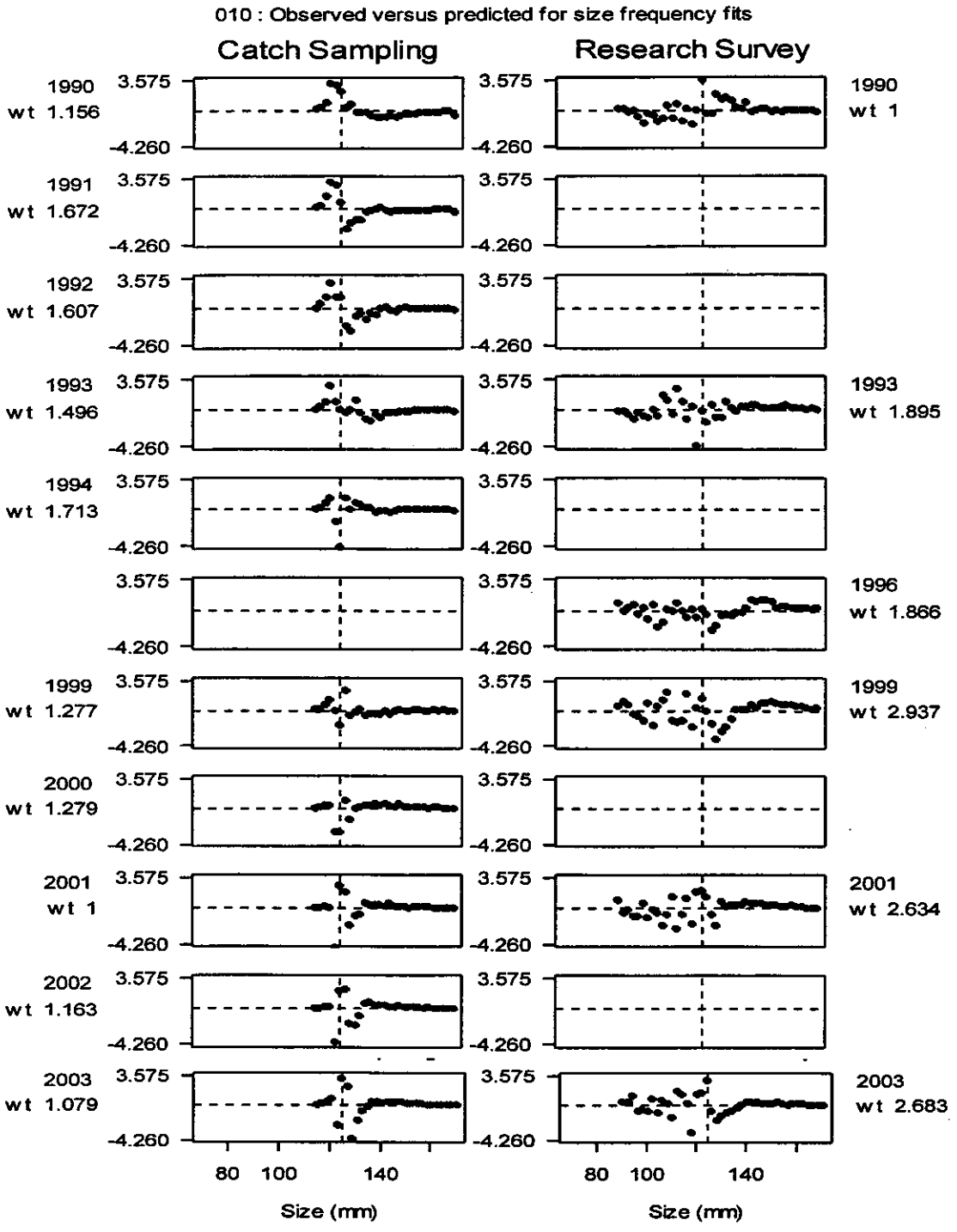

Figure 43: Residuals from the fits to proportions-at-length data seen in Figure 42 from the base case MPD fit for PAU 7.

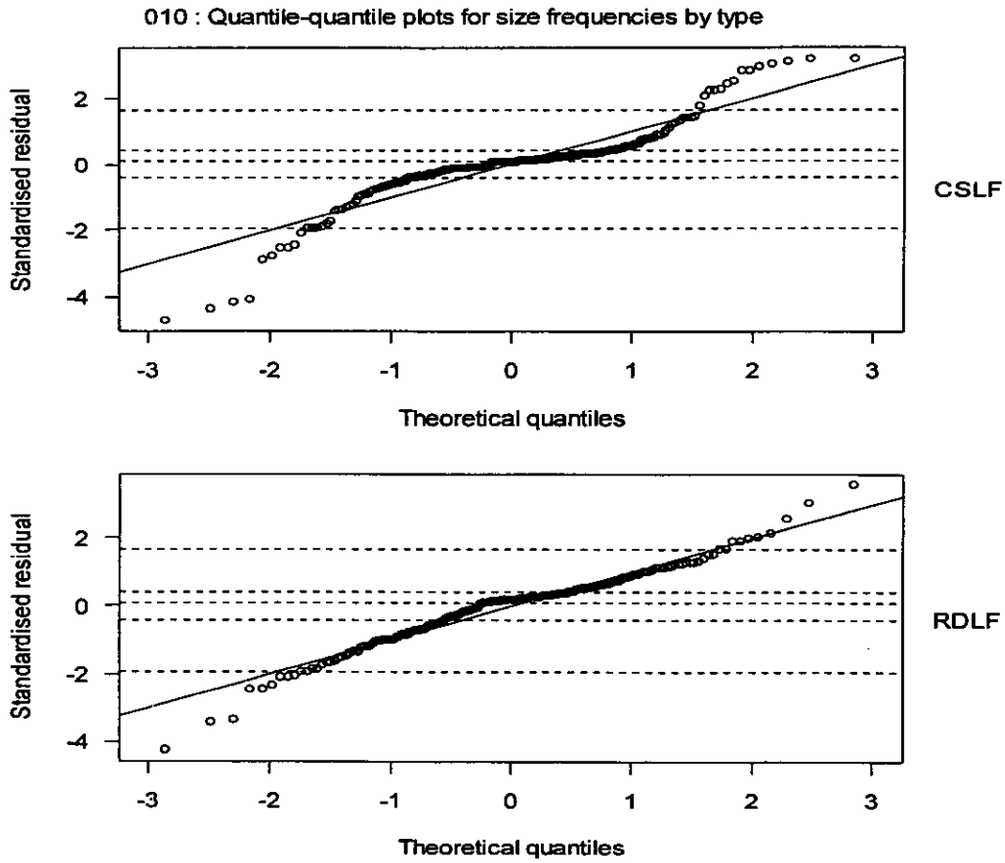

Figure 44: Q-Q plot of residuals for the fits to proportions-at-length from commercial catch sampling (top) and research diver surveys (bottom) from the base case MPD fit for PAU 7.

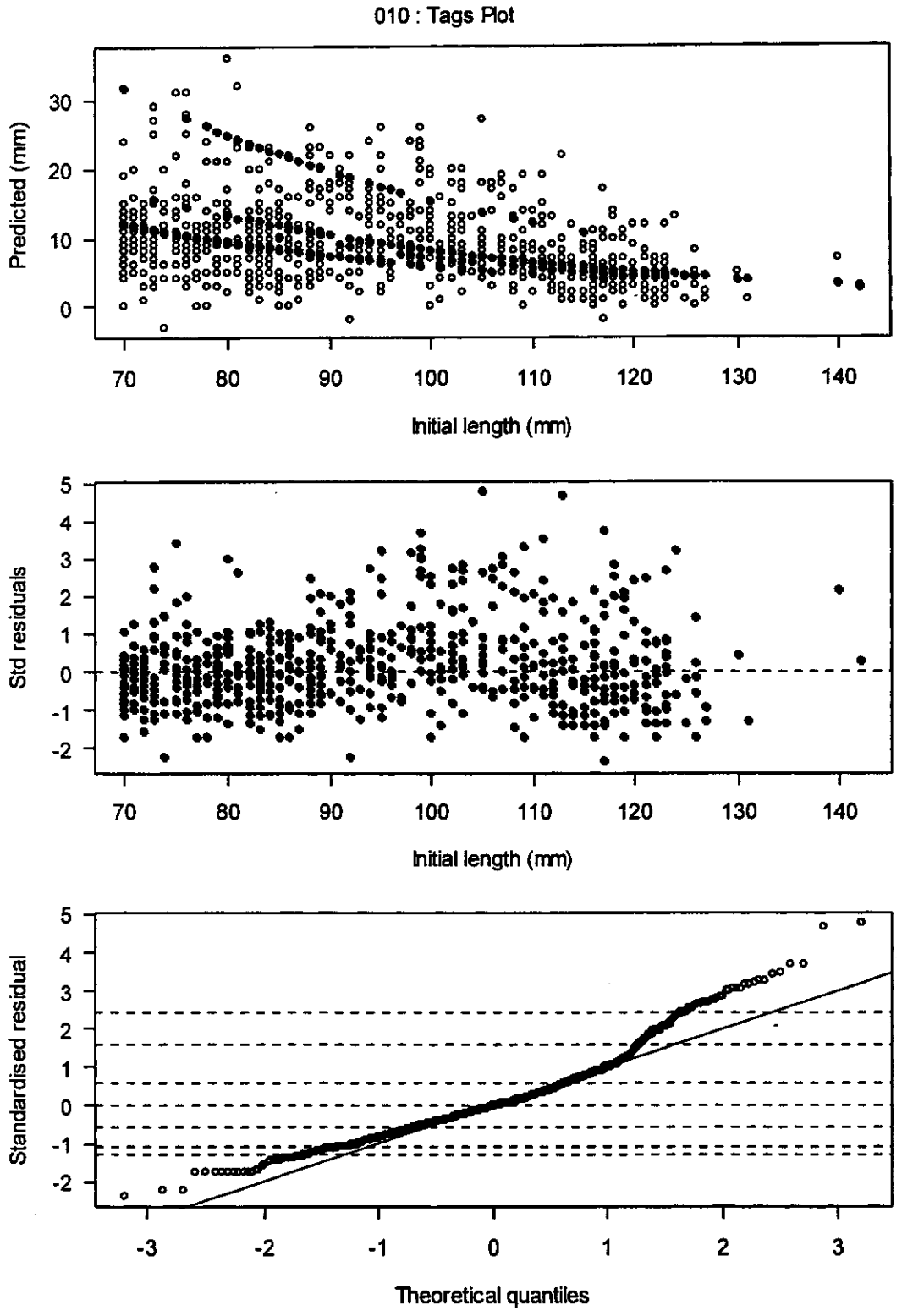

Figure 45: Top: predicted (closed circles) and observed (open circles) increments vs initial length of tagged paua from the base case MPD fit for PAU 7; middle: standardised residuals plotted against initial length; bottom: Q-Q plot of standardised residuals. For each length, there can be more than one predicted increment because different animals were at liberty for different periods.

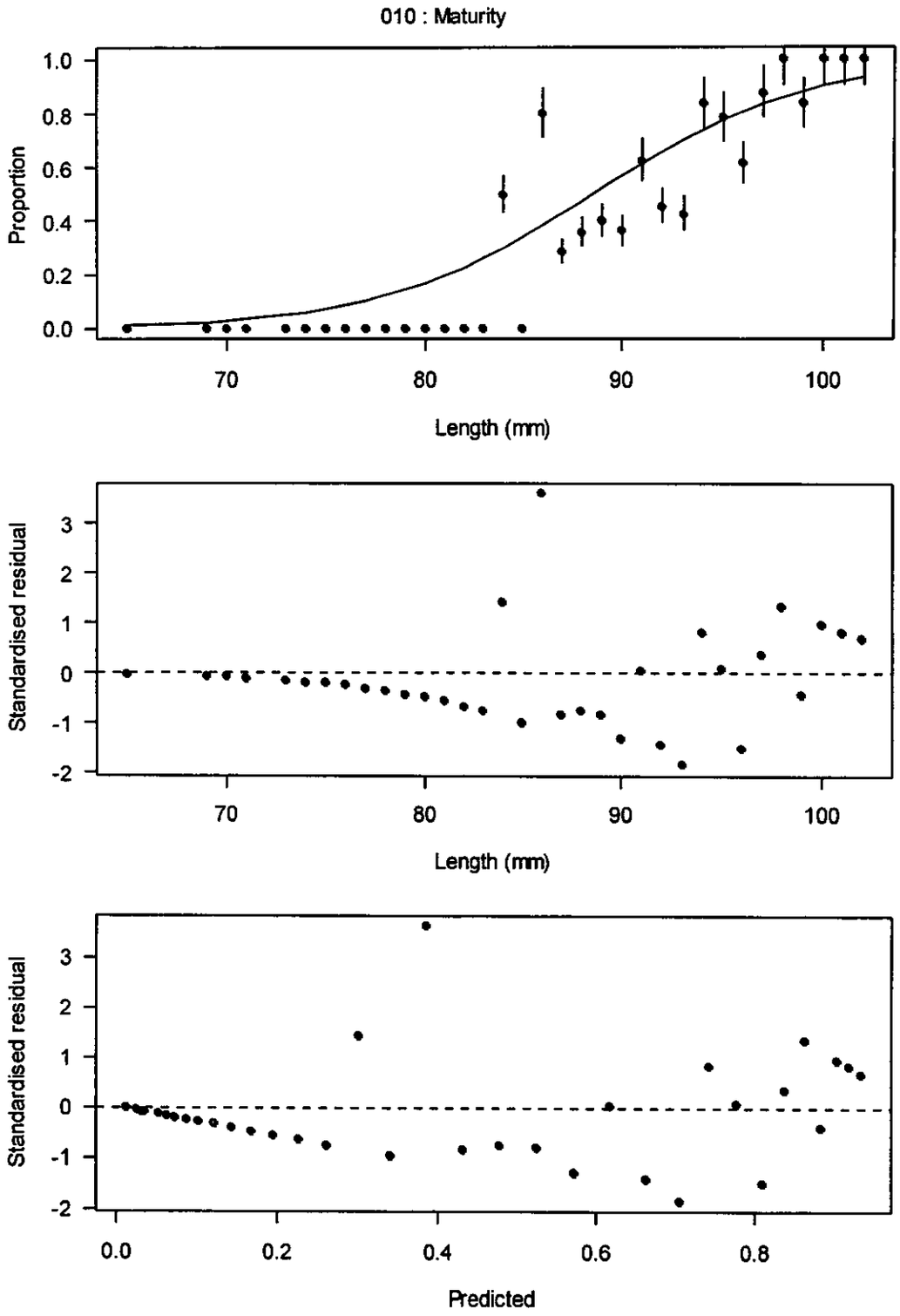

Figure 46: Top: predicted (line) and observed (circles) proportion mature-at-length from the base case MPD fit for PAU 7; middle: standardised residuals plotted against length; bottom: standardised residuals plotted against predicted proportion.

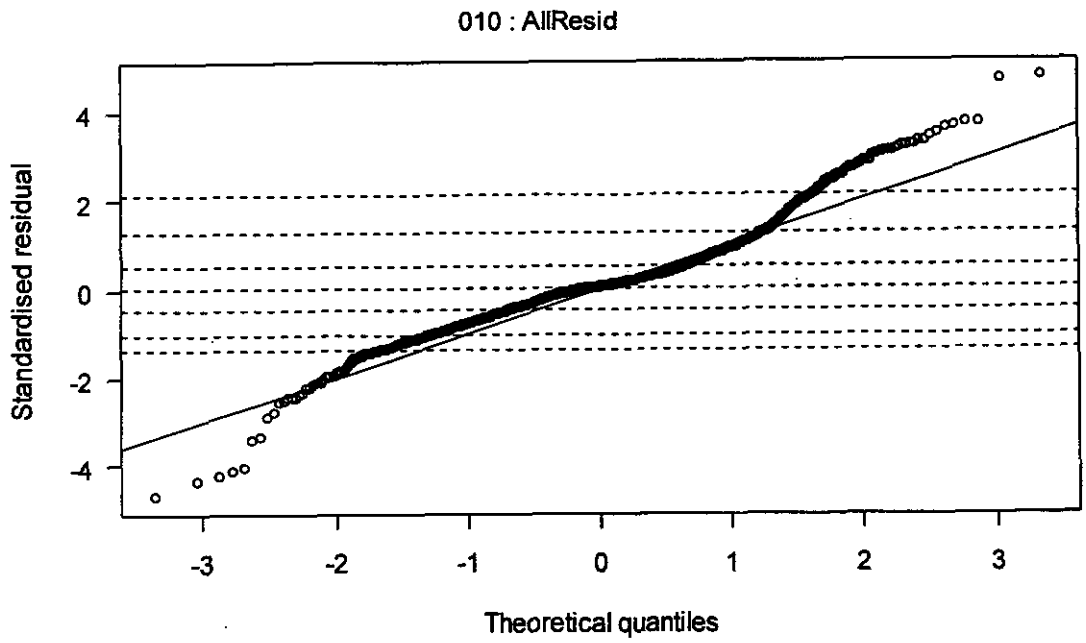

Figure 47: Q-Q plot of the normalised standard residuals from all datasets used by the model in the base case MPD fit.

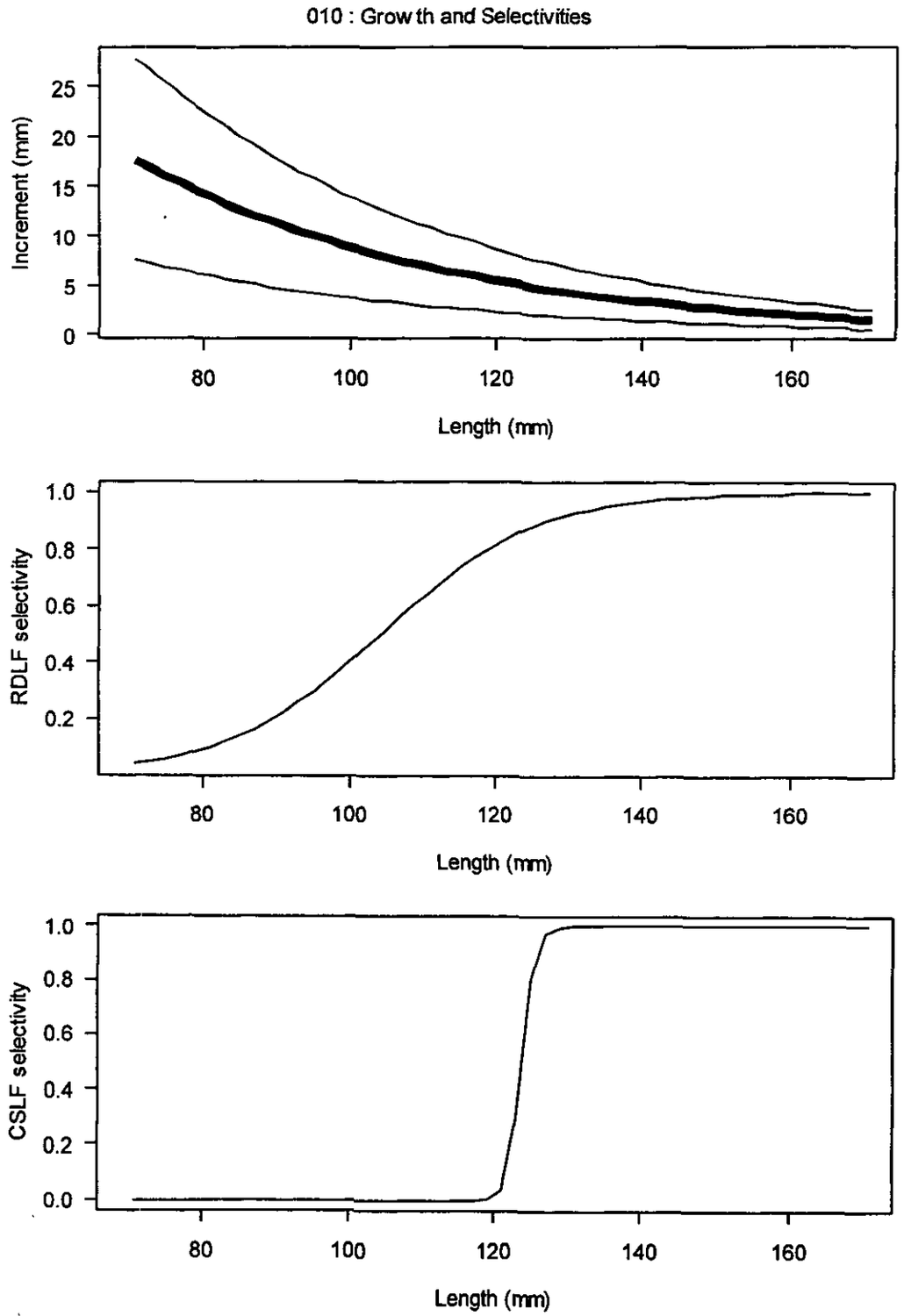

Figure 48: Top: predicted annual growth increment (thick line) *vs* initial length of paua, shown with one standard deviation around the increment (thin line); middle: research diver survey selectivity; bottom: commercial catch sampling selectivity.

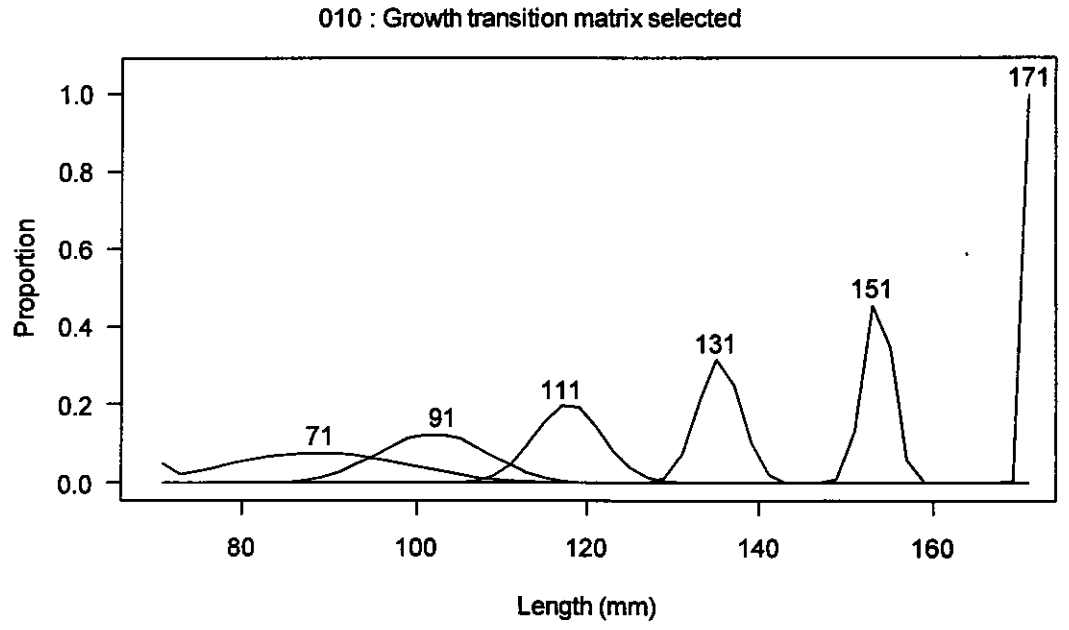

Figure 49: Sections of the growth transition matrix from the base case MPD fit in PAU 7. These are, for each initial length shown, the probability distribution of expected length after growth.

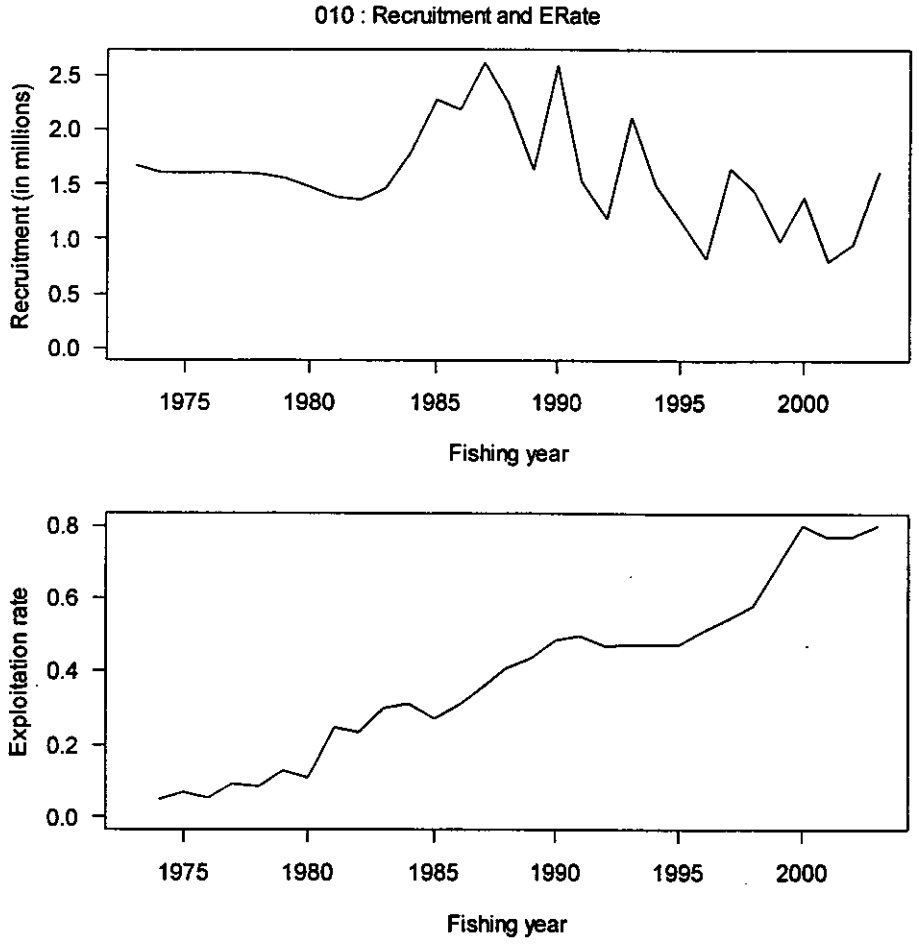

Figure 50: Recruitment in millions of animals (top) and exploitation rate (bottom) from the base case MPD fit in PAU 7.

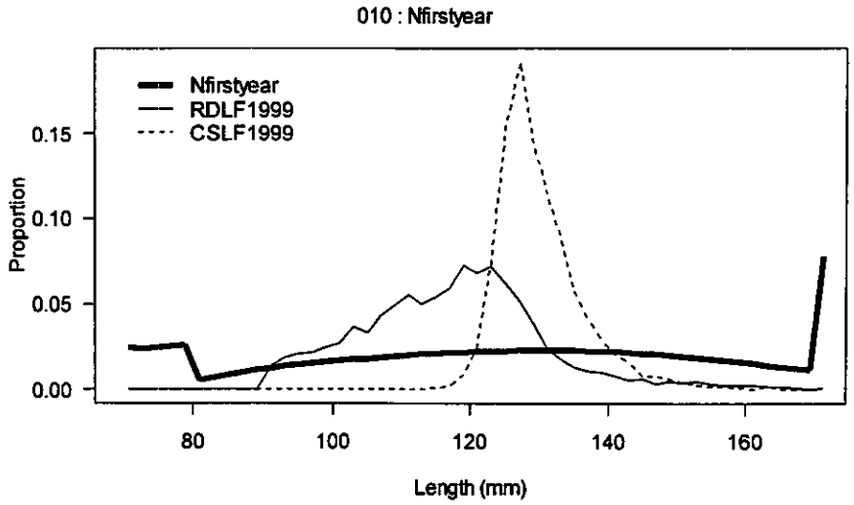

Figure 51: Comparison of length frequencies in the virgin population from the base case MPD fit in PAU 7 (heavy line), research diver surveys in 1999 (thin line) and commercial catch sampling in 1999 (dashed line).

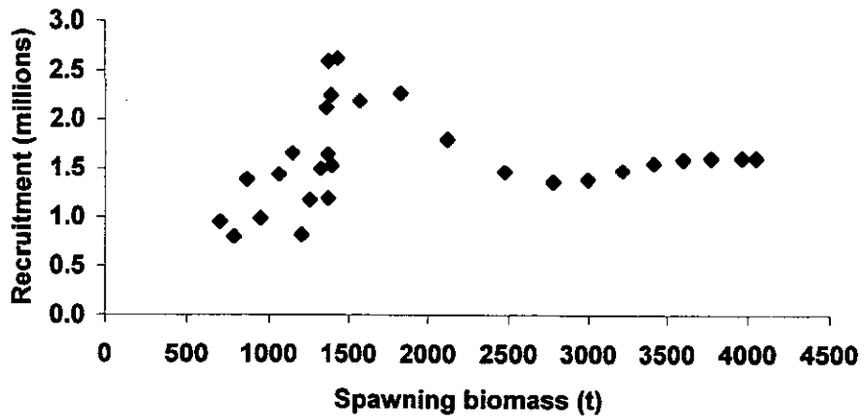

Figure 52: Recruitment plotted against spawning biomass two years earlier from the base case MPD fit in PAU 7.

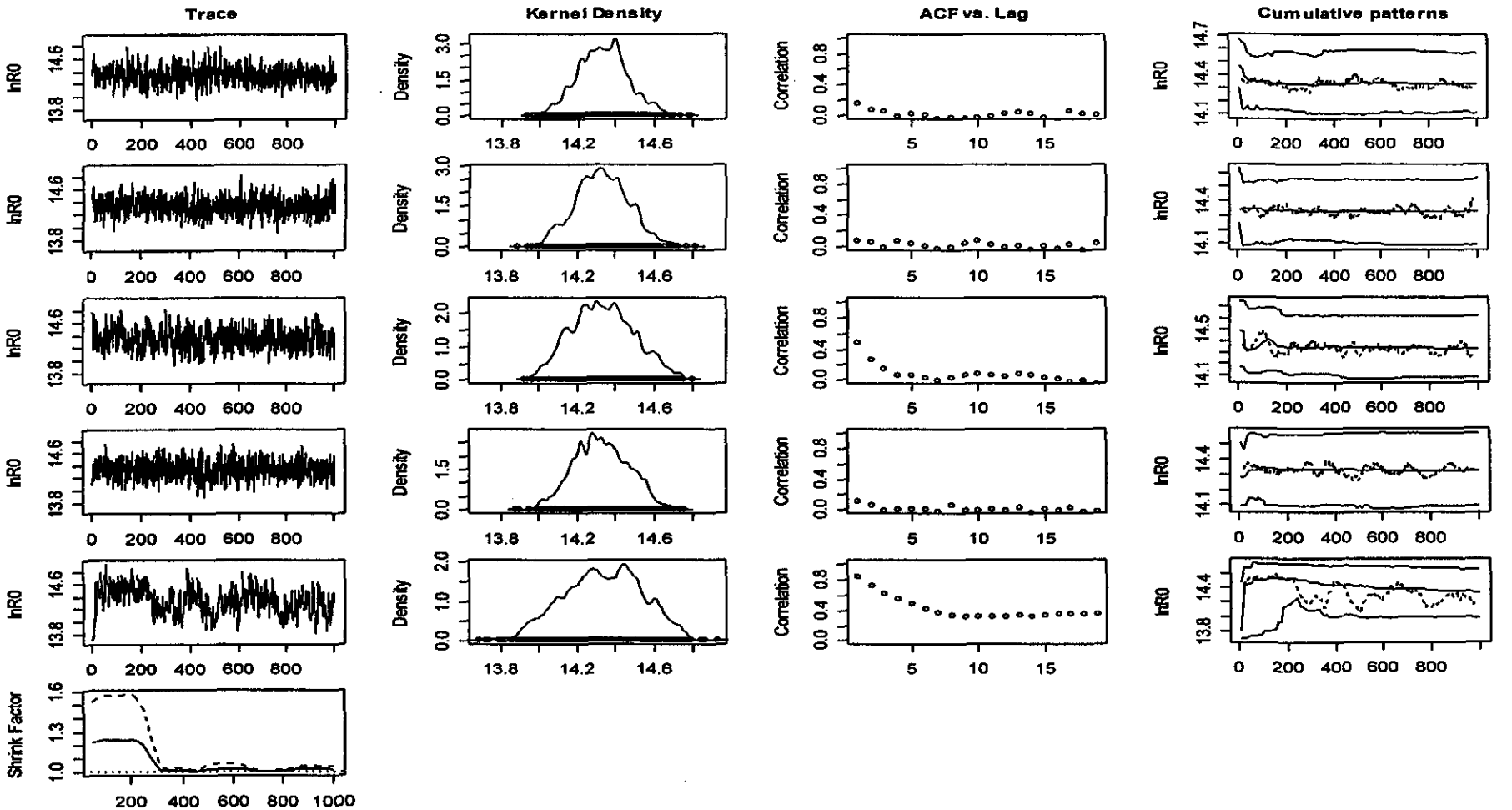

Figure 53: Diagnostics from the five McMC chains for the parameter ln(*R0*). Left: traces; second from left: posterior distribution; second from right: serial autocorrelation; right: the cumulative fifth and 95th percentiles of the traces, the cumulative median and the running mean over 40 samples.

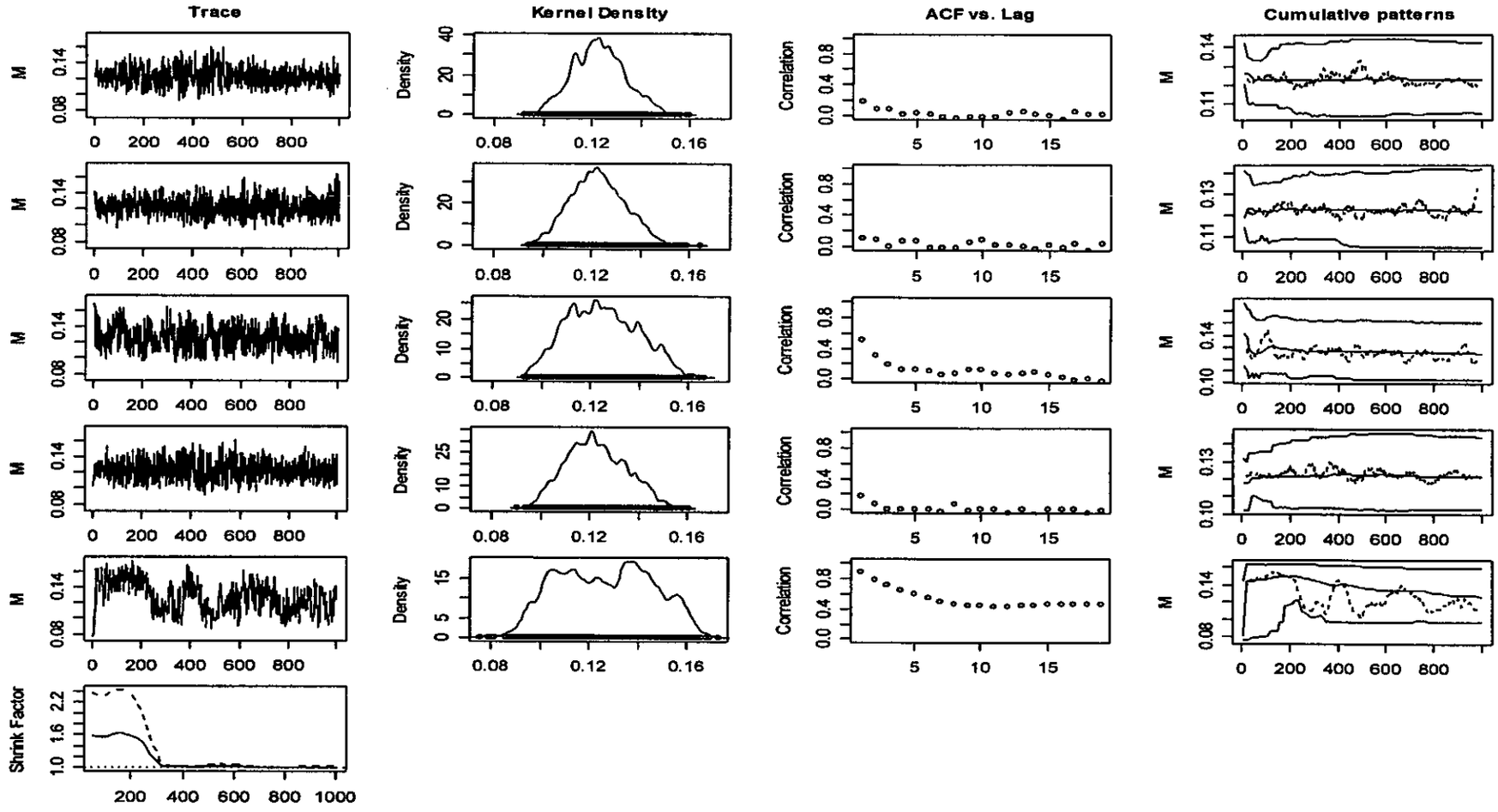

Figure 54: Diagnostics from the five McMC chains for the parameter *M*. Caption as for Figure 53.

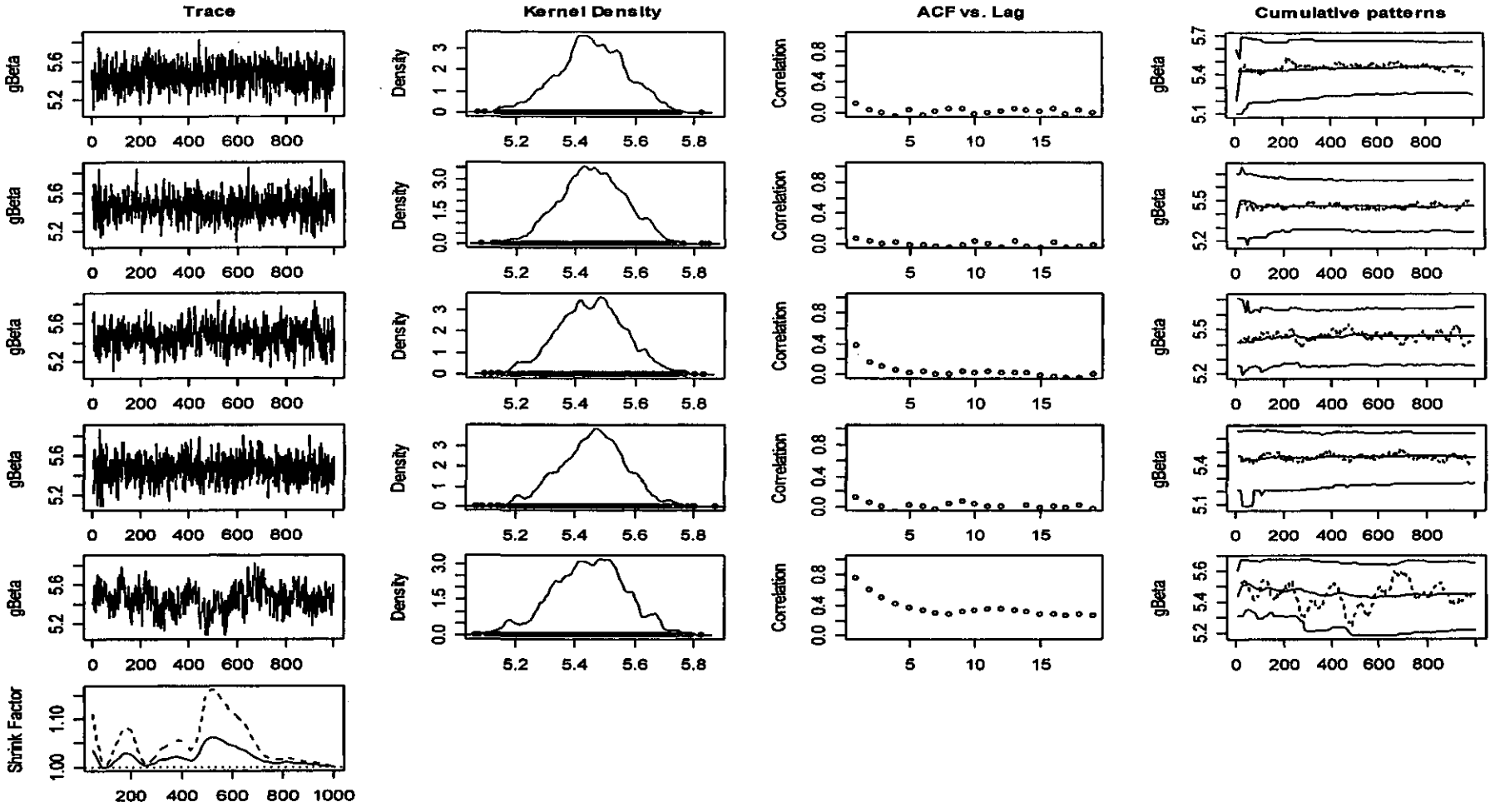

Figure 55: Diagnostics from the five McMC chains for the parameter g_β. Caption as for Figure 53.

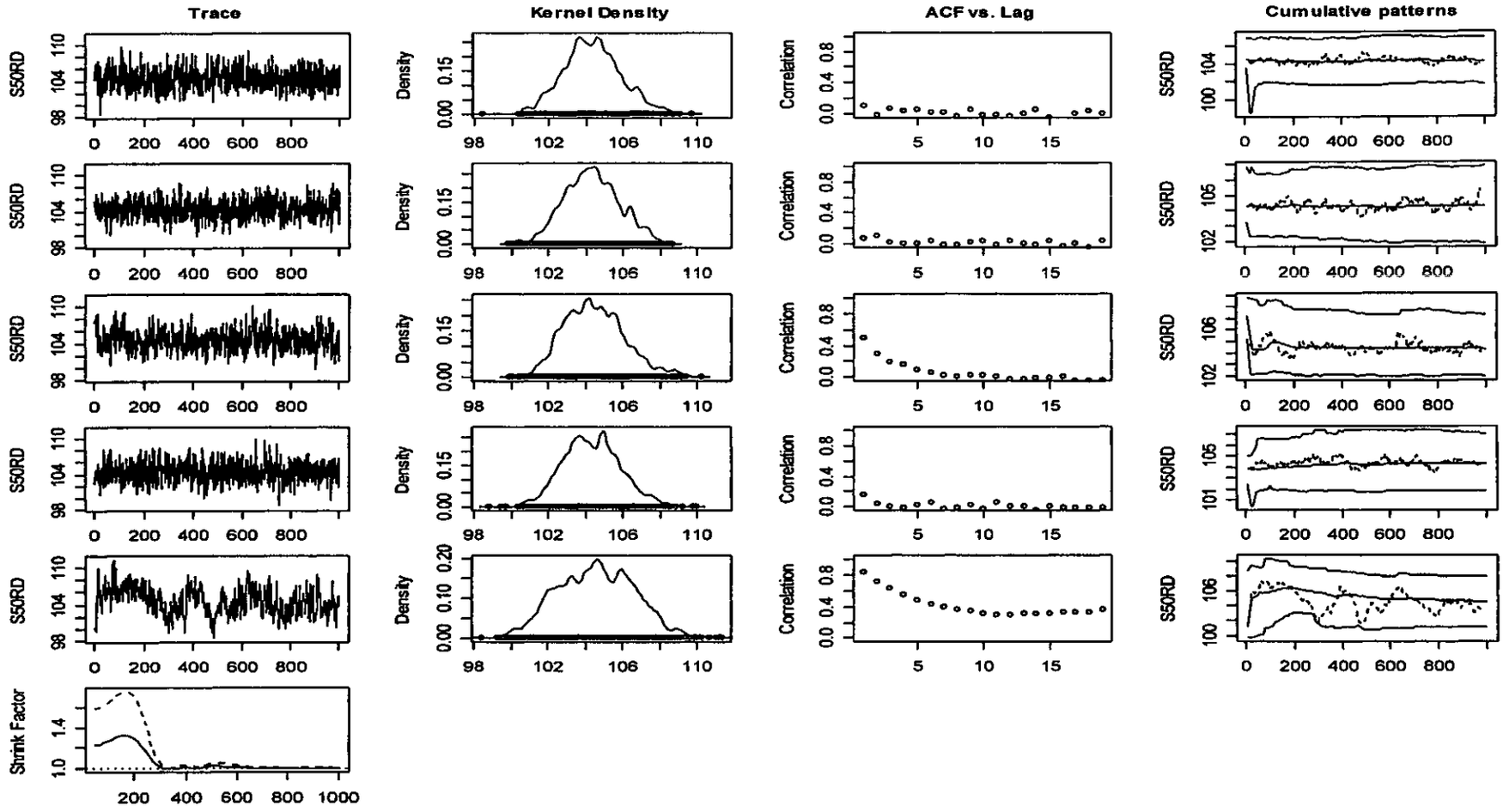

Figure 56: Diagnostics from the five McMC chains for the parameter T_{50}. Caption as for Figure 53.

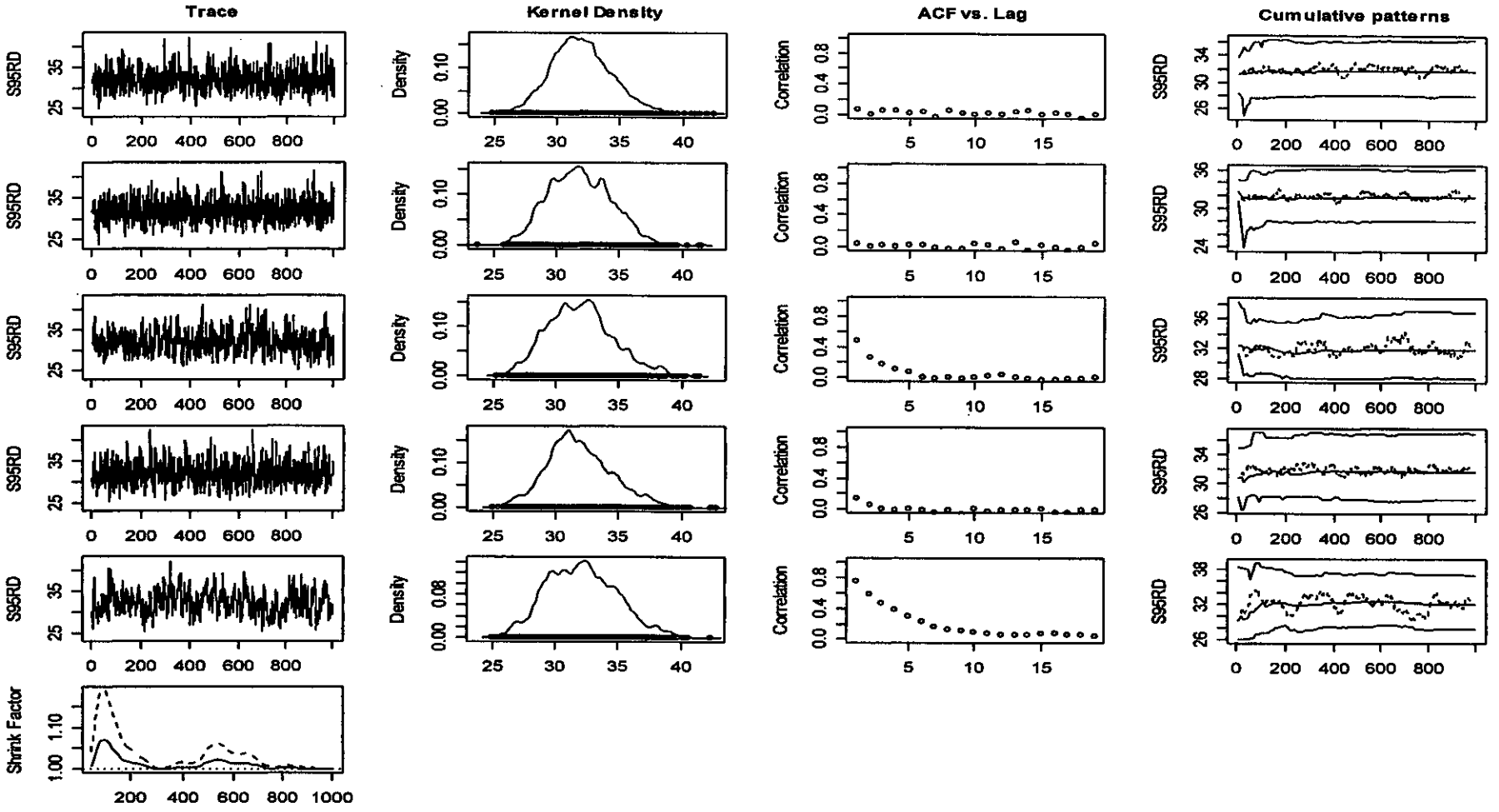

Figure 57: Diagnostics from the five McMC chains for the parameter T_{95-50}. Caption as for Figure 53.

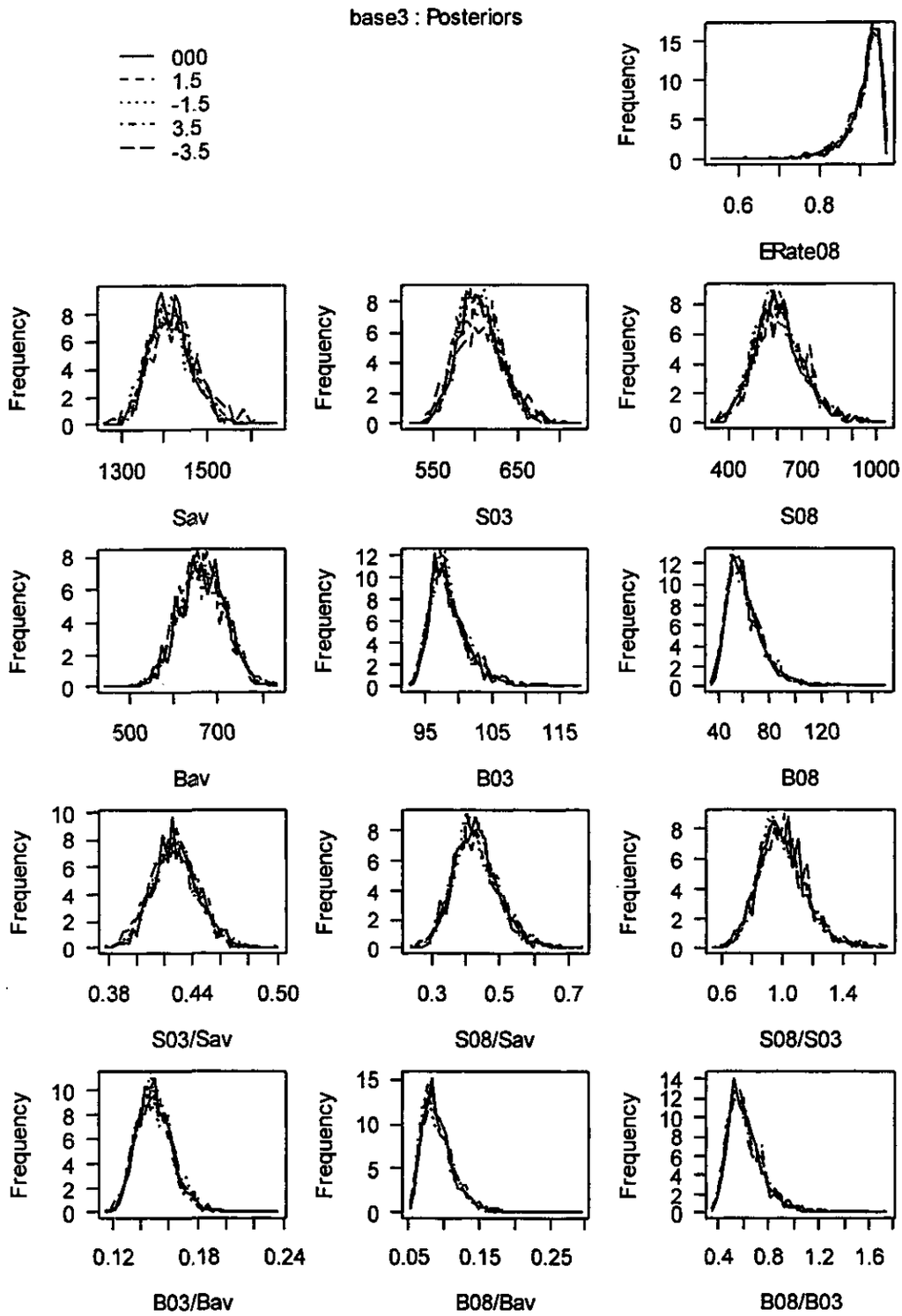

Figure 58: Posterior distributions of parameters and indicators from each of the five chains described in the text for the base case for PAU 7.

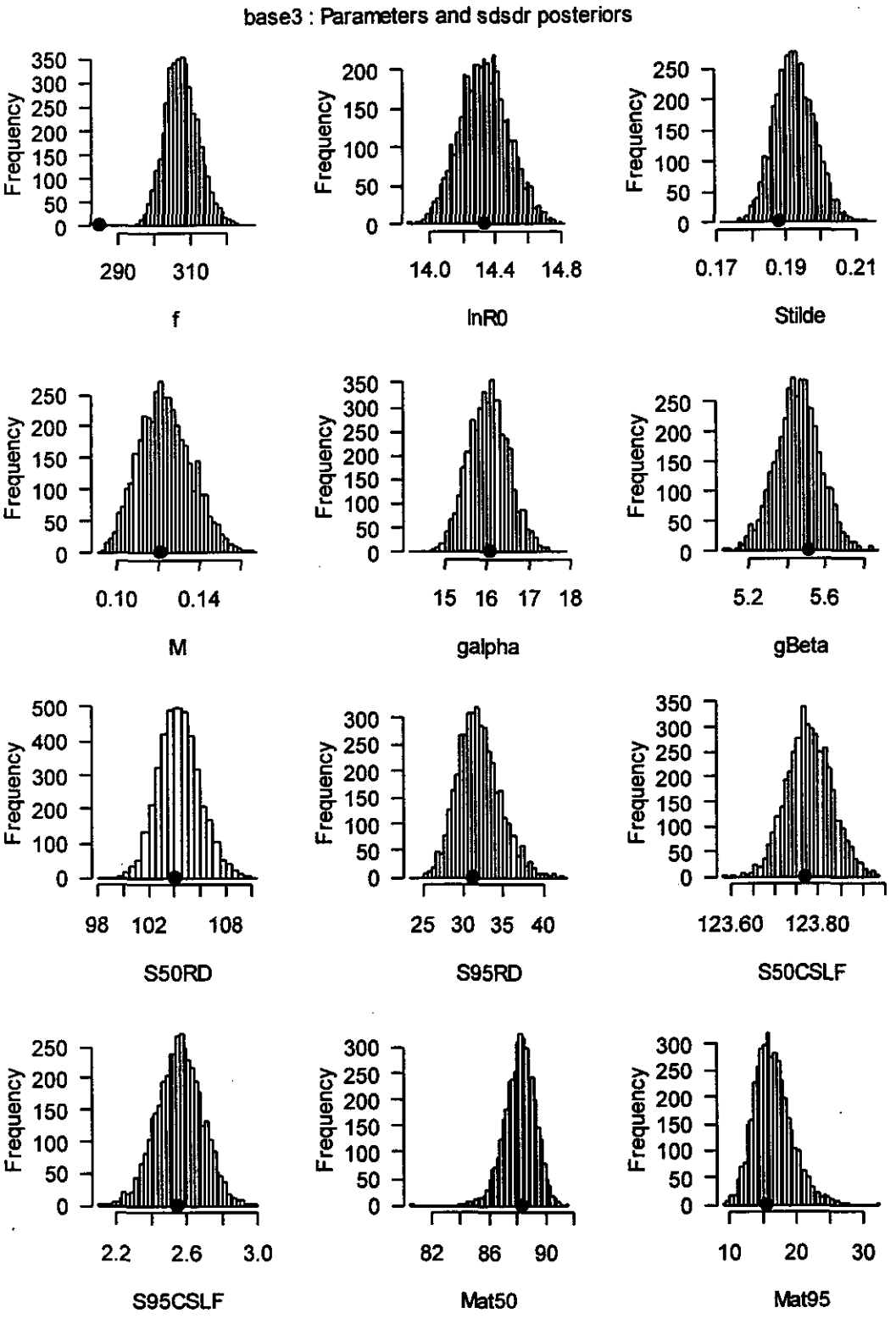

Figure 59: Posterior distributions of parameters and indicators from the combined chain for the base case for PAU7. The dark point shows the MPD estimate.

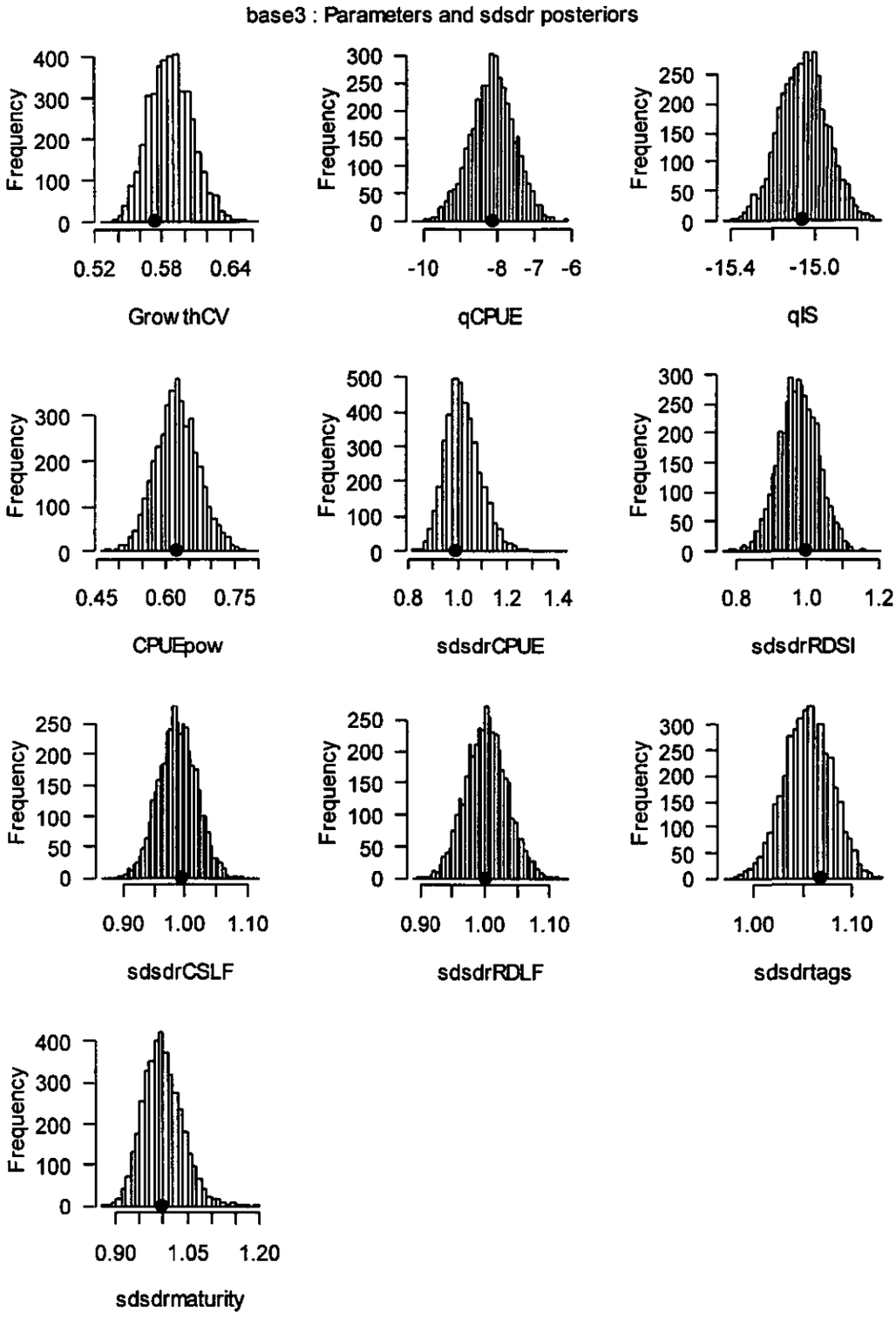

Figure 59: ***continued.***

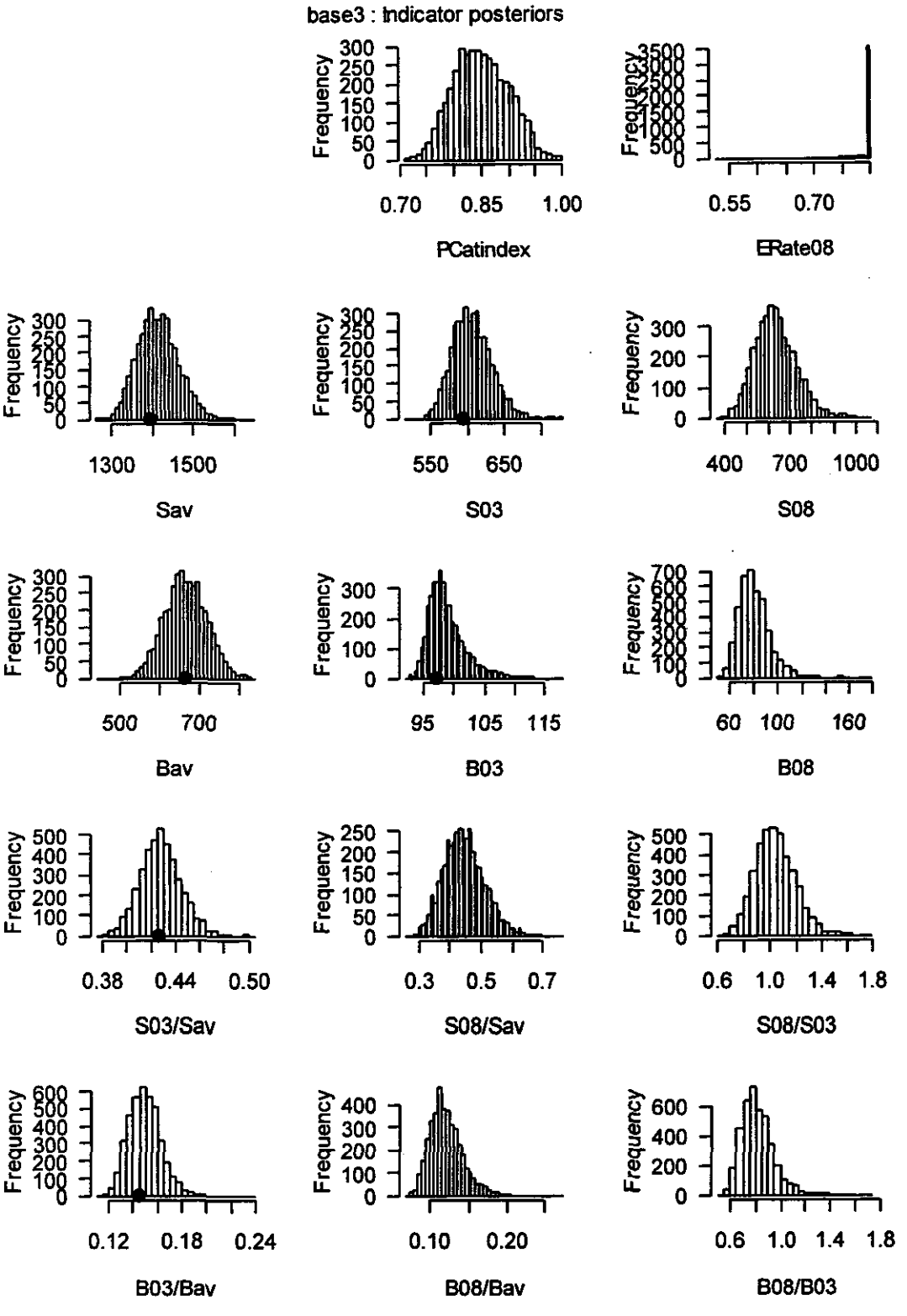

Figure 59: ***continued.***

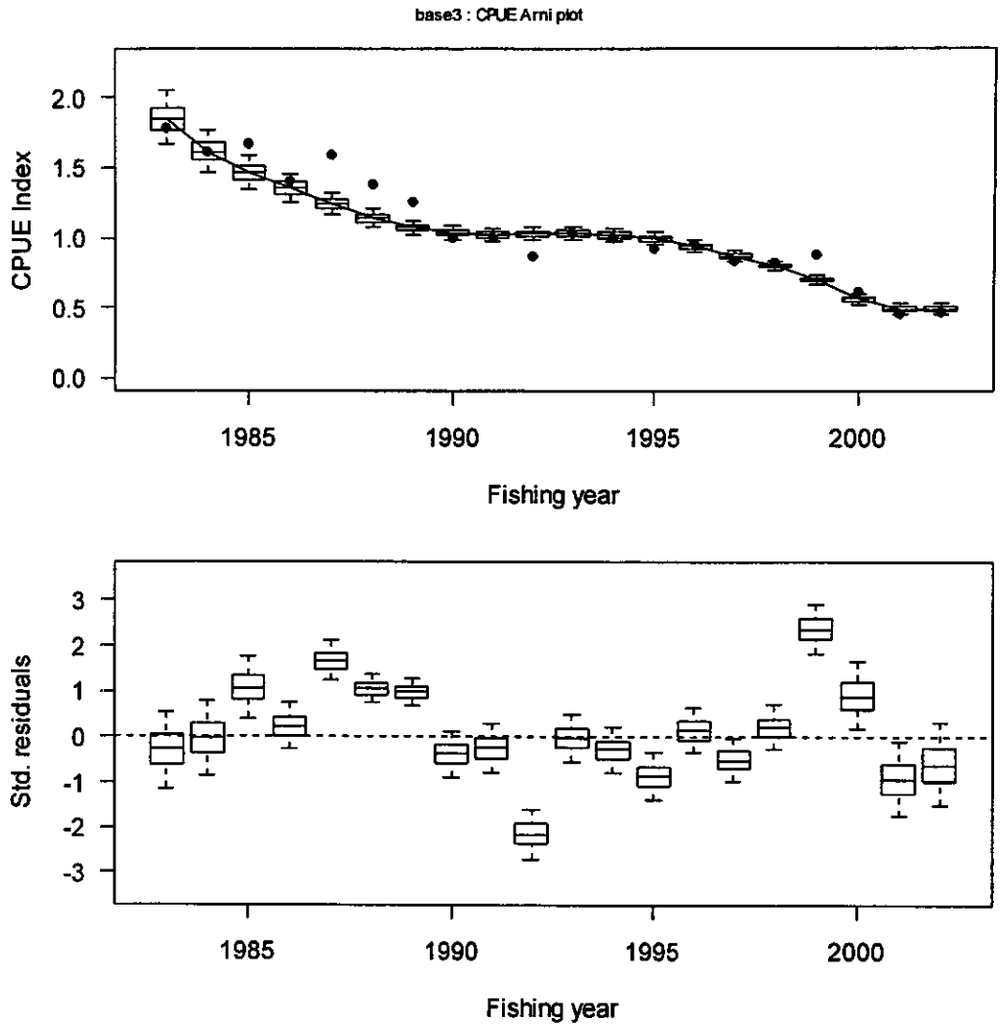

Figure 60: The posterior distributions of the fits to CPUE data (top) and the posterior distributions of the normalised residuals.

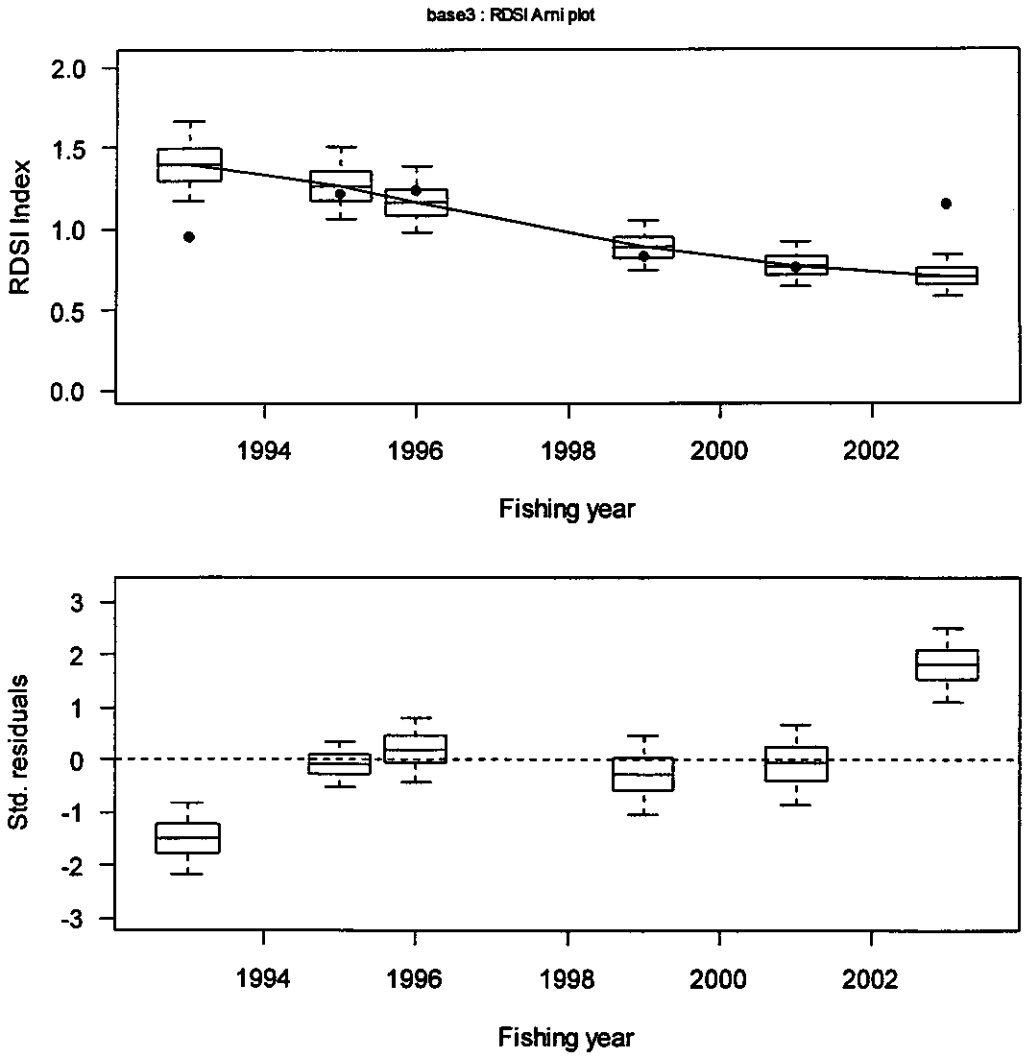

Figure 61: The posterior distributions of the fits to RDSI data (top) and the posterior distributions of the normalised residuals.

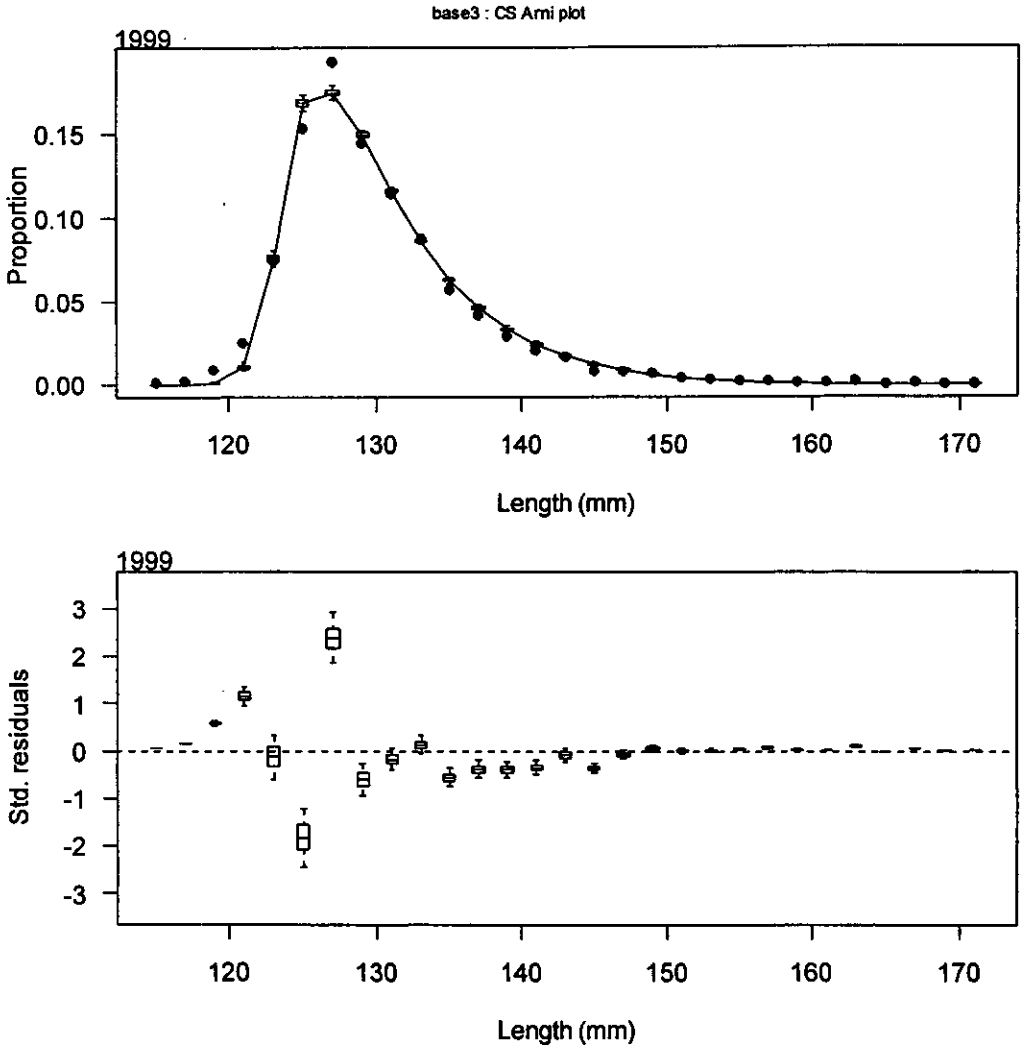

Figure 62: The posterior distributions of the fits to commercial catch sampling proportions-at-length from 1999 (top) and the posterior distributions of the normalised residuals.

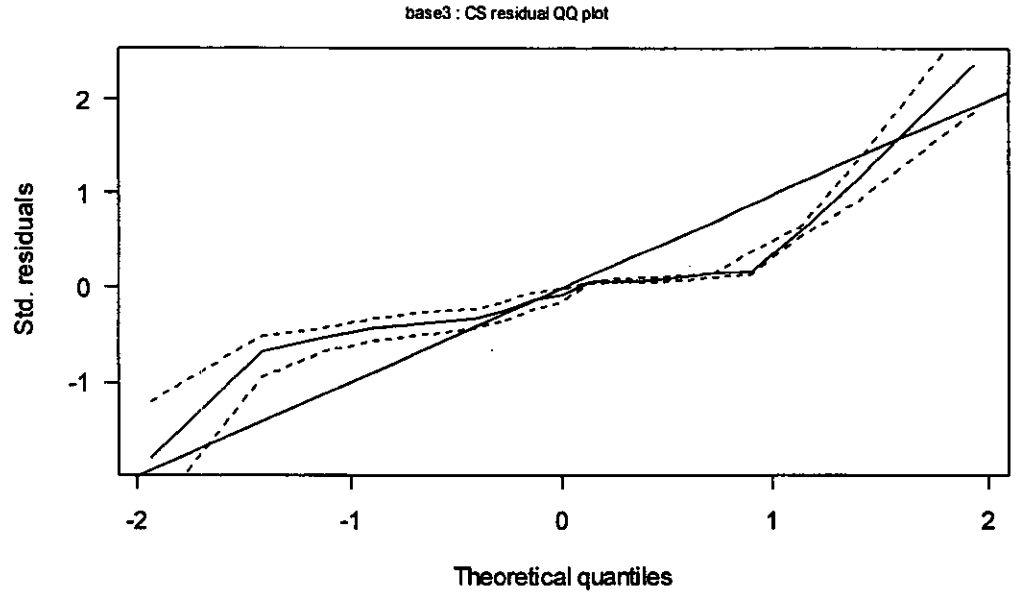

Figure 63: Q-Q plot of the normalised residuals from Figure 62.

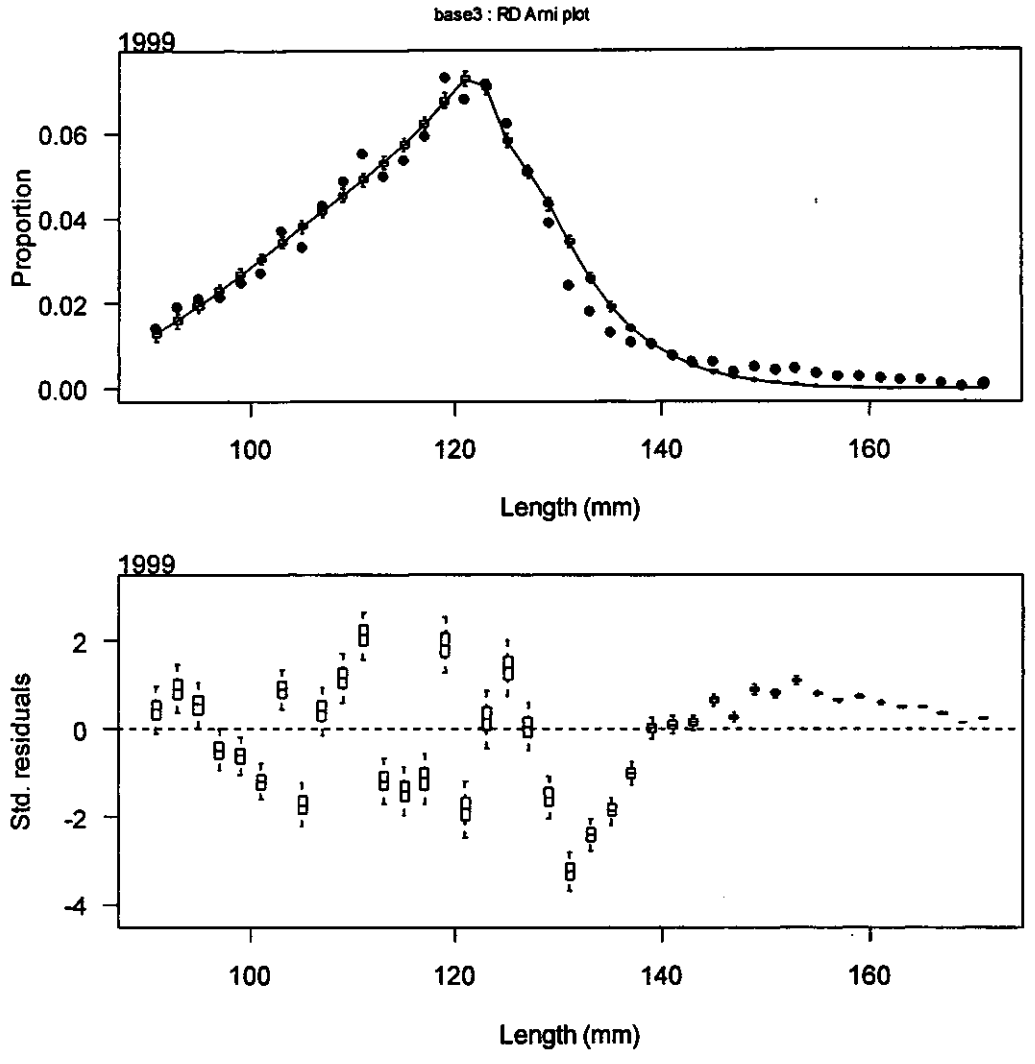

Figure 64: The posterior distributions of the fits to research diver survey proportions-at-length from 1999 (top) and the posterior distributions of the normalised residuals.

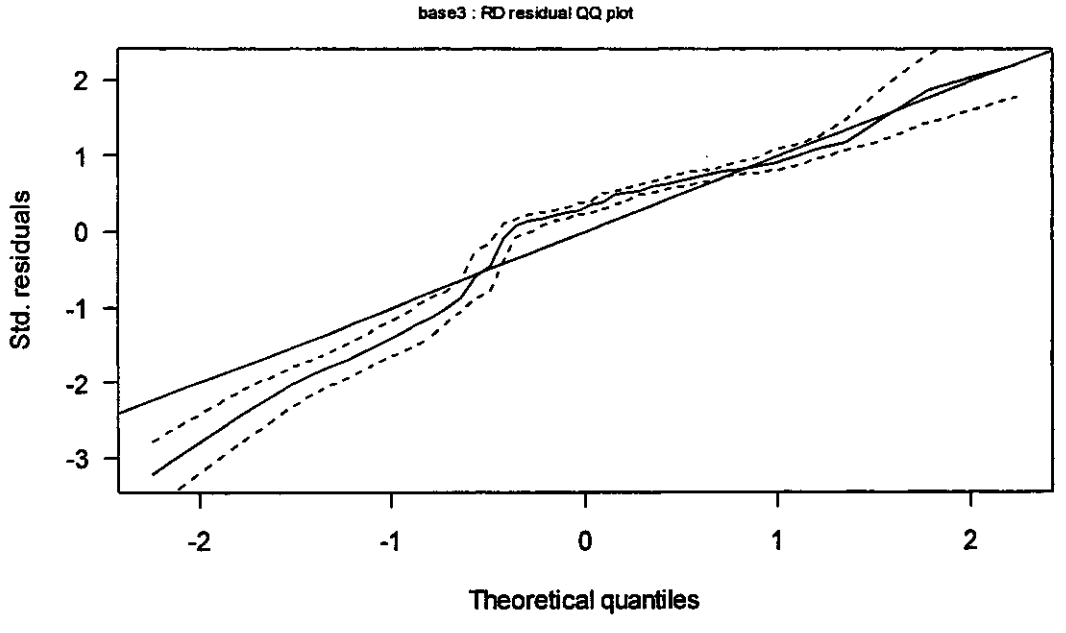

Figure 65: Q-Q plot of the normalised residuals from Figure 64.

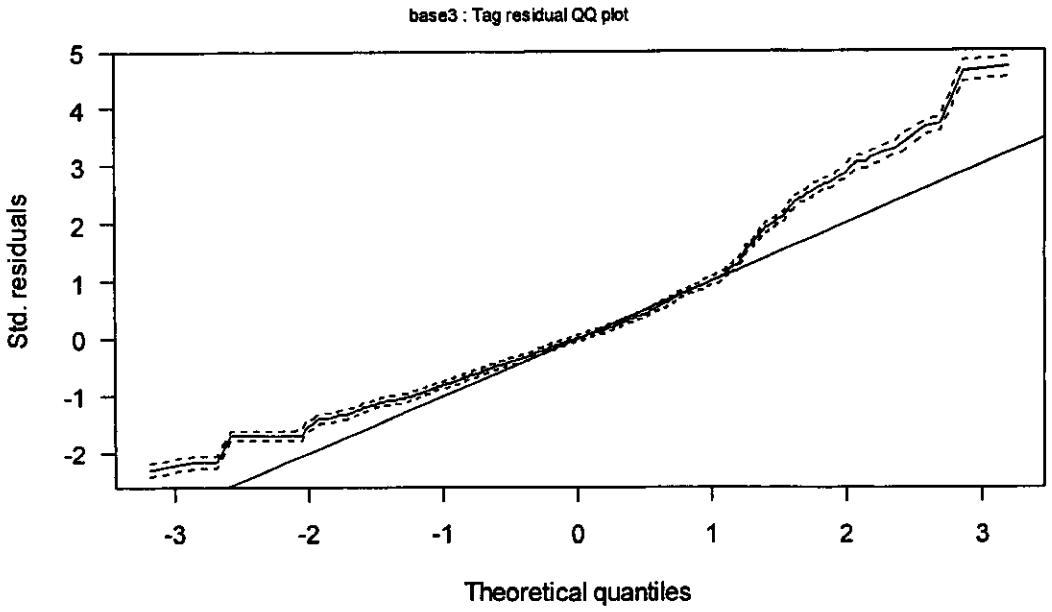

Figure 66: Q-Q plot of the normalised residuals from the posterior distributions of fits to the tag-recapture data.

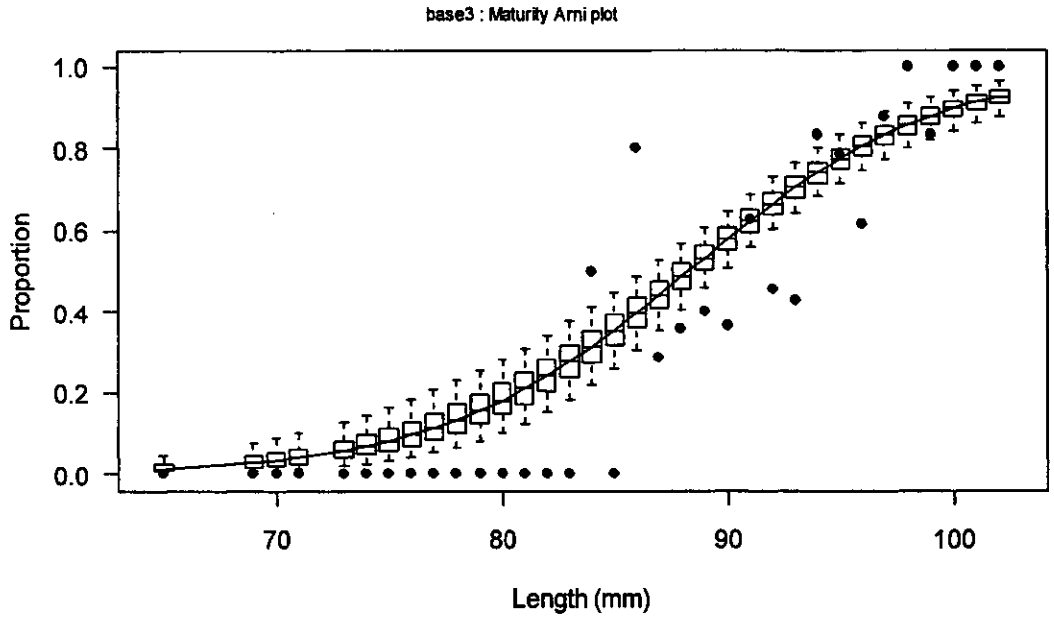

Figure 67: Posterior distribution of the fit to the maturity-at-length data.

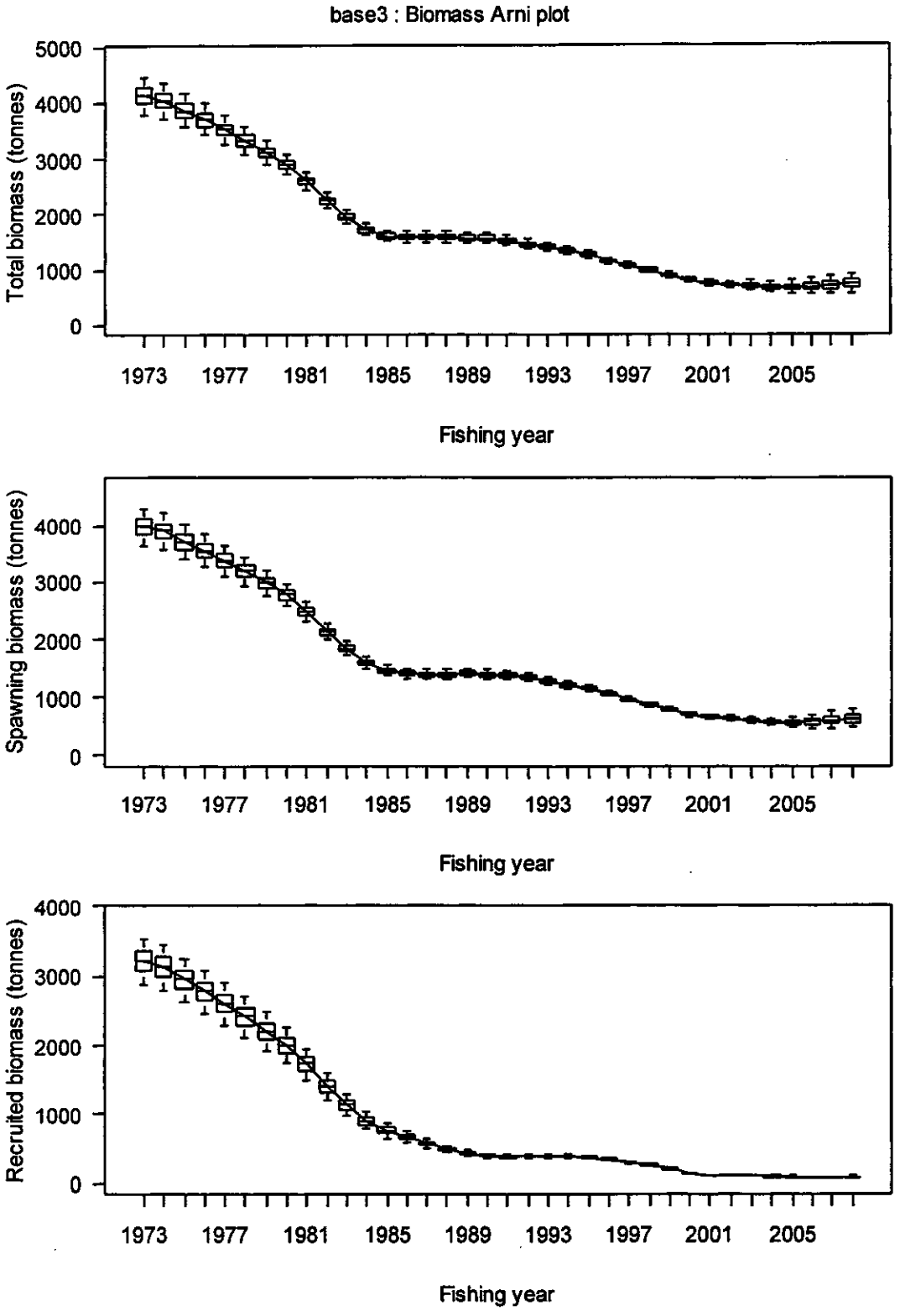

Figure 68: The posterior biomass trajectories for total (top), spawning (middle) and recruited (bottom) biomass for the base case for PAU 7. For each year, the figure shows the median of the posterior (horizontal bar), the 25th and 75th percentiles (box) and 5th and 95th percentiles of the posterior.

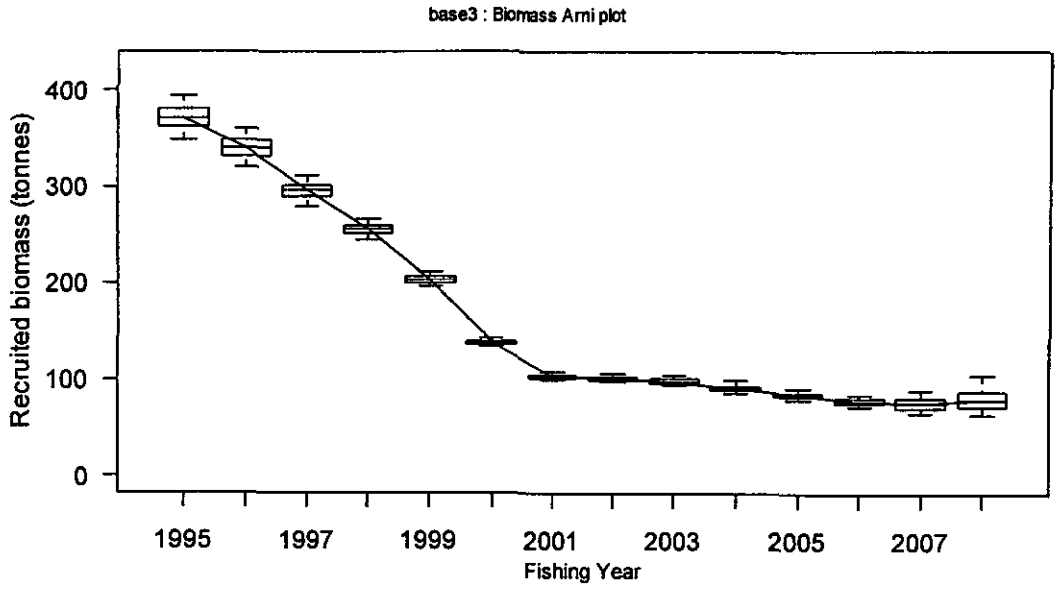

Figure 69: Posterior distribution of the biomass trajectory for recruited biomass from 1995 onwards.

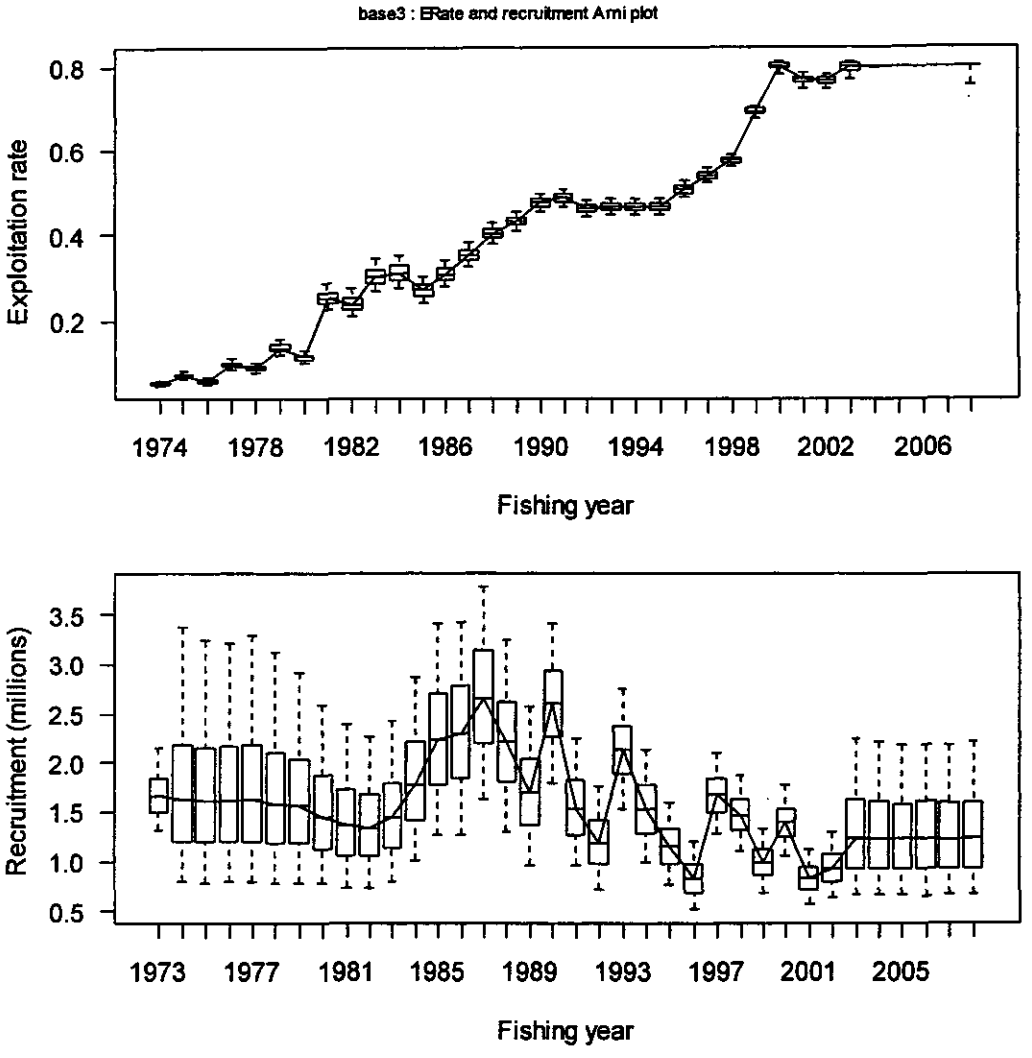

Figure 70: The posterior trajectories of exploitation rate (upper) and recruitment (lower) for the base case for PAU 7.

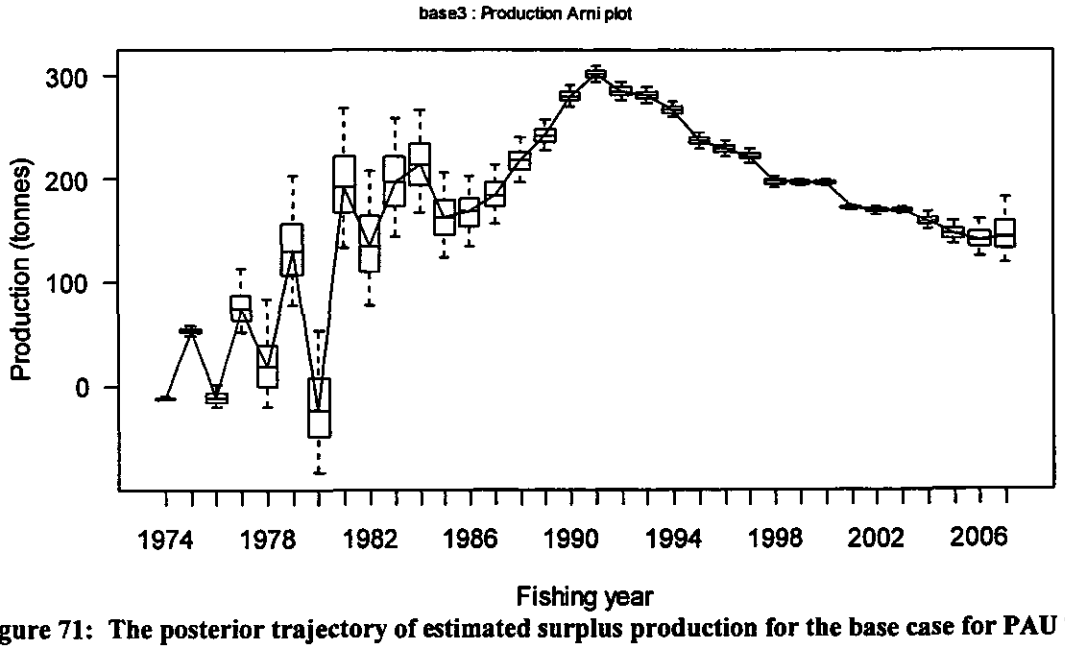

Figure 71: The posterior trajectory of estimated surplus production for the base case for PAU 7.

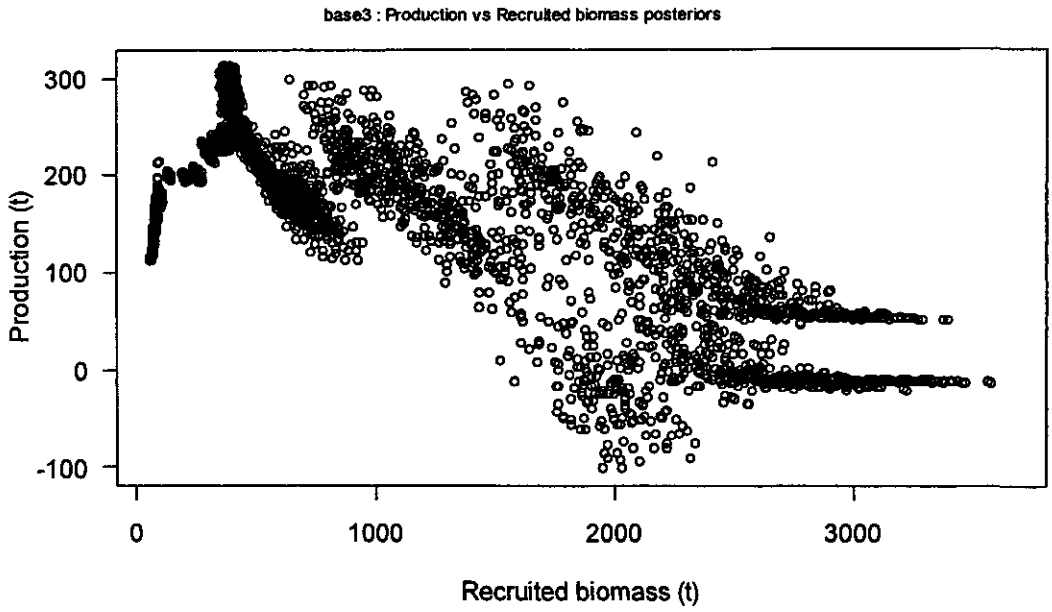

Figure 72: Production plotted against recruited biomass from 200 MCMC samples, sampled uniformly from the population of 4000 samples.

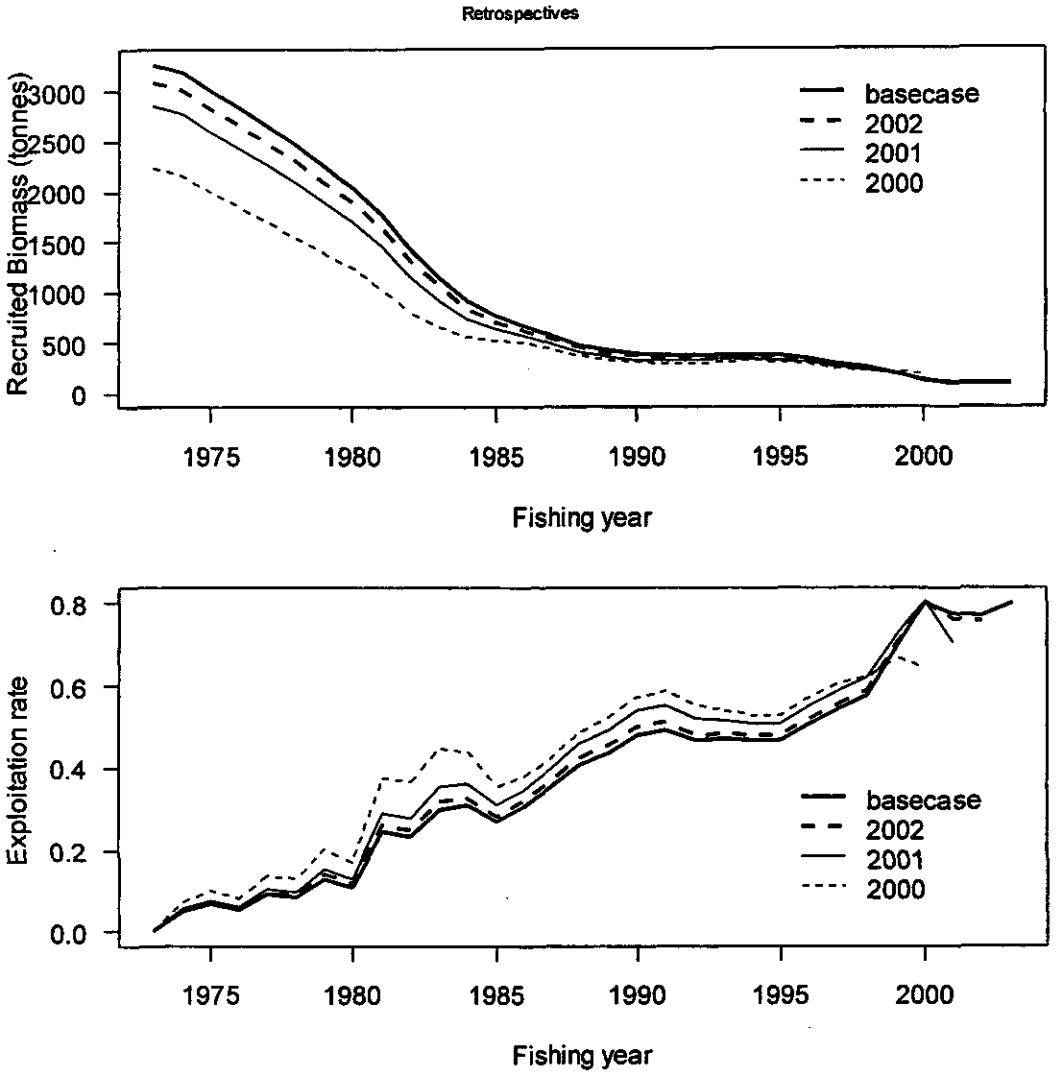

Figure 73: Recruited biomass (upper) and exploitation rate (lower) trajectories from the MPD estimates in a retrospective analysis. The key refers to datasets labelled by the last of data they include. The "base case" includes 2003 data.

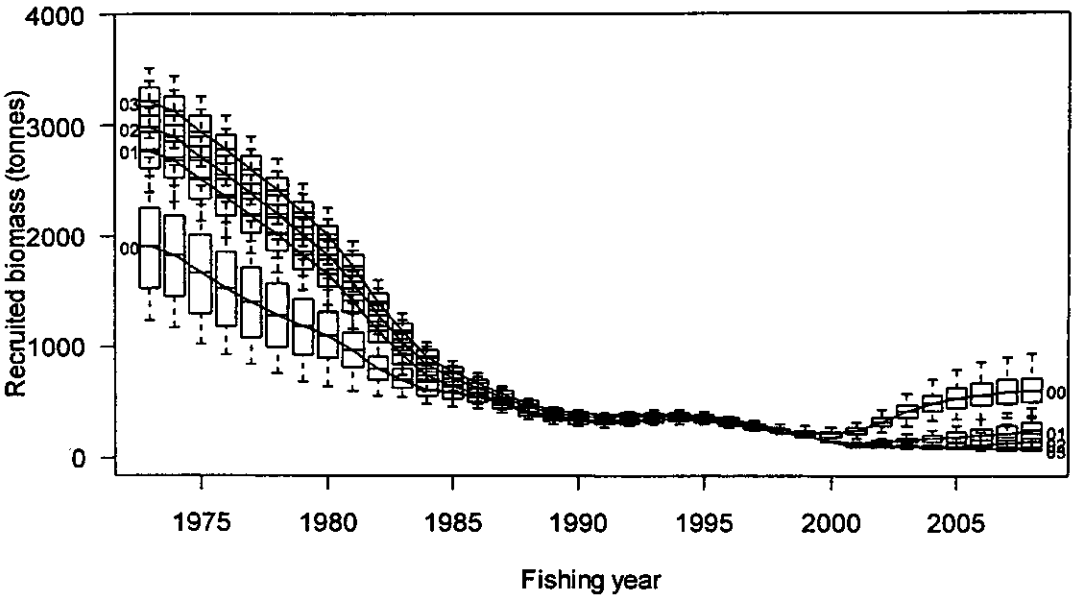

Figure 74: The posterior trajectories of the recruited biomass from retrospective analysis for PAU 7. Numbers beside each plot represents the last year of data used for the analysis.

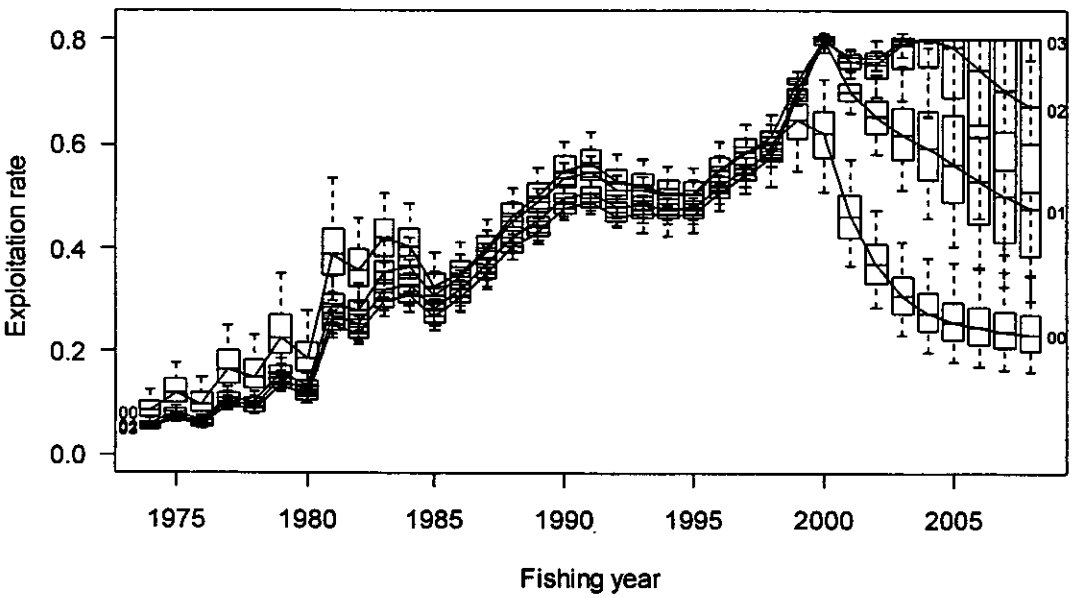

Figure 75: The posterior trajectories of the exploitation rate from retrospective analysis for PAU 7. Numbers beside each plot represents the last year of dataset used for the analysis.

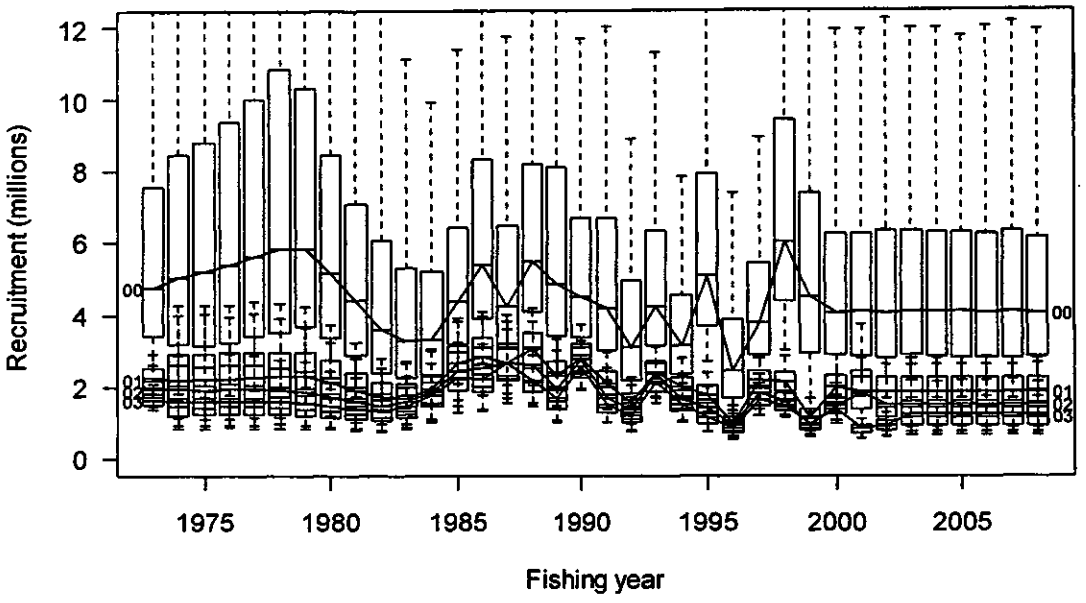

Figure 76: The posterior trajectories of the recruitment from retrospective analysis for PAU 7. Numbers beside each plot represents the last year of dataset used for the analysis.

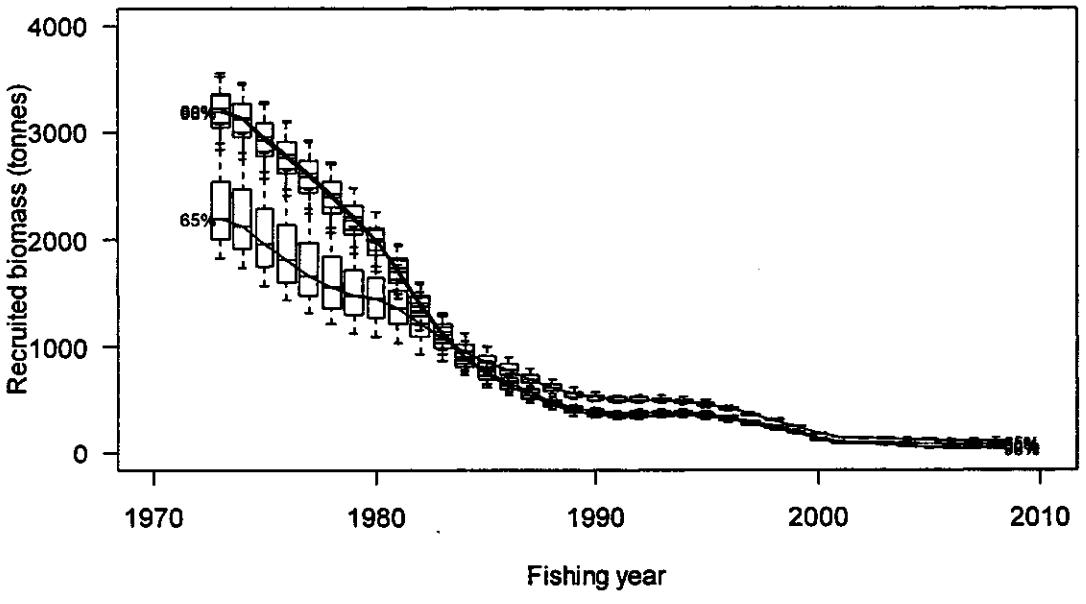

Figure 77: The posterior trajectories of the recruited biomass from a sensitivity analysis of maximum exploitation rate for PAU 7. Numbers beside each plot represents the maximum exploitation rate for that analysis (80% is the base case).

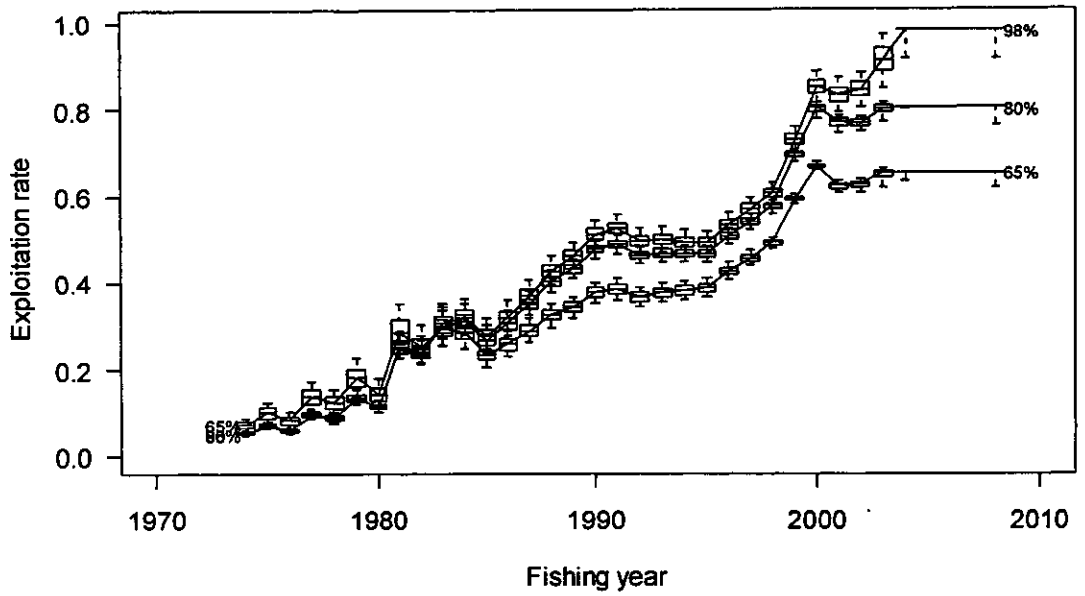

Figure 78: The posterior trajectories of the exploitation rate from sensitivity analysis on maximum exploitation rate for PAU 7. Numbers beside each plot represents the maximum exploitation rate for the analysis.

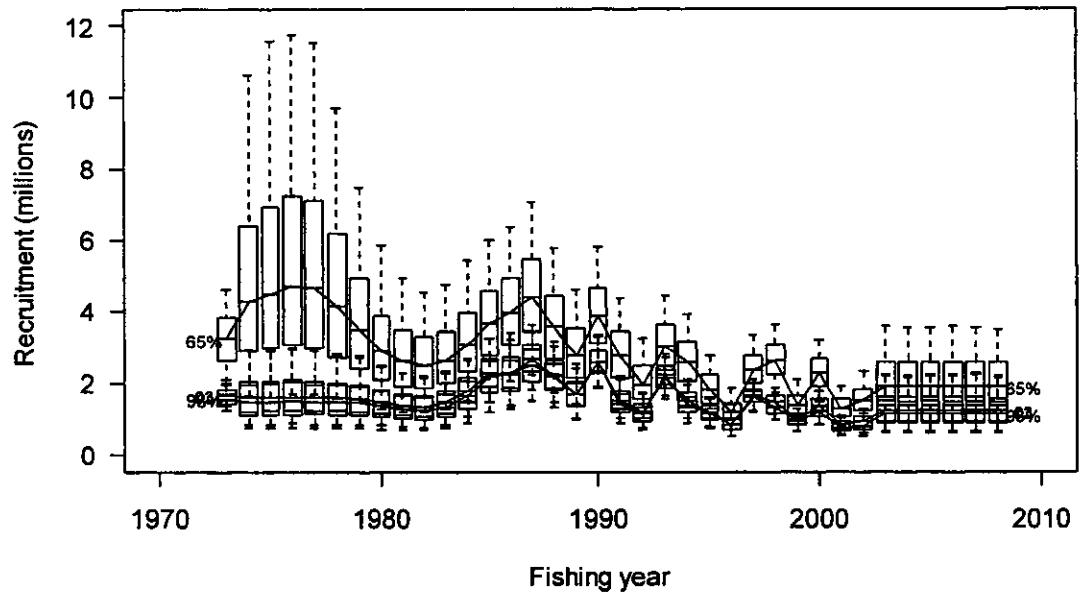

Figure 79: The posterior trajectories of the recruitment from sensitivity analysis on maximum exploitation rate for PAU 7. Numbers beside each plot represents the maximum exploitation rate for the analysis.

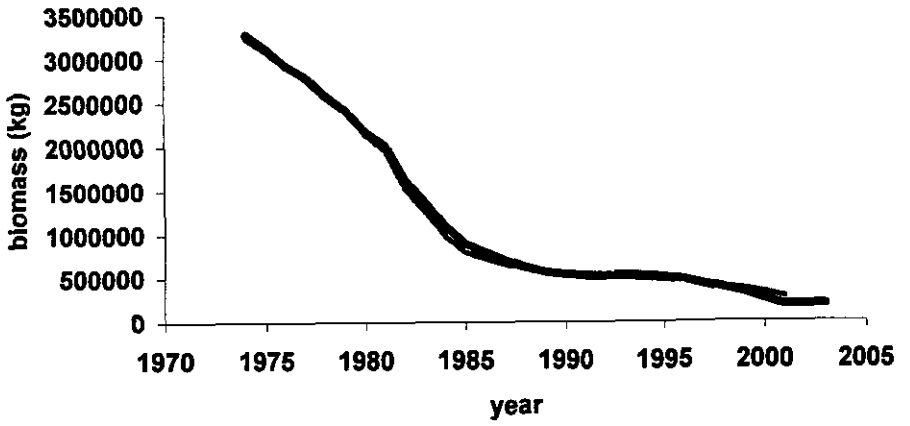

Figure 80: Comparing recruited biomass at the start of the year from the 2001 (lighter line) and 2003 base case MPDs.

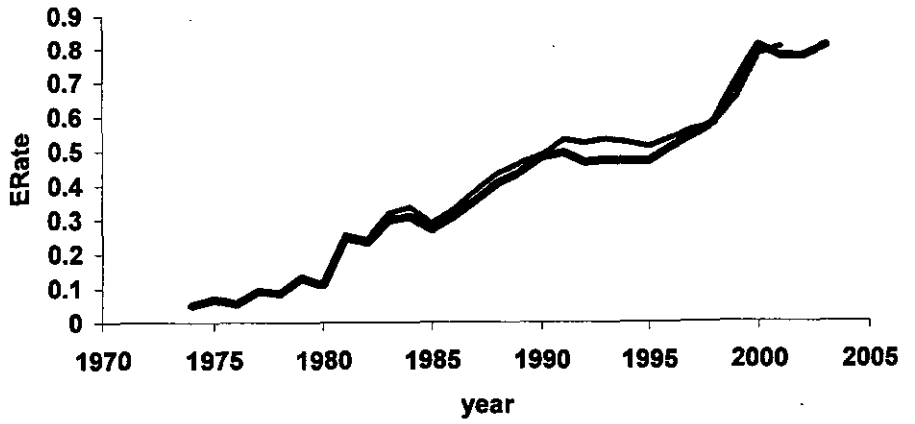

Figure 81: Comparing exploitation rates from the 2001 (lighter line) and 2003 base case MPDs.

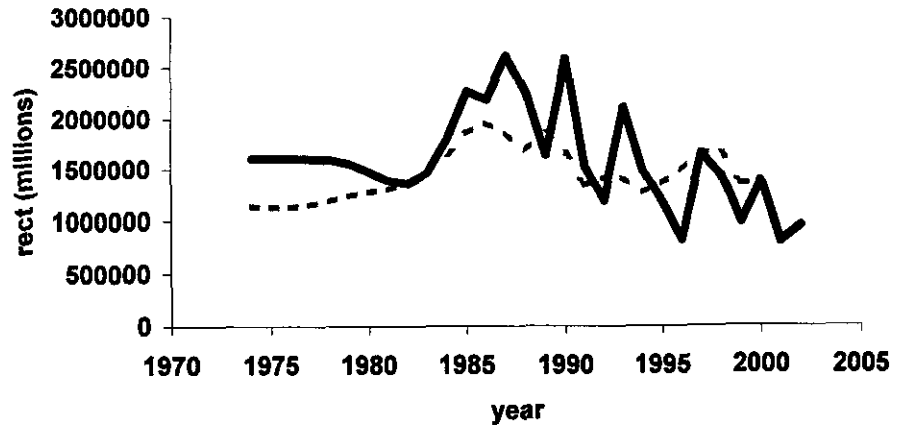

Figure 82: Comparing recruitment (millions) to the model from the 2001 (lighter line) and 2003 base case MPDs.

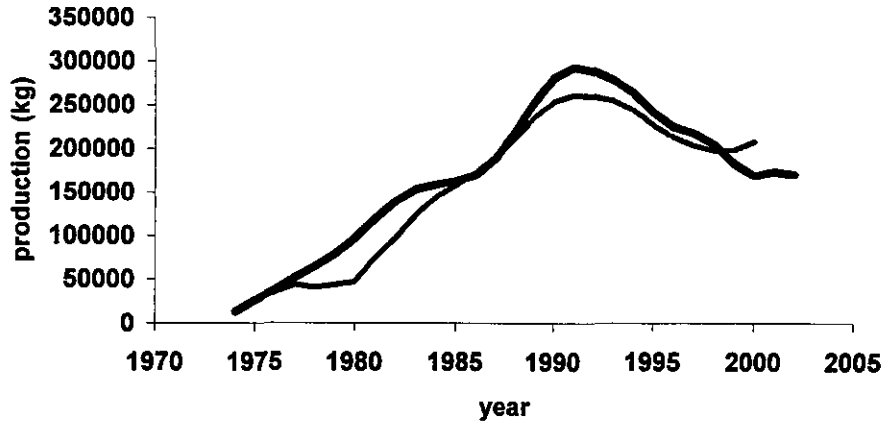

Figure 83: Comparing surplus production from the 2001 (lighter line) and 2003 base case MPDs.

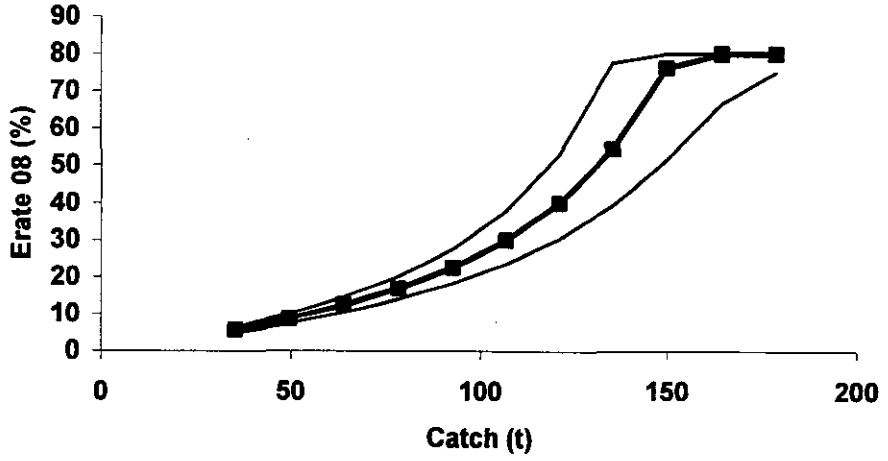

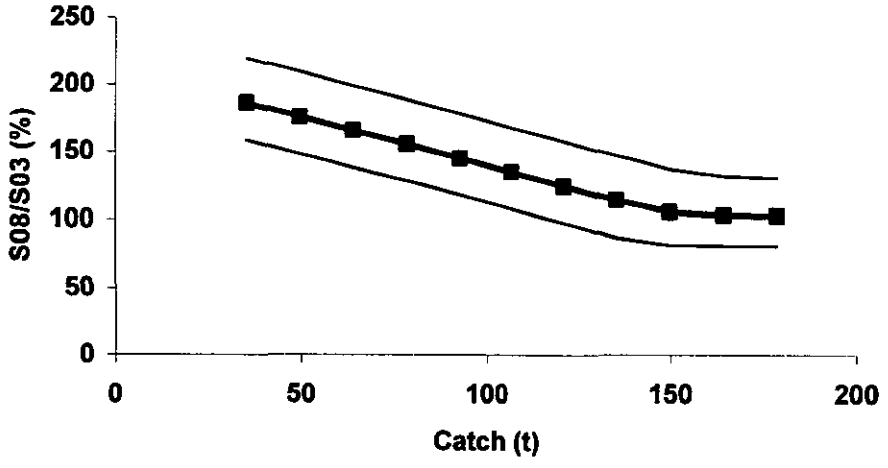

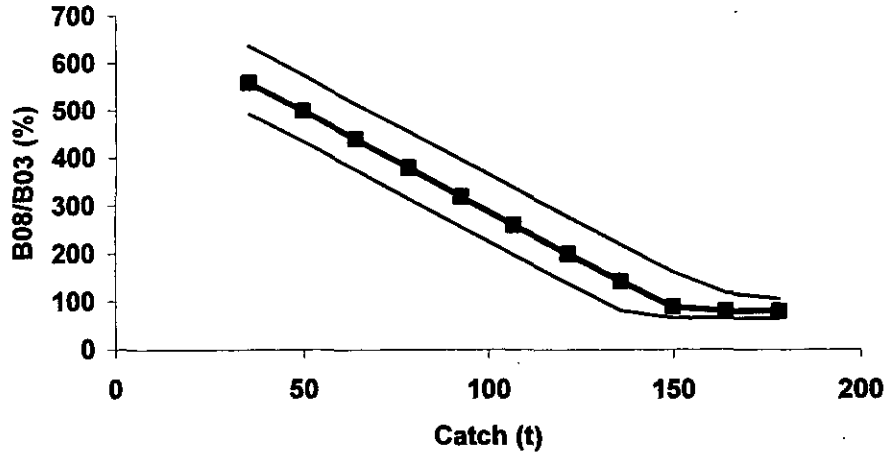

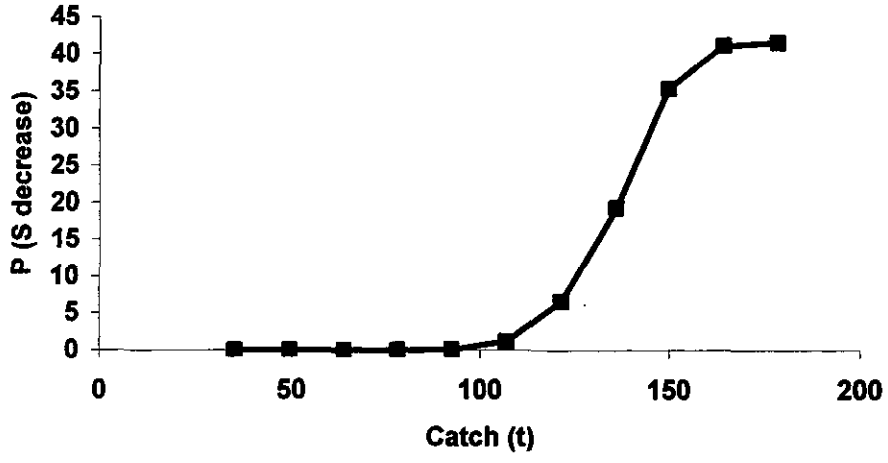

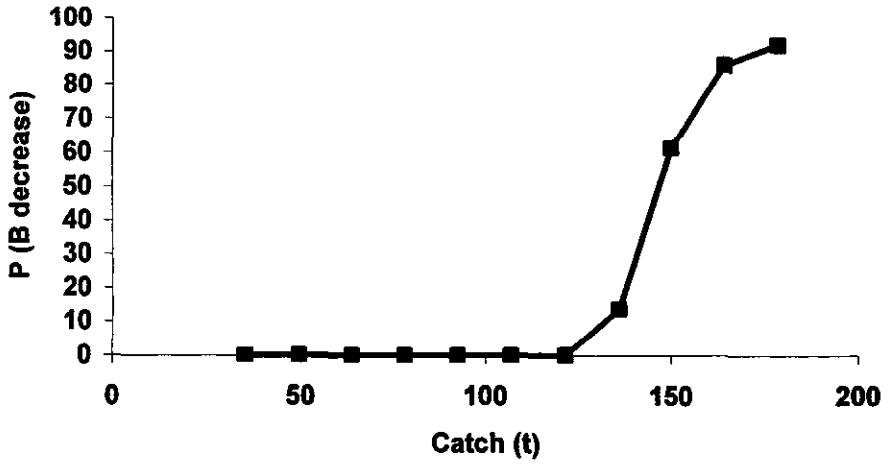

Figure 84: Results of 5-year forward projections made from the parameter vectors in 4000 samples from MCMC simulations. Each figure shows an indicator plotted against eleven different levels of total catch.